

1981-7

Final.

A STUDY OF THE RESPONSE TO EXPLOITATION OF
THE SVARTSENGI GEOTHERMAL FIELD, SW - ICELAND

Jonathan R. Regalado⁺,
UNU Geothermal Training Programme,
National Energy Authority,
Grensásvegur 9, 108 Reykjavík,
Iceland

⁺ Permanent address:
Philippine National Oil Company,
Energy Development Corporation Building,
Merritt Road,
Fort Bonifacio, Metro Manila,
Philippines

ABSTRACT

The response of the Svartsengi geothermal reservoir during the first 1600 days of exploitation is investigated. Two models to describe its behaviour and forecast its response to future exploitation are proposed. The first model revolves around the concept of the unit response function of the reservoir derived from drawdown and flowrate data only. The second model is built upon a hydrological idea of flow along a porous rectangular trench called an esker.

Based on the energy requirements of the region for the next 25 years, both models yield longterm drawdown estimates which are well within the operational limits imposed by the system. The unit response function model gives a much lower estimate of drawdown over the same period.

<u>LIST OF CONTENTS</u>	Page
ABSTRACT.....	3
1. INTRODUCTION.....	11
1.1 Purpose of the Study.....	11
1.2 Statement of the Problem.....	11
1.2.1 The main problem.....	11
1.2.2 The subproblems.....	11
1.2.3 Scope and limitation.....	12
1.2.4 Outline of solution to the problem.....	12
2. REVIEW OF BASIC GEOTHERMAL FEATURES.....	13
2.1 Brief Historical Sketch.....	13
2.2 Some Geological Features.....	14
2.2.1 The Reykjanes area.....	14
2.2.2 The Svartsengi area.....	14
2.2.3 Subsurface geology of Reykjanes area.....	14
2.3 Resistivity Measurements.....	15
2.4 Hydrological Features.....	15
2.5 Chemical Features of the Reservoir Fluids.....	16
3. RESERVOIR PROPERTIES AND WELL DESIGN AND PERFORMANCE FEATURES.....	18
3.1 General Description of the Field.....	18
3.2 Casing String Design.....	18
3.3 Reservoir Density and Pressure.....	19
3.4 Reservoir Temperature Distribution.....	20
3.4.1 Vertical temperature distribution.....	20
3.4.2 Horizontal temperature distribution.....	20
3.5 Temperature-Pressure Saturation Relation.....	21
3.6 Enthalpy and Flowrate Measurements.....	21
4. WELL TESTING.....	22
4.1 Well Interference Testing.....	22
4.2 Results of Previous Interference Tests.....	22
4.3 Well Testing Project.....	23

	Page
4.3.1 The use of the unit response function in well test analysis.....	23
4.3.2 The definition of the unit response function....	24
4.3.3 The numerical approximation of the unit response function.....	24
4.4 Multiple Rate Test Results. Test A.....	26
4.4.1 Type curve matching solution.....	26
4.4.2 Semi-log analysis of measured drawdown.....	27
4.4.3 Semi-log analysis of computed unit response function.....	27
4.5 Single Rate Test Results. Test B.....	28
4.5.1 Type curve matching of measured data.....	28
4.5.2 Type curve matching of computed unit response function values.....	28
4.6 Multiple Rate Test Results. Test C.....	29
4.6.1 Type curve matching of computed unit response function values.....	29
4.6.2 Semi-log analysis of unit response function values.....	30
4.7 Multiple Rate Test Results. Test D.....	30
4.8 A Summary of Interference Test Results.....	30
5. RESERVOIR MODELS.....	31
5.1 Need of a Model.....	31
5.2 The Earlier Model.....	32
5.2.1 Model description.....	32
5.2.2 Model tests.....	33
5.2.3 Drawdown projections.....	33
5.3 The Unit Response Function Model.....	34
5.3.1 Model description.....	34
5.3.2 Model tests.....	35
5.3.3 Drawdown projections.....	35
5.4 The Esker Model.....	36
5.4.1 Model description.....	36
5.4.2 Mathematical formulation of the esker model.....	36

	Page
5.4.3 Test of the model.....	37
5.4.4 Projected drawdowns.....	38
6. RESULTS AND RECOMMENDATIONS.....	39
6.1 Summary of Results	39
6.2 Recommendations.....	41
ACKNOWLEDGEMENTS.....	41
NOMENCLATURE.....	43
REFERENCES.....	44
TABLES.....	47
FIGURES.....	53
APPENDIX A Drawdown history.....	105
APPENDIX B Flowrate history.....	108
APPENDIX C Total mass output history.....	110

LIST OF TABLES

	Page
2.1 Chemical composition of formation water at Svartsengi.....	47
4.1 Calculated and measured drawdown (1st 10 days) used for calculating reservoir parameters S and T.....	48
4.2 Calculated and measured drawdown used for calculating reservoir parameters S and T.....	49
4.3 Calculated and measured drawdown used for calculating reservoir parameters S and T.....	50
4.4 Summary of well interference test results.....	51
5.1 Summary of drawdown projections for different energy requirements for the next 25 years.....	52

LIST OF FIGURES

	Page
2.1	Quake epicenters and fissure swarms in the Reykjanes peninsula53
2.2	Geological map of the western Reykjanes peninsula54
2.3	Seismic structure section of the Reykjanes thermal brine area55
2.4	Iso-resistivity map at 1000m depth.....56
2.5	A resistivity cross-section along line A-A' in Fig. 2.257
2.6	Section along the Reykjanes peninsula showing possible infiltration streamline and hybrid convection model58
3.1	The drillholes and the surface geology of the Svartsengi geothermal field....59
3.2	SW-NE vertical section showing some geological features60
3.3	Early pressure logs showing differences in fluid densities61
3.4	Initial pressure distribution62
3.5	Horizontal pressure distribution at 1000m reference depth63
3.6	SG-4 Completion and early P-T logs64
3.7	SG-3 Temperature log.....65
3.8	A vertical section showing temperature distribution66
3.9	Temperature profile at 350m depth67
3.10	Temperature distribution at 700m depth68
3.11	Pressure-Temperature saturation relation.....69
3.12	Typical bore output characteristics of Svartsengi wells70
4.1	Results of initial measurements of storativity(S) and transmissivity(T)71
4.2	Measured drawdown (0-970 days).....72
4.3	Flowrate data used for test A (76-10-18 to 76-10-28).....73
4.4	Flowrate and drawdown data for test B and C (77-02-25 to 77-04-06).....74
4.5a	Definition of boundaries for equation (1).....75
4.5b	Linear interpolation scheme for equation (5).....75
4.6	Type curve matching with computed U.R.F. for the first 10 days76
4.7	Semi-log plot of drawdown data for first 10 days.....77
4.8	Semi-log plot of the unit response function for first 10 days.....78
4.9	Type curve matching with measured drawdown from 77-02-25 to 77-03-17...79
4.10	Type curve matching with unit response function data from 77-02-25 to 77-03-17.....80
4.11	Type curve matching with values of unit response function from 77-02-28 to 77-04-06.....81
4.12	Semi-log plot of unit response function from 77-02-28 to 77-04-06.....82
4.13	Semi-log plot of 0-10 day drawdown. Computed from unit response function for 0-900 days.....83

4.14	Drawdown history (0-1600 days).....	84
5.1	Reservoir configuration of previous model	85
5.2	Discrete pumping rates	86
5.3	Measured vs calculated drawdown for previous model	87
5.4	Unit response function for previous model	88
5.5	Future production requirements	89
5.6	Forecasted drawdowns for previous model	90
5.7	Results of numerical two phase flow calculations for wells for different reservoir pressures at 1000m depth	91
5.8	Unit response function (0-900 days).....	92
5.9	Unit response function (0-900 days).....	93
5.10	Unit response function (0-900 days).....	94
5.11	Measured and fitted drawdown from U.R.F. (0-900 days).....	95
5.12	Unit response function (0-1600 days).....	96
5.13	Measured vs computed drawdown (0-1600 days)	97
5.14	Projected unit response function (0-25 years).....	98
5.15	Calculated drawdowns from unit response function	99
5.16A	Flow in an esker by pumpage from a well.....	100
5.16B	Auxiliary hydraulic system for calculating the hydraulic proper- ties of an esker.....	100
5.16C	Svartsengi reservoir configuration	101
5.16D	Equivalent two-well system	101
5.17	Measured vs computed drawdown (0-1600 days)	102
5.18	Projected esker model (0-25 years).....	103
5.19	Calculated drawdown from esker model	104

1 INTRODUCTION

1.1 Purpose of the Study

This work is the final product of a 6-month training at the UNU Geothermal Training Programme, at the National Energy Authority in Reykjavík, Iceland in the summer of 1981.

The programme started with a 4 week lecture course on all relevant aspects of geothermal energy which were augmented with short field excursions. The author's course of study in reservoir engineering consisted of the following: supervised reading on groundwater hydrology (2 weeks), supervised reading on advanced well testing methods (2 weeks) field excursions to geothermal fields in Iceland (2 weeks), practical field training in well testing (2 weeks) and a general report on a reservoir engineering study of the Svartsengi geothermal area in Iceland (11 weeks).

The choice of the problem in this exercise and the emphasis placed upon certain aspects were purposely chosen in order to provide the writer with useful learning experience and knowledge of geothermal energy utilization, consistent with the nature and scope of his responsibilities at the Philippine National Oil Company in his home country.

1.2 Statement of the Problem

1.2.1 The main problem. Briefly stated, this work is addressed to the following problem:

"To determine the response of the Svartsengi geothermal field during the first 1600 days of exploitation and to construct models based upon continuous pressure and mass output measurements describing its behaviour and predicting its response to future production."

1.2.2 The subproblems. The subproblems are:

- A. To determine the initial properties and state of the reservoir as to its:
 - 1) Chemistry
 - 2) Pressure

- 3) Temperature
 - 4) Enthalpy
 - 5) Transmissivity
 - 6) Storativity
- B. To determine some important changes and the extent to which they have occurred in some of the above properties over the first 1600 days of production.
- C. To find a hydrological model which explains the observed behaviour and to base upon this model a mathematical simulation of performance of the field when energy is produced according to future production requirements.

1.2.3 Scope and limitation. This study is limited to the examination of the changes in mass output measurements and the corresponding drawdown in water level as input to the proposed reservoir models. Effects of forecasted drawdown on well performance are also studied.

1.2.4 Outline of solution to the problem.

To arrive at a reasonable description of the characteristics of the Svartsengi geothermal field and to forecast its response to future exploitation, a survey of existing production, geological, geophysical and geochemical data is undertaken. This effort could lead to the identification of various reservoir properties and the relationships between them that would constitute an initial conceptual model.

The analytic work is confined mainly to mass output and observed drawdowns during the prescribed period. Two models based on these measurements are proposed. These models express the relationships between drawdown and flow rates and identify reservoir parameters which are subsequently calibrated by matching the calculated against the measured drawdowns.

Forecasts of drawdowns are calculated over the next 25 years based on future energy requirements of the region. Finally, effects of the drawdown projections upon well performance are estimated.

2 REVIEW OF BASIC GEOTHERMAL FEATURES

2.1 Brief Historial Sketch

What is now known as the Svartsengi geothermal field was conceived during the early 1950's when the possibility of heating the Sudurnes region was discussed. This venture seemed viable in the light of the example of Reykjavík which had geothermal heating since 1944.

To this end the initial plans for regional geothermal heating for Keflavík, Njardvík and the Keflavík airport were completed in 1961. Eight years later, in 1969, Orkustofnun (NEA) conducted geophysical and geological exploration of the region which identified a potential geothermal field about 5 km north of Grindavík near an area called Svartsengi.

In 1971-72 two holes (SG-2 and SG-3) were drilled which proved that the prospective area was a high-temperature field producing 235°C brine of high salinity which could not be used directly for space heating. A test pilot plant employing a heat exchanger arrangement was proposed and operated in the early part of 1974 to 1975. Several process arrangements were tried and the results served as input to the design of the present power plant.

Following detailed resistivity measurements conducted in 1973, two more successful boreholes, SG-4 and SG-5, were drilled in 1974. These wells completed to depths of 1713 m and 1519 m respectively gave individual flowrates of 60-80 kg/s brine at 235°C.

At this time excalation of oil prices and uncertainty of supply made it imperative to develop the Svartsengi project further. Consequently, more investments and efforts were made which lead to the initial production for district heating in November 1976. By means of a novel heat exchange process, two-phase mixture from SG-4 was used to heat warm fresh water to 95°C which supplied heat for Grindavík only.

Presently, Svartsengi field is operated by the Sudurnes Regional Heating, a consortium of seven separate towns and villages in the Reykjanes peninsula and the state. Eleven holes have been drilled to date which provide 125 MW_t of heating and 8 MW_e of electricity to these localities.

2.2 Some Geological Features

2.2.1 The Reykjanes area. The Reykjanes geothermal area is located at the extreme SW end of the active volcanic belt which runs across Iceland in a SW-NE trend (Fig. 2.1). Arranged in echelons and intersecting the belt are five active fissure swarms. High temperature areas and magnetic anomalies are observed at these intersections.

Reykjanes is the smallest of the 17 high temperature fields in Iceland (Bodvarsson 1961), all of which are found in the active volcanic belt. Early chemical investigations revealed reservoir temperatures of 250-290°C. Visible thermal activity is limited to about 1 km² (Bjornsson et al. 1970).

2.2.2 The Svartsengi area. The Svartsengi is a part of the Reykjanes peninsula and lies within the second westernmost fissure swarm called the Grindavík swarm (Fig. 2.1). This is one of the intensely fractured NE-SW trending fault zone that crosses the belt of quake epicenters. It is believed that tectonic activity increases the permeability of the formations thus creating a hydraulic channel along the earthquake belt which controls the geothermal characteristics of the area.

Fig. 2.2 shows the surface geology of the field. The Thorbjörn and Svartsengisfell mountains form the prominent features. The production area lying north of Thorbjörn and west of Svartsengisfell is covered with postglacial lava flows. Active surface geothermal manifestations are almost absent except for some steam emanating from lava fractures east of Svartsengisfell, visible only under certain weather conditions (Jónsson 1978). Hydrothermal alterations are limited to about 1-2 km² (Arnorsson, et al. 1975) and consist of patches of clay alteration in the hyaloclastite formations in the slopes of Thorbjörn and Svartsengisfell (Jonsson 1978).

2.2.3 Sub surface geology of Reykjanes area. According to Bjornsson et al. (1970) studies of explosion seismology and exploratory drilling indicate that the crustal structure of the Reykjanes area may be divided into 4 layers (Fig. 2.3). Layer 1 which extends from the surface to about 900 m depth consists of porous, fresh breccias, pillow lavas and individual lava flows with a density of 2.1-2.5 g/cm³ and porosity of 23-32% as measured from drill cores recovered from 300-510 m.

Layer 2 extending from about 900 to 2600 m has proven to be composed mainly of basaltic lava flows with thick interbeds of hyaloclastites. A core recovered at 1370 m gives a porosity of 19%.

Layer 3 which covers a depth from about 2.6 km to about 8.5 km corresponds to a typical "oceanic layer" while layer 4 corresponds to the upper mantle (Björns-son et al. 1970).

Drilling in this area showed that good aquifers were encountered within the basaltic formation of layer 2 instead of within the high porosity hyaloclastite formation of layer 1. It is believed that the scoriaceous contacts between lava flows and interbeds are quite porous & permeable which, together with joint fractures & faults, act as channels of geothermal fluids.

2.3 Resistivity Measurements

Extensive resistivity studies have been conducted in the Svartsengi geothermal field. These show that the field extends along a SW-NE direction and is predominantly controlled by the tectonic fracture system in the area (Georgsson 1979, 1981).

A 5 ohm-meter resistivity contour which increases with depth has been found to show the possible lateral extent of the field (Fig. 2.4).

Fig. 2.5 shows that the horizontal cross-section of the iso-resistivity area increases with depth from at least 5 km² at 200 m to over 7 km² at 600 m below sea level. These findings however do not substantiate the presence of less permeable rock formations which could define the horizontal boundaries of the reservoir. (Georgsson 1979).

2.4 Hydrological Features

Studies in the hydrology of the Svartsengi area reveal a fresh water lens of meteoric origin floating on saline water in the uppermost part of the ground (Ingimarsson, et al. 1978). Subsequent resistivity measurements verified this and gave an estimate of its thickness as 40-60 m (Georgsson 1979). Beneath the fresh water lens are pockets

of cold sea water intrusions.

The recent hydrologic reservoir mechanism is as follows: Deep meteoric water percolates approximately 3 km down from the infiltration area near Kleifarvatn lake and flows westward along the earthquake zone, a permeable channel created by tectonic movements. This flow picks up heat from the lower rock formation and mixes with the intrusive cold sea water forming a saline geothermal fluid. Convection occurs in regions where fissure swarms intersect the earthquake zone resulting in rising of hot fluids which are capped by an impermeable layer at about 600 m below the surface. Figure 2.6 shows the proposed model and calculations show a mass flux of 20 kg/S km^2 along the earthquake zone and an estimated reservoir pressure which agrees with the pressure measured at point C (Kjaraan et al. 1980).

2.5 Chemical Features of the Reservoir Fluids

Geothermal fluids in the Reykjanes Peninsula exhibit variable degree of salinity. This has been attributed to different degrees of mixing of fresh water with the intrusive sea water and ground water in the downflow zones around the geothermal fields (Arnórsson 1978). In Svartsengi, fluids from geothermal boreholes give a base temperature of 240°C and a high salinity, about two-thirds that of sea water. It has been shown from chemical analysis that these fluids are about 67% sea water but deuterium measurements give only 57% sea water. This difference may be due to flashing in the upflow zones which tap the geothermal reservoirs (Kjaraan et al. 1979).

Quartz equilibrium temperatures calculated from chemical analysis of fluid samples at well-head conditions are in good agreement with measured aquifer temperatures (Arnórsson 1978). This implies that flashing occurs in the well, not in the aquifer, which poses a problem of calcite deposition in the boreholes.

Table 2.1 gives a representative list of chemical compositions of reservoir fluids at Svartsengi showing high concentrations of dissolved solids particularly silica and calcium ions.

Calcite is found to be very abundant not only in the upflow zones of the Reykjanes and Svartsengi fields where flashing occurs but also below the flashing zones (Tómasson and Kristinsdóttir 1972). In wells SG-4, SG-5 and SG-6, calcite deposition at 350-400 m has been found to create serious operating problems which requires periodic cleaning of SG-5 and SG-6 once every 7-8 months. It has been decided to drill wider boreholes and install 13-3/8" production casing instead of 9-5/8". This will reduce the frequency of costly periodic cleaning and increase well output to nearly double. The latter advantage is due to high reservoir permeability (1 darcy) and reduced flow resistance in the borehole.

3 RESERVOIR PROPERTIES AND WELL DESIGN AND PERFORMANCE FEATURES

3.1 General Description of the Field

The production area is situated on a flat land, sited north of Thorbjorn and west of Svartsengisfell mountains. The size of the reservoir is small, the most porous area is estimated at 2 km² and believed to be rectangular shaped, bounded by impermeable formations on all sides except on the SW side.

The 11 wells that have been drilled to date are aligned in a SW-NE direction in an area of about 0.64 km² and are spread at an average distance of 250 m between adjacent wells.

All boreholes are productive except for SG-4 which has a broken liner at about 70 m and is presently used as an observation well. SG-1 is a shallow hole which supplied fresh water in the early drilling operations. Figure 3.1 shows the location of drillholes. SG-12 and SG-13 are to be drilled.

The depth of the wells ranges from 239 m (SG-2) to 1734 m (SG-6). Wells SG-2, SG-3, SG-10 are shallow (239-425 m) and located in an upwelling zone where a major fault intersects the earthquake zone and controls an upflow of boiling water. This upflow cools as it reaches the caprock, flows downward and is heated up again. Thus a convection cell is formed which gives the reservoir a characteristic temperature of 240°C.

Wells SG-9 and SG-11 are intermediate in depth (994-1141 m) while SG-4, SG-5, SG-6 and SG-8 are deep wells (1519-1734 m), three of which SG-4, SG-6 and SG-8 have intercepted deep aquifers. SG-5 and SG-7 appear to feed from the basaltic layer at 700-1200 m (Fig. 3.2).

3.2 Casing Design

All wells are completed with slotted liners except SG-7 which is a barefoot well. There are three casing designs in Svartsengi. The

shallow wells have 8-5/8" production casing except SG-10 which has a 13-3/8" liner. The deep wells SG-4, SG-5 and SG-6 have 9-5/8" casings while wells SG-1, SG-8, SG-9 and SG-11 all have 13-3/8" casings.

3.3 Reservoir Density and Pressure

Figure 3.3 shows some initial pressure logs from 3 different wells taken when the reservoir may be considered in its "undisturbed" state. SG-1 is a shallow well, SG-3 a production well located at the upwelling zone where boiling occurs while SG-4 is a deep well connected to a zone of compressed liquid. It can be seen that the pressure within the deeper part of the aquifer is a least 16 kp/cm^2 lower than the pressure at the boiling zone.

With the exception of SG-1 and SG - 2 all the wells have nearly equal densities at an average of 854 kg/m^3 . The low density of fluids at SG-2 maybe due to boiling and the high density in SG-1 maybe due to sea water intrusion.

Interpretation of pressure gradient profiles of Svartsengi bores suggests that the wells are connected to a common widespread compressed hot water (240°C) reservoir 1000 m beneath the surface. With the exception of SG-2 all wells have nearly equal hydrostatic pressure of 83.5 kg/cm^2 to within $\pm 2.5 \text{ kg/cm}^2$ referred at a common datum of 1000 m. SG-2 is the only underpressured well indicating boiling in its vicinity.

Fig. 3.4 showing a vertical section of the field pressure measurements suggests an almost even pressure distribution with depth between wells SG-6 to SG-9 in the deep well area. A horizontal pressure distribution is shown in Fig. 3.5, but it is quite difficult to see any horizontal pressure trend from these measurements.

3.4 Reservoir Temperature Distribution

Fig. 3.6 shows pressure and temperature logs taken from surveys of SG-4. The temperature profile during completion and heat up ('76-07-12) indicates a rapid increase in temperature from 300 to 600 m followed by an isotherm at 240°C down to 1700 m. This trend is typical of the deep wells at Svartsengi.

The shallow wells on the other hand show a different temperature trend. The temperature log of SG-2 shown in Fig. 3.7 exhibit only a slight increase in temperature with depth over the entire column from 165°C at about 80 m to 220°C at 400 m.

With reference to Fig. 3.2, the deep well temperatures from 0-600 m may reflect rock temperatures in this region while those from 600 to 1700 m could indicate true reservoir fluid temperatures. The shallow well temperatures are also indicative of reservoir fluid temperatures.

3.4.1 Vertical temperature distribution

A vertical temperature section in a SW-NE direction is illustrated in Fig. 3.8. There appears to be a high temperature gradient between 400 to 700 m in the deep well area from SG-4 to SG-9. Below this the temperature trend changes gradually with depth.

In the shallow well area, the temperature gradient is quite pronounced within the vicinity of wells SG-6 and SG-3. This may be due to an outflow of fluid escaping from the deep aquifer which causes rapid heating of the formation in this zone.

3.4.2 Horizontal temperature distribution

Fig. 3.9 is a temperature distribution at 350 m which shows the area around SG-6 as the hottest horizontal section within the field. The temperature drops in all directions away from SG-6.

The horizontal temperature distribution at 700 m (Fig. 3.10) depth on the other hand shows a nearly even distribution in a SW-NE direction. The north and south edges of the field seem to be hotter as suggested by higher temperatures in SG-11 and SG-4.

3.5 Temperature-Pressure Saturation Relation

A temperature-pressure relation for geothermal fluids in Svartsengi is shown in Fig. 3.11. The boiling point curve is constructed from a pressure log from SG-4. It appears that there are three degrees of saturation depending upon the location of the feed zones in the wells.

Fluids in shallow wells SG-2, SG-3, SG-10 are saturated as expected since these wells are located near the upwelling zone where reservoir fluids boil as they rise through the fault. Fluids in SG-5, SG-7, SG-9 and SG-11 are nearly saturated suggesting that those wells feed from an upflow coming from the upwelling zone which runs through the basalt layer from 750 to 1200 m. Fluids in SG-4, SG-6 and SG-8 are all undersaturated, highly compressed and appear to be fed from the lower part of the aquifer. Thus it may be said that the reservoir is basically single phase liquid dominated with nearly uniform temperature of 235-240°C. These observations agree with the proposed model found in Fig. 3.2 (Kjaran et al. 1979).

3.6 Enthalpy and Flowrate Measurements

The results of enthalpy measurements using the Russel Jones formation are available only for wells SG-7, SG-8, SG-9, SG-10 and SG-11. These give an average enthalpy of 1074 kJ/kg which is slightly higher than both the average enthalpies based on silica temperature (1004 kJ/kg) and steam brine mixture temperature (1000 kJ/kg).

Fig. 3.12 shows some of the results of flowrate measurements. It can be seen that at a given wellhead pressure, bores with larger production casing diameters give higher flowrates than those with smaller sized casings. SG-4 (9-5/8") gives 70-85 kg/s at 10-15 bars absolute while SG-8 and SG-11, both with 13-3/8" give 140-180 kg/s. SG-7 has not yet been tested at higher flowrates but it appears to follow the 13-3/8" casing characteristics. So far, no detectable change has been reported in the enthalpy and fluid composition since the start of production in October 1976.

4 WELL TESTING

4.1 Well Interference Testing

An urgent question that must be answered early in the exploitation of a geothermal field is initial assessment of reservoir capacity. This requires determination of deliverability rate and estimation of that part of the reserves which can be economically recovered.

Short period pressure transient tests are usually used and could give acceptable determination of deliverability during the early stages of production. However, it is necessary to obtain extended observations of mass output and pressure to detect decline, to establish performance models and to estimate reserves.

Interference testing has been reported to give adequate answers to the above questions. It can be accomplished in a reasonably short period of time and provide important information on reservoir capacity early in the life of a reservoir (Chang et al. 1979).

In Svartsengi, interference well testing has been used to: a) determine storativity (S) and transmissivity (T) of the reservoir, b) monitor field drawdown, and c) detect the presence of geological boundaries.

4.2 Results of Previous Interference Tests

Using interference tests reservoir parameters S and T were determined and reported by previous workers (Eliasson, et al. 1977). By varying the flowrate of SG-4 and observing the corresponding drawdown in observation well SG-5, three sets of data were recorded and analyzed using the semi-log analysis. Fig. 4.1 shows the summary of their results which gave an average transmissivity (T) of $0.012 \text{ m}^2/\text{s}$ and a storage coefficient (S) of 0.012.

Extended observations of drawdown data in SG-5 as one or more wells were being discharged were recorded and analyzed on a semi-log plot shown in Fig. 4.2. Results show that the pressure front has reached impermeable boundaries in about 10-20 days. This is indicated where the curve begins

to deviate from the straight line representing Theis solution for a well in an infinite reservoir. In this paper, type curve matching with Theis solution is used in the time interval where it is applicable.

4.3 Well Testing Project

As part of his training program in reservoir engineering, the writer reviewed and recalculated the values of transmissivity and storativity by using type-curve matching and semi-log analysis together with values of the unit response function of the reservoir. Reasonable results were obtained which are comparable in magnitude with values reported previously.

Calculations of S and T were made on the drawdown and flowrate measurements taken during the following schedules.

Test A: Multi-rate well test analysis using drawdown data for the first 10 days of production between 76-10-18 to 76-10-28, Fig. 4.3 .

Test B: Single-rate well test analysis using drawdown data during an increase of flowrate from 30 to 45 kg/s between 77-02-25 to 77-03-17 (Fig. 4.4)

Test C: Multi-rate well test analysis using drawdown data between 77-02-28 to 77-04-06 (Fig. 4.4).

Test D: Multi-rate well test analysis using computed unit response function for the first 900 days of production (Fig. 4.14 and 5.8). Appendix A and B contain the list of flowrate-drawdown history.

4.3.1 The use of the unit response function in well test analysis

Standard well test analyses (e.g. pressure build & fall-off tests) suffer from one major drawback in that flowrates must be kept constant as close as possible to a step function. The requirement of constant rate is sometimes difficult to meet due to reservoir changes and other factors (Barelli and Palama 1980). Pressure variations taken at varying flowrates to be usable must therefore be processed properly before the methods of standard well test analyses could be applied.

The processing of flowrate-drawdown records involves the solution to the linear diffusion equation in a porous medium subject to appropriate boundary condition. The definition and solution to this equation are well known from the paper of Barelli and Palama (1980). Here, only a brief outline of the method of formulating the diffusion problem and computing the unit response function are presented.

4.3.2 The definition of the unit response function

Barelli defines the unit response function $P_r(\vec{r}, t)$ as the solution of the following boundary value problem:

$$\begin{aligned} n \nabla^2 p_r(\vec{r}, t) - \frac{\partial p_r(\vec{r}, t)}{\partial t} &= 0 && \text{in } V, \\ p_r(\vec{r}, t) &= 0 && \text{on } S_1, \\ p_r(\vec{r}, 0) &= 0 && \text{in } V, \\ A_2 K \nabla p_r(\vec{r}, t) \cdot \vec{n} &= U(t) && \text{on } S_2, \\ \nabla p_r(\vec{r}, t) \cdot \vec{n} &= 0 && \text{on } S_3 \end{aligned} \quad (1)$$

Fig. 4.5 shows the boundaries as defined. It can be shown that the solution to this system of equations is a superposition of solutions of the form

$$p_d(t) = q(0+) p_r(\vec{r}, t) + \int_0^t p_r(\vec{r}, \tau) q^1(t-\tau) d\tau \quad (2)$$

4.3.3 The numerical approximation of the unit response function

In terms of water level drawdown h and discrete changes in pumping rates q , the equation (2) can be written as

$$h(t) = q(0+) F(t) + \sum_{i=1}^n \Delta q_i F(t-\tau_i) \quad (3)$$

Where we have used n pairs of measured values of drawdown and flowrate. $F(t)$ is the unknown function.

Further if the number of variables N_0 and the time interval of interest T are specified, then a set of values

$$F(0), F\left(\frac{T}{N_0-1}\right), F\left(\frac{2T}{N_0-1}\right), \dots, F(T) \quad (4)$$

can be written as a linear combination with the measured values of h and q. For instance if a data point $(t_b, F(t_b))$ falls within the time interval $t_i < t < t_{i+1}$ the following relationship can be written

$$F(t_b) = (t_{i+1} - t_b)F_i + (t_b - t_i)F_{i+1} \quad (5)$$

$F(0)$ may be set equal to zero leaving $r = N_0 - 1$ unknowns.

Using this procedure for n number of observations a set of n simultaneous linear equations in N_0 unknowns in the interval T follows. This is of the form

$$\begin{aligned} C_1 &= a_{11}x_1 + a_{12}x_2 + \dots + a_{1r}x_r \\ C_2 &= a_{21}x_1 + a_{22}x_2 + \dots + a_{2r}x_r \\ &\vdots \\ C_n &= a_{n1}x_1 + a_{n2}x_2 + \dots + a_{nr}x_r \end{aligned} \quad (6)$$

where: C's are the observed drawdown $h_i(t)$'s

x's are the unknown functions F_i 's

a's are the differences in adjacent time interval $(t_i - t_j)$'s

Equation 6 was solved by the method of least squares using a computer program "UNIT" written specifically for this purpose. The object of the least squares solution is to find a set of values x_1, x_2, \dots, x_r such that

$$\sum_{i=1}^n (a_{i1}x_1 + a_{i2}x_2 + \dots + a_{ir}x_r - C_i)^2$$

is a minimum.

Hence, within specified boundary conditions, a set of values of the unit response function can be calculated from drawdown and flowrate data. This can be used to determine reservoir parameters using any of the appropriate standard methods of well test analysis.

4.4 Multiple Rate Test Results. Test A.

In order to calculate the reservoir parameters S and T, the unit response function of the reservoir for the first 10 days of production was computed using the drawdown and flowrate data from well SG-5 and SG-4 respectively.

A computer program "UNIT" together with a smoothing routine "DENSE" calculated values of the response function which were plotted on a log-log scale. Using a unit flowrate, conventional type curve matching with Theis solution for the case of a well in an infinite reservoir was used. Fig. 4.2, a semi-log plot showing drawdown vs. time for the first 970 days of production validates this assumption if the time of interest is confined to within the first 10-15 days.

4.4.1 Type curve matching solution

Fig. 4.6 illustrates a type curve matching solution with the values of the unit response function computed for the first 10 days. Using the following values:

$$\begin{aligned} \text{At match point: } W(u) &= 1.0 \\ u &= 1.0 \\ s &= 0.7 \text{ cm} \\ t &= 0.24 \text{ d} \\ \text{Reservoir data: } \dot{m} &= 1.0 \text{ kg/s} \\ \rho &= 825 \text{ kg/m}^3 \\ r &= 241.0 \text{ m} \end{aligned}$$

the transmissivity and storativity are computed as:

$$T = \frac{\dot{m}}{4\pi \rho S} = \frac{1.0}{4\pi \times 825 \times 0.7 \times 10^{-2}} = 0.0135 \frac{\text{m}^2}{\text{s}}$$
$$S = \frac{4Tt}{r^2} = \frac{4 \times 0.0135 \times 0.24 \times 24 \times 3600}{(241)^2} = 0.019$$

Table 4.1 gives a summary of data and results of calculating the unit response function for the first 10 days.

4.4.2 Semi-log analysis of measured drawdown

The drawdown data taken during the first 10 days (Table 4.1) was also analyzed using the semi-log analysis. Taking an average flowrate of 46 kg/s and the values of slope and intercept shown in Fig. 4.7, calculations give the values of S and T as:

give the value

$$m = 31.05 \text{ cm/decade}$$

$$t_0 = 0.62 \text{ d}$$

$$\dot{m} = 46 \text{ kg/s}$$

$$\rho = 825 \text{ kg/m}^3$$

$$T = \frac{\dot{m}}{4\pi m\rho} = \frac{46}{4\pi \times 31.05 \times 825 \times 10^{-2}} = 0.0142 \frac{\text{m}^2}{\text{s}}$$

$$S = \frac{2.246Tt}{r^2} = \frac{2.246 \times 0.0102 \times 0.6 \times 24 \times 3600}{(241)^2} = 0.02$$

4.4.3 Semi-log analysis of computed unit response function

Figure 4.8 is a semi-log plot of the unit response function for the first 10 days of production. The following calculations give results of S and T comparable to those obtained earlier; Here,

$$m = 0.616 \text{ cm/decade}$$

$$t_0 = 0.35 \text{ day}$$

$$\dot{m} = 1.0 \text{ kg/s}$$

$$\rho = 825 \text{ kg/m}^3$$

$$T = \frac{\dot{m}}{4\pi m\rho} = \frac{1.0}{4\pi \times 0.616 \times 825 \times 10^{-2}} = 0.015 \frac{\text{m}^2}{\text{s}}$$

$$S = \frac{2.246Tt}{r^2} = \frac{2.246 \times 0.015 \times 0.35 \times 24 \times 3600}{(241)^2} = 0.017$$

4.5 Single Rate Test Results. Test B.

Table 4.2 gives a summary of measured & calculated drawdowns taken during a single rate test in Feb. 28, 1977 when flowrate in SG-4 was increased by 15 kg/s. The measured drawdown is plotted on a log-log scale (Fig. 4.9) and analyzed as follows:

4.5.1 Type curve matching of measured data

At Matchpoints. $W(u) = 1.0$
 $u = 1.0$
 $s = 13.5 \text{ cm}$
 $t = 0.24 \text{ d}$
 $\dot{m} = 15 \text{ kg/s}$
 $\rho = 825 \text{ kg/m}^3$

$$T = \frac{\dot{m}}{4\pi\rho s} = \frac{15}{4\pi \times 825 \times 13.5 \times 10^{-2}} = 0.0107 \text{ m}^2/\text{s}$$

$$S = \frac{4Tt}{r^2} = \frac{4 \times 0.0107 \times 0.24 \times 24 \times 3600}{(241)^2} = 0.015$$

4.5.2 Type curve matching of unit response function values

Fig. 4.10 shows the curve-matching process where the matchpoint gives the following values:

$W(u) = 1.0$
 $u = 1.0$
 $s = 0.9 \text{ cm}$
 $t = 0.15$
 $\rho = 825 \text{ kg/m}^3$
 $\dot{m} = 1.0 \text{ kg/}$

Calculations of S and T give:

$$T = \frac{\dot{m}}{4\pi\rho s} = \frac{1.0}{4\pi \times 825 \times 0.9 \times 10^{-2}} = 0.0107 \text{ m}^2/\text{s}$$

$$S = \frac{4Tt}{r^2} = \frac{4 \times 0.0107 \times 0.15 \times 24 \times 3600}{(241)^2} = 0.0096$$

4.6 Multi-rate Well Test Results. Test C

Finally, the values of the unit response function obtained from the multi-rate test from 77-02-28 to 77-04-06 was analyzed by type-curve matching as shown in Fig. 4.11 . Table 4.3 gives the details.

4.6.1 Type curve matching of unit response function

<u>At Matchpoints.</u>	$W(u) = 1.0$
	$u = 1.0$
	$s = 1.3 \text{ cm}$
	$t = 0.41 \text{ d}$
	$\dot{m} = 1.0 \text{ kg/s}$
	$r = 241 \text{ m}$

$$T = \frac{\dot{m}}{4\pi\rho S} = \frac{1.0}{4\pi \times 825 \times 1.3 \times 10^{-2}} = 7.42 \times 10^{-3} \frac{\text{m}^2}{\text{s}} = 0.00742 \text{ m}^2/\text{s}$$

$$S = \frac{4Tt}{r^2} = \frac{4 \times 7.42 \times 10^{-3} \times 0.41 \times 24 \times 3600}{(241)^2} = 0.018$$

The value of T obtained is quite lower than those obtained before and there seems to be a change in reservoir properties towards the latter period of the test as seen from the trend of the curve.

4.6.2 Semi-log analysis of unit response function

A semi-log plot of the unit-response function for 30 days is given in Fig. 4.12. The trend is similar to the drawdown plot for the first 910 days shown in Fig. 4.2 where a straight line could be drawn in the early part of the curve before it gets steeper at the end when boundary effects become apparent.

Calculations of S and T are as follows:

$$\begin{aligned} m &= 1.32 \text{ cm/decade} \\ t_0 &= 0.6 \text{ d} \\ \dot{m} &= 1.0 \text{ kg/s} \\ r &= 241 \text{ m} \end{aligned}$$

$$T = \frac{\dot{m}}{4\pi m \rho} = \frac{1.0}{4\pi \times 1.32 \times 10^{-2} \times 825} = 7.3 \times 10^{-3} \text{ m}^2/\text{s}$$

$$S = \frac{2.246 T t}{r^2} = \frac{2.246 \times 7.3 \times 10^{-3} \times 0.6 \times 24 \times 3600}{(241)^2} = 0.014$$

4.7 Multi-rate Well Test Results. Test D

The unit response function computed from production data from 0 to 900 days has been computed for modelling purposes as presented in the next chapter. Fig. 4.13 is a semi-log plot for the first 14 days of drawdown. A straight line is shown through $t < 3.6$ days to get estimates of S and T, this gives:

$$m = 1.024 \text{ cm/decade}$$

$$t_0 = 0.08 \text{ d}$$

$$\dot{m} = 1.0 \text{ kg/sec}$$

$$r = 241 \text{ m}$$

$$T = \frac{\dot{m}}{4\pi m \rho} = \frac{1.0}{4\pi \times 1.024 \times 10^{-2} \times 825} = 9.42 \times 10^{-3} \text{ m}^2/\text{s}$$

and

$$S = \frac{2.246 T t}{r^2} = \frac{2.246 \times 9.42 \times 10^{-3} \times 0.08 \times 24 \times 3600}{(241)^2} = 2.5 \cdot 10^{-3}$$

4.8 A Summary of Interference Test Results

Table 4.4 gives a summary of calculated values of storativity (S) and transmissivity (T) for different tests and test analysis performed in Svartsengi geothermal fields.

The range of values of T lie within 0.0074 to 0.015 m²/S while those of S is within 0.0025 to 0.020. The average values of T and S are 0.011 m²/S and 0.015 respectively almost equal to those reported earlier (Kjaran et al. 1980). It is noted that multi-rate tests carried over longer periods (Test C and D) tend to give much lower average values of S and T.

5 RESERVOIR MODELS

5.1 Need of a Model

Essential to an optimum utilization of a geothermal resource is the notion of a model of the reservoir under exploitation. This may be a combination of conceptual and mathematical descriptions of relationships between field properties stated within a framework of known physical principles and consistent with results of field measurements.

With a model on hand, solutions to the following basic reservoir engineering problems may be sought: a) What plan of development gives an optimum return on investment? b) How many wells, what drilling pattern are to be drilled? c) What recovery techniques are suited to the requirements of the power plant? d) What will be the ultimate recovery of reserves given a variety of economic constraints and available choices of recovery techniques?

In an undeveloped field, volumetric estimates of reserves, the fraction that can be economically recovered and the technically suitable recovery technique can be made from geophysical and geological data (Atkinson et al. 1977).

On the other hand, when production and well test data are available, a hydrological model may be proposed together with known geological and geophysical constraints.

This chapter cites some earlier work done on reservoir modelling in Svartsengi and presents two other models. The first is based on the idea of a unit response function derived from actual production data. This model gives lower long term estimates of drawdown as compared to the earlier one under identical production requirements. The second model is built around the concept of an esker, a geological formation consisting of a long ridge of sand and gravel found in previously glaciated regions. It gives higher projections of drawdowns compared with the unit response function model but slightly lower projections compared with the earlier model.

These models will be referred to as the unit response function (URF) model and the esker model.

5.2 The Earlier Model

5.2.1 Model Description

Based on available information, Kjaran et al. (1980) proposed a rectangular configuration for the Svartsengi geothermal reservoir which is oriented approximately in a SW-NE direction. Fig. 5.1 gives the orientation, dimensions of the reservoir and the coordinates of some representative wells. No estimate of the length of the rectangular field is given. However, in the mathematical formulation of the model it is assumed that the production wells are very much nearer the NE than the SW boundary. Hence from a mathematical point of view the SW side of the rectangular field is far enough and its effect can be ignored in the development of the model.

Starting from this assumption, a boundary value equation for fluid flow in a porous medium was formulated. It can be shown that the solution is

$$h(x,y,t) = \frac{1}{a \cdot b \cdot S} \sum_{n=0}^{\infty} \sum_{m=0}^{\infty} C_{nm} \phi_{nm}(x,y) \phi_{nm}(\xi,\eta) \int_0^t Q(\tau) e^{-(t-\tau)/K_{nm}} d\tau \quad (1)$$

where:

- h : water drawdown in observation well, m
- a : length of rectangular trench, m
- b : width of rectangular trench, m
- S : storage coefficient
- Q : mass flowrate, m^3/s
- (x,y) : coordinates of observation well, m
- (ξ,η) : coordinates of blowing well, m
- T : transmissivity, m^2/s

and matrices C_{nm} , ϕ_{nm} and K_{nm} are defined in the following way:

$$C_{nm} = \begin{cases} 4 & n \neq 0, m \neq 0 \\ 2 & n \neq 0 \text{ \& } m = 0, \text{ or } n = 0 \text{ \& } m \neq 0 \\ 1 & n = 0 \text{ \& } m = 0 \end{cases}$$

$$K_{nm} = \frac{S}{\pi^2 T \left(\frac{m^2}{a^2} + \frac{n^2}{b^2} \right)}$$

$$\phi_{nm} = \cos \frac{m\pi x}{a} \cos \frac{n\pi y}{b}$$

This gives the dependence of drawdown $h(x,y,t)$ as a function of reservoir dimensions, distance between observation and flowing wells, flowrates and time after the start of production.

For discrete pumping rates Q_i shown in Fig. 5.2 the drawdown $h(x,y,t)$ may be expressed as:

$$h(x,y,t) = \frac{1}{abs} \sum_{n=0}^{\infty} \sum_{m=0}^{\infty} C_{nm} \phi_{nm}(x,y) \phi_{nm}(\xi,\eta) K_{nm} \sum_{L=1}^N Q_i e^{ti-tN/K_{nm}} (1-e^{-(ti-ti-1)/K_{nm}}) \quad (2)$$

This form of the solution was used for numerical calculations of drawdown $h(x,y,t)$ (Halldorsson 1981).

5.2.2 Model tests

To evaluate the merits and adequacy of the proposed model, Equation (2) was evaluated using drawdown and flowrate data for the first 1600 days of production. The results of these calculations were compared with measured drawdown as shown in Fig. 5.3 (Halldórsson 1981). There appears to be a good agreement between calculated and measured drawdowns during the first 1600 days of exploitation.

5.2.3 Drawdown projections

On the basis of the above results drawdown projections were made for the next 25 years. From Equation 2, a unit response function (Fig. 5.4) was computed on a yearly basis. When taken together with different combinations of flow rates from a given set of production schedules shown in Fig. 5.5 it gave the calculated drawdowns in Fig. 5.6.

Based on this model, it is anticipated that for an average district heating utilization of 4700 hours/year a drawdown of 200 m could be expected in 25 years. Whereas, for an additional 8 MW electricity at 6000 hours per year a drawdown of 250 m may occur.

The practical limit to the allowable drawdown in waterlevel at Svartsengi is 200 m which corresponds to a pressure drop of approximately 16 bars at a withdrawal rate of 60 kg/s. This drop in water level brings the well-head pressure to 7 bars, the minimum limit set for system operation (Fig.5.7).

Furthermore, as drawdown increases, flashing and calcite deposition gradually occurs deeper into the bore which makes cleaning more difficult.

5.3 The Unit Response Function Model

5.3.1 Model description

In the previous chapter, the definition of the unit response function as a superposition of linear solutions to a boundary value problem is presented. A numerical solution using the method of least squares was used to get calculated values of drawdown from a given set of short period flow tests. These values were used to estimate the magnitude of storativity and transmissivity which gave acceptable results.

The present model is based on the actual response of the reservoir without any reference to geological or geophysical constraints. This method may be called the 'black-box' approach. From drawdown data, the unit response function is computed for the first 900 days of production and extrapolated to give it a predictive characteristic.

The same set of drawdown data used in the earlier model was corrected for earthquake effects and utilized to construct and test the model. Fig. 5.3 shows this effect as a spike at about 200 days which adds to the actual drawdown. The unit response function based on field data for the first 900 days is shown in Fig. 5.8. The curve is smooth everywhere and shows a prominent change in slope at about 600 days. This change is also present in Fig. 5.9 and 5.10 where the unit response is plotted on log-log and semi-log scales. As pointed earlier, boundary effects are also apparent after 10-15 days. The change in the unit response function at 600 days may be due to: a) downward encroachment of colder water from the upper basaltic layer in the outflow zone, b) horizontal encroachment of colder liquids into the main body of the aquifer, and c) diminished natural outflow from the reservoir due to reservoir pressure drop after about 2 years of production. These possible causes should be verified by careful measurements and observations in the output characteristics of the wells. For instance the shallow wells may be observed to see any change in degree of saturation of the fluids coming from them.

5.3.2 Model tests

Using the calculated unit response function in Fig. 5.8 together with the corresponding flowrate (Fig. 4.14) a set of calculated drawdown values was obtained and compared with the measured values as shown in Fig. 5.11. It is seen that the model adequately follows reasonably short period trends over the specified time interval.

Fig. 5.12 shows the unit response function plus a logarithmic curve fitted towards the end from 650 to 1600 days.

This unit response function model was likewise tested to see if drawdowns calculated from it agree with observed values as shown in Fig. 5.13. Unfortunately there were no drawdown measurements made between 973 to 1239 days and those taken from 1230 to 1613 days are suspect as they were measured from SG-4 where cold water intrusion due to a broken casing at 70 m was earlier reported. A rigid validation of the model is quite difficult to make and only gross qualitative features of the model such as trend agreement would justify its use.

5.3.3 Drawdown projections

To forecast drawdowns for the next 25 years, the projected unit response function shown in Fig. 5.14 was run together with production schedules listed in Fig. 5.5 . It is seen in Fig. 5.15 that for an average district heating requirement of 4700 hours/year a drawdown of 105 m could be expected in 25 years (curve D). For an additional 8 MW electricity of 6000 hours/year a drawdown of 120 m approximately is anticipated (curve B). Curves A and C are drawdowns calculated for different load factors in Fig. 5.5.

5.4 The Esker Model

5.4.1 Model description

Geological and geophysical data suggest the Svartsengi geothermal reservoir possessing geometric properties similar to those of an esker and may be treated mathematically as such.

Gustafsson cites a typical esker to have a width of 300-600 m but the length of its individual groundwater basins can extend to several kilometers (Gustafsson et al. 1976). Figure 5.16A is a top view of an esker showing its dimensions and the flow due to pumping from a well. If the observation and pumping wells are sufficiently far apart, the latter may be replaced by a drain across the esker as shown in Fig. 5.16B.

5.4.2 Mathematical formulation of the esker model

Gustafsson shows that if the following assumptions hold:

- the aquifer is homogeneous, isotropic and of infinite extent;
- the wells penetrate the aquifer completely;
- the aquifer is boarded by an impermeable strata above and below;
- the flow in the esker is laminar and unidimensional;
- the release of water from storage is instantaneous and proportional to decline in head, and
- the wells discharge at a constant rate,

then the following differential equation in the non-steady state may be written for the auxiliary system of Fig. 5-16B.

$$\frac{\partial^2 h}{\partial x^2} = \frac{S}{T} \frac{\partial h}{\partial t} \quad (3)$$

$$h(x, 0) = h(\infty, t) = h_0 \quad (4)$$

$$\frac{\partial h}{\partial x}(0, t) = - \frac{Q}{2TB} \quad (5)$$

The Svartsengi geothermal field is believed to possess the configuration of a rectangular trench as shown in Fig. 5.16C where one of the shorter sides is absent as suggested by drawdown data. Using the method of images (Kjaran pers. comm.), the preceding formulation is equivalent to a two-well system sketched in Fig. 5.16D.

This mathematical transformation has been shown to yield the following solution

$$s = \frac{1}{2\sqrt{\pi}} \cdot \frac{Qx}{TB} \cdot D(w_1) + \frac{1}{2\sqrt{\pi}} \cdot \frac{Q(2l-x)}{TB} \cdot D(w_2) \quad (6)$$

$$w_1 = \frac{x^2 S}{4Tt} \quad , \quad w_2 = \frac{(2l-x)^2 S}{4Tt} \quad (7)$$

$$D(w) = \frac{e^{-w}}{\sqrt{w}} - \sqrt{\pi} + 2 \int_0^{\sqrt{w}} e^{-z^2} dz \quad (8)$$

which gives the drawdown s in terms of pumping rate Q , reservoir parameters S and T , width of the trench B , distance between observation and flowing well x , distance of flowing well from the closed vertical boundary and time after the start of production t .

5.4.3 Test of the model

Assuming that the preceding assumptions hold and the reservoir to have the configuration shown in Fig. 5.16C, drawdowns were calculated using the relevant reservoir dimensions and properties and flowrate data covering the first 1600 days of production. The computed drawdowns were compared with the observed values as shown in Fig. 5.17.

It can be seen that a reasonably good fit is obtained during the first 200 days after which the model gives a consistently lower estimate of drawdown up to about 970 days. It is difficult to evaluate the model against measured drawdowns after 1200 days due to reliability of the measurements obtained during this period. That the model gives consistent overestimates after 970 days may be noted also in the same figure.

5.4.4. Projected drawdowns

Fig. 5.18 shows the projected drawdowns using the esker model for the next 25 years for a unit pumping rate. Using the schedule of future requirements in heating and electricity, drawdowns were calculated as shown in Fig. 5.19 . For an average yearly district heating utilization of 4700 hours, a water level drop of 200 m is anticipated (curve D). For an additional production of 8 MW electricity at 6000 hours per year, a drawdown of 255 M may be expected (curve B).

These projections are in close agreement with those obtained by Kjaran et al. (1980), but give higher estimates than those obtained from the unit response function model.

A summary of projected drawdowns for the next 25 years based on the three models is given in Table 5.1.

6 RESULTS AND RECOMMENDATION

The main object of this study is to determine the response to exploitation of the Svartsengi geothermal field during the first 1600 days of production and to devise models to describe its behaviour and forecast drawdown in water level based on future energy requirements.

A survey of geological, geophysical, geochemical and production information were made to see how these factors contribute to a total picture describing the reservoir, its properties and behaviour. Two models were proposed to describe the extent of drawdowns that may be expected based on projected load requirements.

6.1 Summary of Results

The main characteristics of the reservoir are as follows:

- a. It lies at the intersection of the main earthquake zone and the Grindavik fissure swarms which account for its high permeability of 1 darcy.
- b. Fresh water recharge is believed to come from the Reykjanes mountain range, possibly Lake Kleifarvatn about 18-20 km NE of the field. It flows along the main earthquake zone and picks up sea water inflow on its way.
- c. Resistivity surveys show that the iso-resistivity area extends along a SW-NE direction and increases with depth to over 7 km², 600 m below sea level.
- d. Reservoir permeability is attributed to scoriaceous contacts between lava flows and interbeds of hyaloclastites and lava intrusions. Joint fractures and faults also contribute to the total permeability of the reservoir.
- e. The size of the field is comparatively small, the most porous area in the order of 2 km² only. Its configuration may be taken as rectangular with impermeable walls except at the SW side.
- f. Well measurements indicate a reservoir temperature of 235-240°C,

a static reservoir pressure of 83.5 kg/cm^2 referred at 1000 m depth, fluid density of 854 kg/m^3 and enthalpy of 1000-1074 kj/kg.

- g. Temperature-pressure saturation relation reveal single phase liquid conditions below 1000 m. Saturation increases upwards and boiling occurs in the upwelling zone, controlled by a major fault though the shallow wells SG-2 and SG-3.
- h. Reservoir fluids have high salinity, approximately 2/3 that of sea water which requires the use of heat exchangers for effective utilization.
- i. Well interference testing has been demonstrated to:
 - a) give good results for calculating reservoir parameters S and T,
 - b) monitor water level drawdown, and
 - c) detect the presence of impermeable boundaries.
- j. The unit response function computed from measurements of flowrate and drawdown could be used to calculate field parameters S and T together with standard well test analysis.
- k. The average values of storativity (S) and transmissivity (T) are 0.011 and $0.015 \text{ m}^2/\text{s}$ respectively. There is a wide variation in the measured values of these parameters.
- l. There appears to be a prominent change in the reservoir properties around 600 days as revealed by the plot of the unit response function. This may be due to horizontal and/or vertical encroachments of colder liquids into the reservoir or diminished natural outflow due to pressure drop after about 2 years of production.
- m. The first of the two proposed reservoir models based on the unit response function calculated from field data gives optimistic results of drawdown in the next 25 years. Based on a yearly average utilization time of 4700 hours a drawdown of 105 m may be expected. An additional 8MW at 6000 hours/yr utilization will give a higher drawdown of 120 m.
- n. The second model based on the geohydrological concept of an esker on the other hand, gives pessimistic estimates. nearly equal to those previously published. For the same load requirements a drawdown of 200 m may be expected due to district heating needs alone

and 255 m for an additional 8 MW of electricity production.

6.2 Recommendations

- a. The use of the unit response function to calculate reservoir parameters S and T has been shown to give acceptable results. However, the values of the function seem to be sensitive to the choice of distribution of points. Here, only a linear distribution has been used. It is recommended that a logarithmic or square root distribution be tried as it could reduce numerical oscillations and give better definition of the unit response function (H. Halldorsson pers. comm.).
- b. In this work the unit response function was calculated using one observation well and one flowing well. This approximation is quite valid since the variations in the drawdown measurements in two or more adjacent wells while other wells are flowing is quite small (G. K. Halldorsson pers. comm.). It may be worthwhile to repeat the calculations using different pairs of observation and pumping wells to get a more accurate model.
- c. Only the simple 'non-leaky' form of the esker model has been tried. In view of the pronounced change in the computed unit response function of the reservoir at around 600 days a 'leaky' esker model may be considered.
- d. Both the esker and the unit response models have to be re-validated in the light of recent and reliable data.

ACKNOWLEDGEMENT

It is said that there are 3 enumerable things in Iceland, the hillocks at Vatnsdalur, the lakes at Arnarvatnsheidi and the small islands at Breidafjordur Bay. If I may add to these, it would be the number of kind persons who in various ways provided the support to the conception and completion of this work. My admiration and gratitude to them are hereby expressed. At the risk of contradiction, I have to re-cite just but a few:

Prof. Jonas Eliasson for extending warm re-assurances during the training period and critically evaluating my work; Dr. Snorri Páll Kjarian for patiently imparting his sound knowledge of reservoir engineering while I stumbled through its rudiments; Mr. Halldór Halldórsson for diligently writing most of the computer programs; Mr. Ásmundur Jakobsson for clearing my way through the software and hardware jungles; Mr. Gísli Karel Halldórsson for providing the field data and technical information; Mr. Sverrir Thorhallsson for pointing out valuable suggestions and corrections to the draft; Dr. Hjalti Franzson for lending able administrative support to the training program, ensuring at all times that the fellows were provided with adequate technical and cultural experiences; Ms. Sólveig Jónsdóttir for cheerfully making all those 'arrangements' which made our stay in Iceland pleasant and fruitful; Ms. Sigríður Valdemarsdóttir and Ms. Aðalheiður Jóhannesdóttir for skillfully typing the draft; Ms. Gyða Guðmundsdóttir and the drawing staff for accurate executions and reproductions of the illustrations and Dr. Ingvar B. Friðleifsson for reviewing the final draft.

I also wish to thank the management of PNOC-EDC Geothermal Division for the leave of absence and the United Nations University for the fellowship which made this work possible.

NOMENCLATURE

η	diffusivity (m^2)
p_r	spatial unit response function ($Pa\ m^{-3}\ s$)
\vec{r}	position vector (m)
t	time (s)
A_2	area of S_2 (m^2)
K	permeability (m^2)
μ	viscosity ($kg\ m^{-1}\ s^{-1}$)
$U(t)$	unit-step function (-)
$F(t)$	unit response function ($Pa\ m^{-3}\ s$)
\dot{m}	mass flow-rate (kg/s)
s	drawdown (cm)
r	distance between observation and flowing well (m)
ρ	reservoir fluid density (kg/m^3)
m	slope of semi-log straight line (cm/decade)
t_0	t intercept of the semi-log plot (day)
S	storativity (-)
T	transmissivity (m^2/s)
$W(u)$	well function (-)
u	Boltzman variable (-)

REFERENCES

- Arnórsson, S. (1978). Major Element Chemistry of the Geothermal Sea-Water at Reykjanes and Svartsengi, Iceland. Mineralogical Magazine, Vol. 42, pp. 209-220.
- Arnórsson, S. and Sigurdsson, S. (1974). The Utility of Waters from High-Temperature Areas in Iceland for Space Heating as Determined by Their Chemical Composition. Geothermics, Vol. 5, No. 4, pp. 127-141.
- Atkinson, P.G., Miller, F.G., and Celati, R. (1977). Analysis of reservoir pressure and decline curves in Serrazzano Zone-Larderello Geothermal Field. Proceedings of the Larderello Workshop on Geothermal Resource Assessment and Reservoir Engineering, Larderello, Italy, pp. 208-232.
- Atkinson, P.G. (1980). Geothermal Reservoir Initial State Baca Location No. 1 - New Mexico Redondo Creek Field. Geothermal Resources Council, Transactions, Vol. 4, pp. 435-438.
- Barelli, A. and Palama, A. (1980). On Some Computational Methods of Unit Response Functions from Varying-Rate Data. Geothermics, Vol. 9, pp. 261-269.
- Björnsson, S., Arnórsson, S. and Tómasson, J. (1970), Exploration of the Reykjanes Thermal Brine Area. Geothermics, Special Issue 2, pp. 1640-1650.
- Bodvarsson, G. (1961). Physical characteristics of natural heat resources in Iceland. Jökull, 11, pp. 29-38.
- Chang, C.R.Y. and Ramey, H.J., Jr. (1979). Well interference Test in the Chingsui Geothermal Field. Proc., Fifth Workshop on Geothermal Engineering, Stanford University, pp. 71-75.
- Elíasson, J. (1980) Reservoir Engineering. Introductory Lectures No. 2. Notes presented at the 1981 UNU Geothermal Training Programme, NEA, Reykjavik, Iceland, 32 p.
- Elíasson, J., et al. (1977). Svartsengi. Straumfræðileg rannsókn á jarðhita-svæði. Orkustofnun Report No. OS ROD 7718 OSSFS 7702.

- Georgsson, L.S. (1979). Svartsengi - Vidnámsmælingar á utanverðum Reykjaneskaga. Orkustofnun Report No. OS 79042/JHD 20, 100 p.
- Georgsson, L.S. (1981). Resistivity Survey on the Plate Boundaries in the Western Reykjanes Peninsula, Iceland. Geothermal Resources Council, Transactions, Vol. 5.
- Gudmundsson, J.S., Thórhallsson, S., Ragnars, K. (1981). Geothermal Electric Power in Iceland: Development in Perspective (Draft). A paper presented at the Electric Power Research Institute, 5th Annual Geothermal Conference and Workshop, June 23-25 19 , San Diego, California.
- Gustafsson, G., Viall, A.B. Falun (1976). A Method of Calculating the Hydraulic Properties of Leaky Esker Aquifer Systems. Nordic Hydrological Conference, Proceedings.
- Halldórsson, G.K. (1981). Vatnsbordslækkun og vinnsla í Svartsengi. Orkustofnun Report No. GKH-81/02,
- Huisman, L. (1972). Ground Water Recovery. Macmillan, London
- Ingimarsson et al. (1978). Evaluation of groundwater level and maximum yield of wells in a fresh water lens in Svartsengi, South-West Iceland. Proceedings of Nordic Hydrological Conference in Helsinki 1978. Papers of workshops, pp. I-61-I-71.
- Ingimarsson, J. and Eliásson, J. (1980). Svartsengi. Grunnvatnsrannsóknir vegna ferskvatnsöflunar fyrir varmaorkuver. Orkustofnun Report No. OS800311 ROD 12.
- Jónsson, J. (1978) Jarðfræðikort af Reykjaneskaga. Orkustofnun Report No. OS JHD 7831.
- Kjaran, S.P. (1981). Reservoir Engineering Lecture Notes. Notes presented at the 1981 UNU Geothermal Training Programme, NEA, Reykjavik, Iceland
- Kjaran, S.P., Eliásson, J., Halldórsson, G.K. (1980). Svartsengi. Athugun á vinnslu jarðhita. Orkustofnun Report No. OS 80021/ROD 10-JHD 17.

Kjaran, S.P., Halldórsson, G.K., Thorhallsson, S. and Eliasson, J. (1979).
Reservoir Engineering Aspects of Svartsengi Geothermal Area. Geothermal
Resources Council Transactions, Vol. 3, pp. 337-339.

Sudurnes Regional Heating. A brochure prepared by the Sudurnes Regional Heating
Corporation.

Thórhallson, S. (1979). Combined Generation of Heat and Electricity from a
Geothermal Brine at Svartsengi in S.W. Iceland. Geothermal Resources Council,
Transactions, Vol. 3, pp. 733-736.

Tómasson, J. and Kristmannsdóttir, H. (1972). High Temperature
Alteration Minerals and Thermal Brines, Reykjanes, Iceland. Contrib.
Mineral. Petrol., Vol. 36, pp. 123-137.

Property	Well 3 (402 m deep)	Well 4 (1670 m deep)
Date	19.04.78	18.04.78
Temperature (°C)	235	240
SiO ₂	447	437
Na ⁺	6959	6837
K ⁺	1140	1060
Ca ⁺⁺	1021	1036
Mg ⁺⁺	0.74	1.08
SO ₄ ⁻⁻	36.1	31.6
Cl ⁻	12440	12593
F ⁻	0.10	0.11
H ₂ S (total)	4.03	6.82
CO ₂ (total)	183	360
TDS	22244	21400

TABLE 2 .1 Chemical composition of formation water at Svartsengi.
 Concentration in mg/kg.
 From Thórhallsson 1979.

Time (day)	Measured drawdown (cm)	Pumping rate (kg/s)	Values of U.R. function (cm)	Calculated drawdown from U.R. function (cm)
0.0000	0.0000	52.40000	-0.1512332E-01	-0.7924619
1.0000	24.0000	40.80000	0.4300462	22.70985
2.0000	37.0000	40.40000	0.8009522	36.98741
3.0000	47.0000	39.20000	1.095113	47.93901
4.0000	56.0000	46.00000	1.319974	55.52404
5.0000	66.0000	56.00000	1.479208	63.57269
6.0000	70.0000	58.00000	1.581649	73.59415
7.0000	84.0000	48.00000	1.631799	81.45112
8.0000	85.0000	53.00000	1.646325	82.08366
9.0000	75.0000	40.40000	1.638195	83.97317
10.0000	86.0000	59.00000	1.623006	78.96674
11.0000	82.0000	46.00000	1.623170	83.84680
12.0000	82.0000	4.500000	1.631217	82.02476

Flowing well: SG-4

Observation well: SG-5

Type of test: Multiple-rate interference test

Date: 76.10.18

TABLE 4.1 Calculated and measured drawdown (1st 10 days)
used for calculating reservoir parameters S and T

Time (day)	Measured drawdown (cm)	Calculated drawdown (cm)	Values of U.R. function (cm)
0.0000	0.0000	0.0000000	0.5305445
1.0000	14.4000	7.958167	1.345729
2.0000	20.0000	20.18594	1.918700
3.0000	29.6000	28.78051	2.181042
4.0000	31.6000	32.71563	2.338003
5.0000	35.2000	35.07005	2.610670
6.0000	40.0000	39.16005	2.883121
7.0000	42.8000	43.24682	3.095338
8.0000	46.4000	46.43008	3.300701
9.0000	48.9000	49.51052	3.549649
10.0000	54.5000	53.24474	3.790991
11.0000	56.0000	56.86486	3.986052
12.0000	60.0000	59.79078	4.147725

Flowing well: SG-4

Observation well: SG-5

Type of test: Single-rate interference test

Date: 77.02.28

Change in flowrate: 15 kg/s

TABLE 4.2 Calculated and measured drawdown used for calculating reservoir parameters S and T

Time (day)	Measured drawdown (cm)	Pumping rate (kg/s)	Values of U.R. function (cm)	Calculated drawdown from U.R. function (cm)
0.0000	0.0000	15.0000	0.1930397	1.210810
1.0000	14.4000	"	0.8831648	12.83972
2.0000	20.0000	"	1.437943	21.88556
3.0000	29.6000	"	1.831338	27.85605
4.0000	31.6000	"	2.103799	31.96261
5.0000	35.2000	"	2.407933	36.10497
6.0000	40.0000	"	2.719836	39.77383
7.0000	42.8000	"	2.924411	42.83707
8.0000	46.4000	"	2.984093	45.63404
9.0000	48.9000	"	3.151146	49.46358
10.0000	54.5000	"	3.562890	53.80637
11.0000	56.0000	"	3.938377	57.09194
12.0000	60.0000	"	4.059822	59.64985
13.0000	63.2000	0	4.124898	61.37248
14.0000	52.0000	"	4.340965	52.96257
15.0000	48.0000	"	4.620440	47.39097
16.0000	45.3200	"	4.842736	45.17842
17.0000	43.6000	"	5.024961	43.80838
18.0000	40.9000	"	5.190765	41.22053
19.0000	40.1000	"	5.347847	39.30303
20.0000	37.4000	"	5.442382	38.49832
21.0000	37.7000	28.0000	5.425007	39.42719
22.0000	57.9000	"	5.424424	57.51901
23.0000	70.2100	"	5.540999	70.26611
24.0000	77.5000	"	5.696845	78.28554
25.0000	85.7000	"	5.823545	85.00056
26.0000	94.0000	"	5.948990	94.39784
27.0000	103.2000	"	6.102590	102.5429
28.0000	106.8300	"	6.281339	107.5006
29.0000	110.8000	0	6.539161	110.5742

Flowing well: SG-4

Observation well: SG-5

Type of test: Multiple-rate interference test

Date: 77-02-28 to 77-04-06

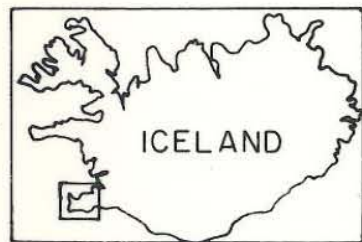
TABLE 4.3 Calculated and measured drawdown used for calculating reservoir parameters S and T





Type of test and analysis		$T(\frac{m^2}{s})$	S
Test A Multi-rate	a) Curve matching of computed URF values	0.0135	0.019
	b) Semi-log analysis of measured drawdown	.0142	.020
	c) Semi-log analysis of computed URF values	0.015	0.017
	Average:	(.014)	(.019)
Test B Single flow-rate	a) Curve matching of measured drawdown	0.0107	0.015
	b) Curve matching with computed USF values	.0107	.0107
	Average:	(.011)	(.013)
Test C Multi-rate	a) Type curve matching of computed URF values	.00742	.018
	b) Semi-log analysis of URF values	.0073	.014
	Average:	(.0074)	(.016)
Test D Multi-rate	a) Type curve matching of computed URF values	.00942	0.0025
	Average:	(.00942)	(0.0025)
Range:		0.0074 - 0.015	0.00250- 0.020
Average		0.011	0.015

TABLE 4.4 Summary of well interference test results

Model	District Heating +8 MW Electricity (8000 hrs/yr) (m)	District Heating +8 MW Electricity (6000 hrs/yr) (m)	District Heating +8 MW Electricity (4000 hrs/yr) (m)	District Heating +8 MW Electricity (4700 hrs/yr) (m)
Previous Model	350	260	220	205
Unit Response Function Model	162	120	105	105
Esker Model	340	255	213	200

Table 5.1 Summary of drawdown projections for various energy requirements for the next 25 years.



-  Geothermal area
-  Quake epicenter
-  Surface fissure swarm
-  Infiltration area

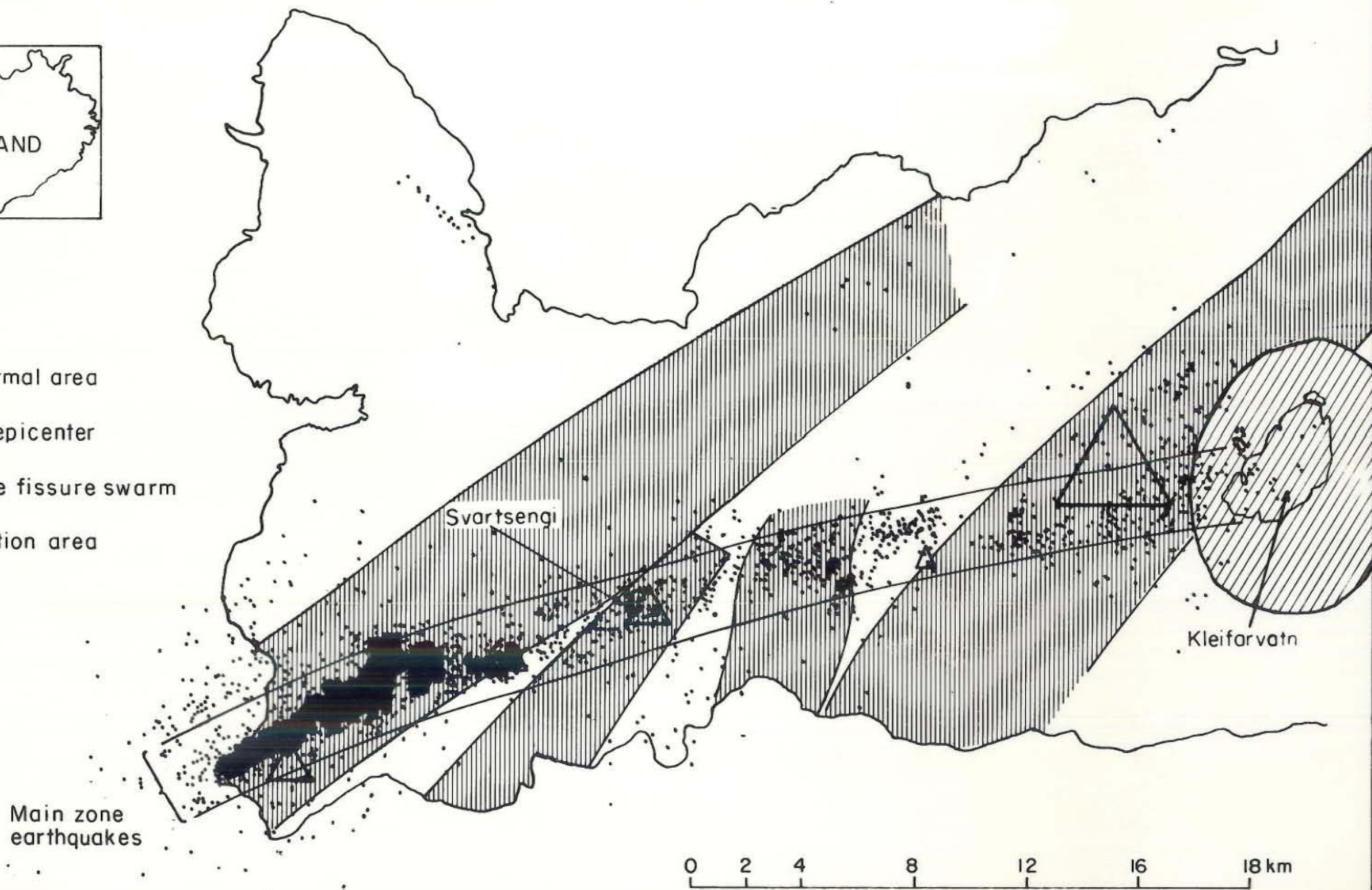
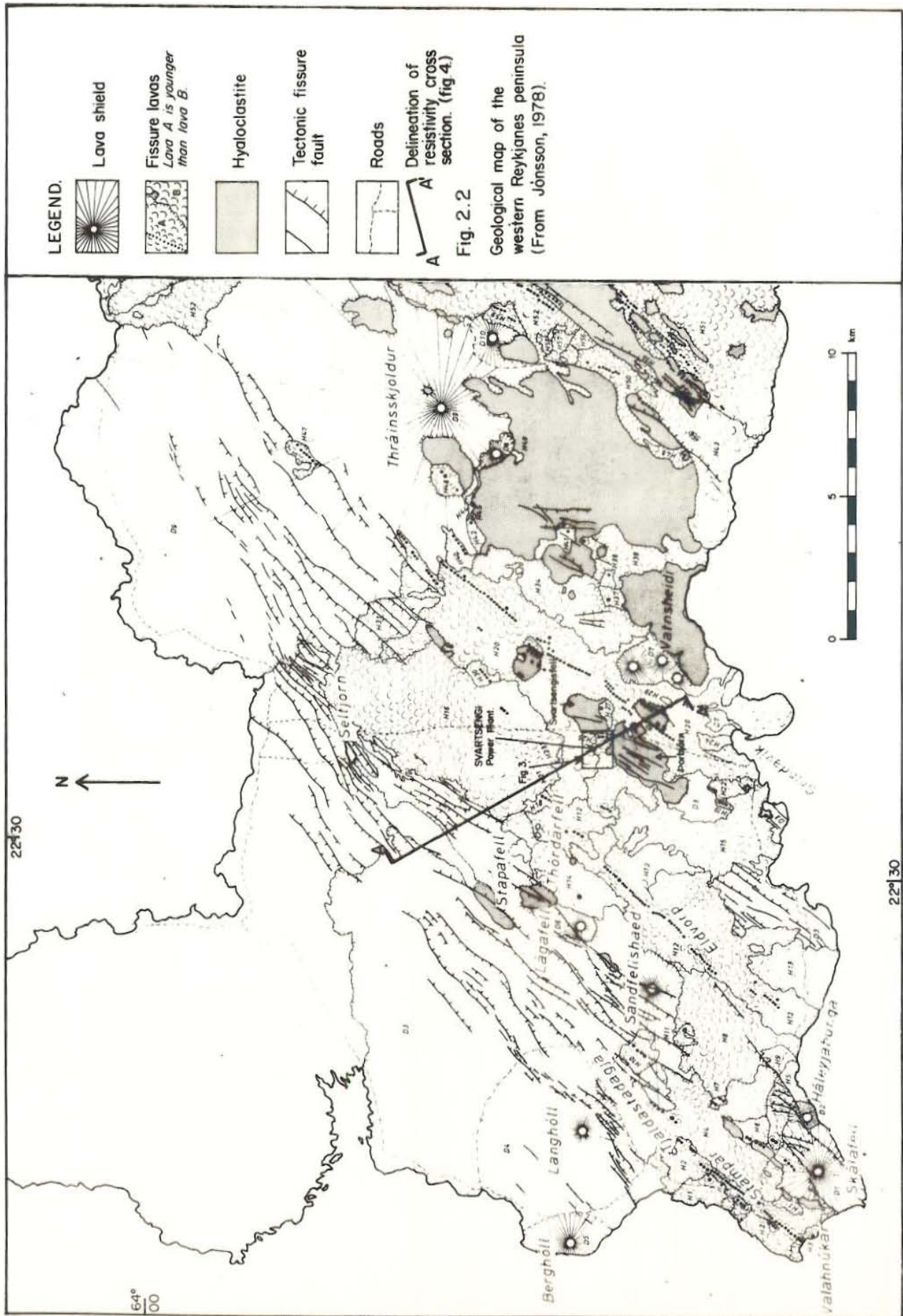


Fig.2.1 Quake epicenters and fissure swarms in the Reykjanes peninsula

'79 06 20 GK/ab Svartse.Reykjon. F-18517 A
(From Kjaran, et al., 1980)



JHD-HSP-900-JRR
81.10.1200-EBF

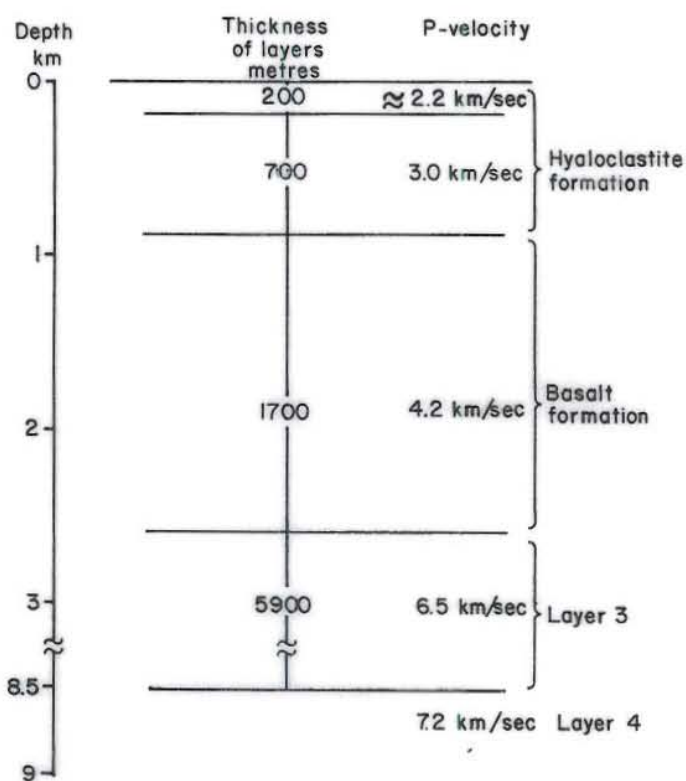
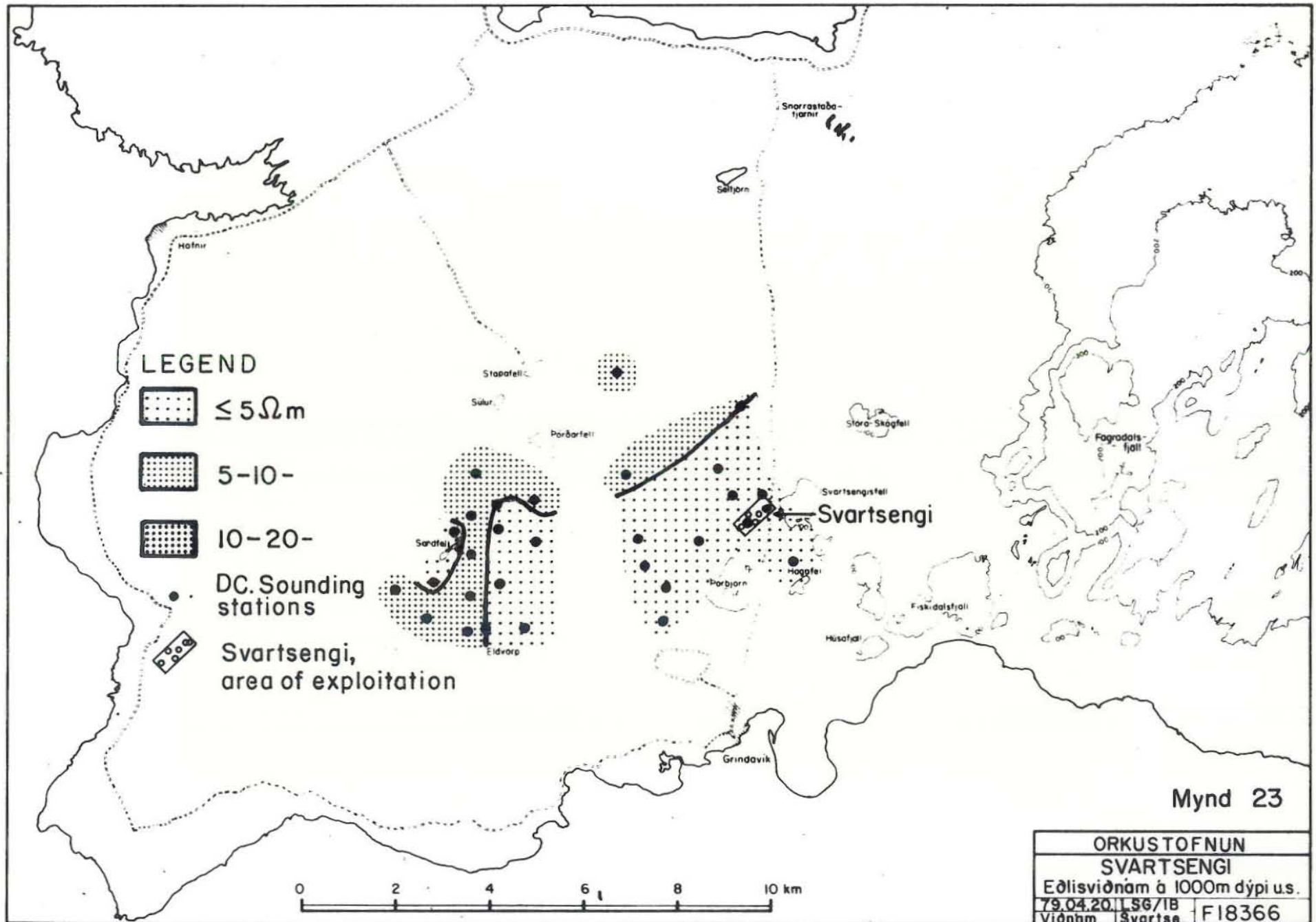


FIG.2.3 Seismic structure section of the Reykjanes thermal brine area. (From Björnsson, et. al, 1970)



Mynd 23

Fig.2.4 Iso-resistivity map at 1000m depth

(From Georgsson, 1979)

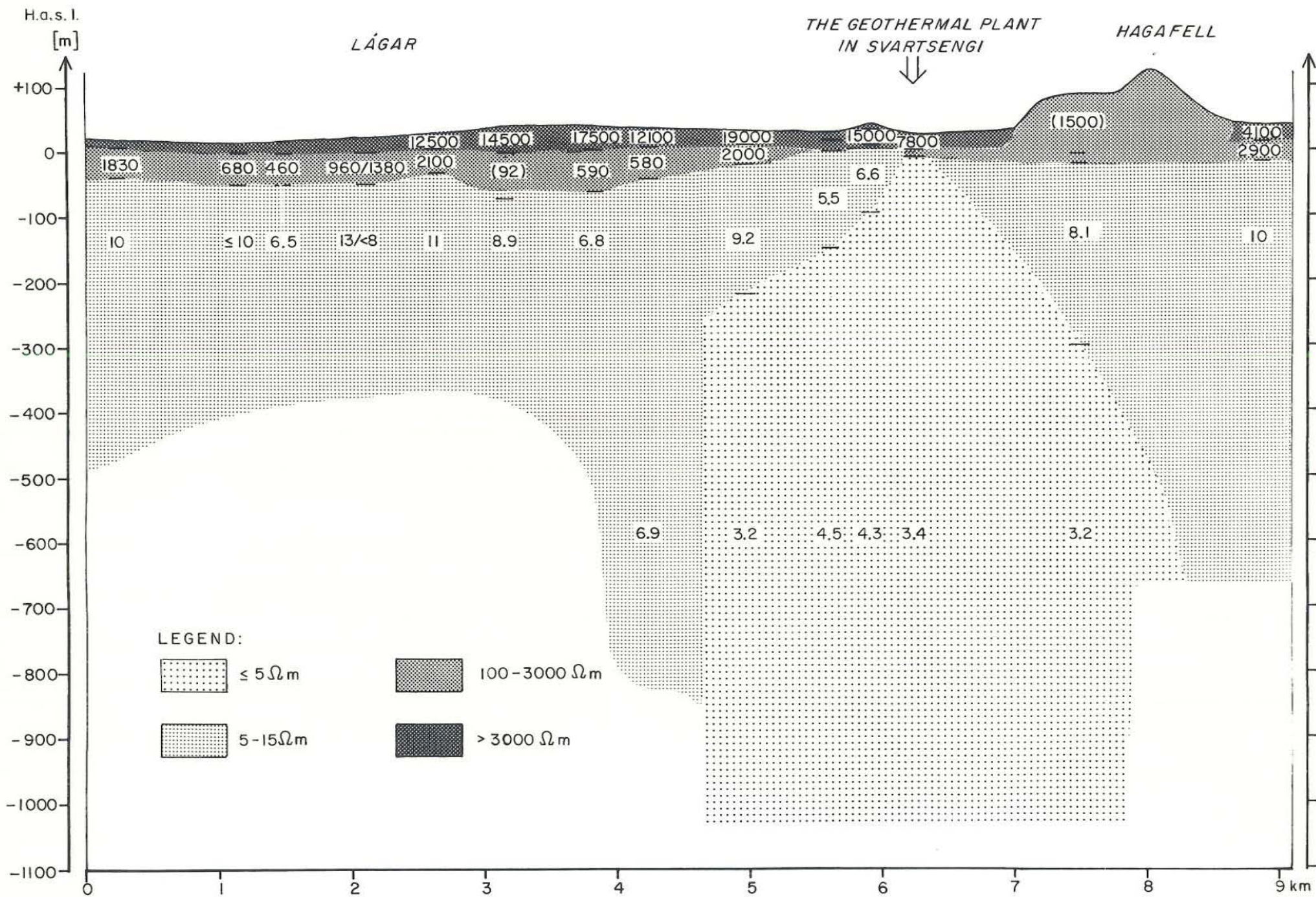


Fig. 2.5. A resistivity cross section along line A-A' in fig. 2.2.

70.09.20 LSG/IS Svartsengi Viðnám. F-18367
 (From Georgsson 1981).

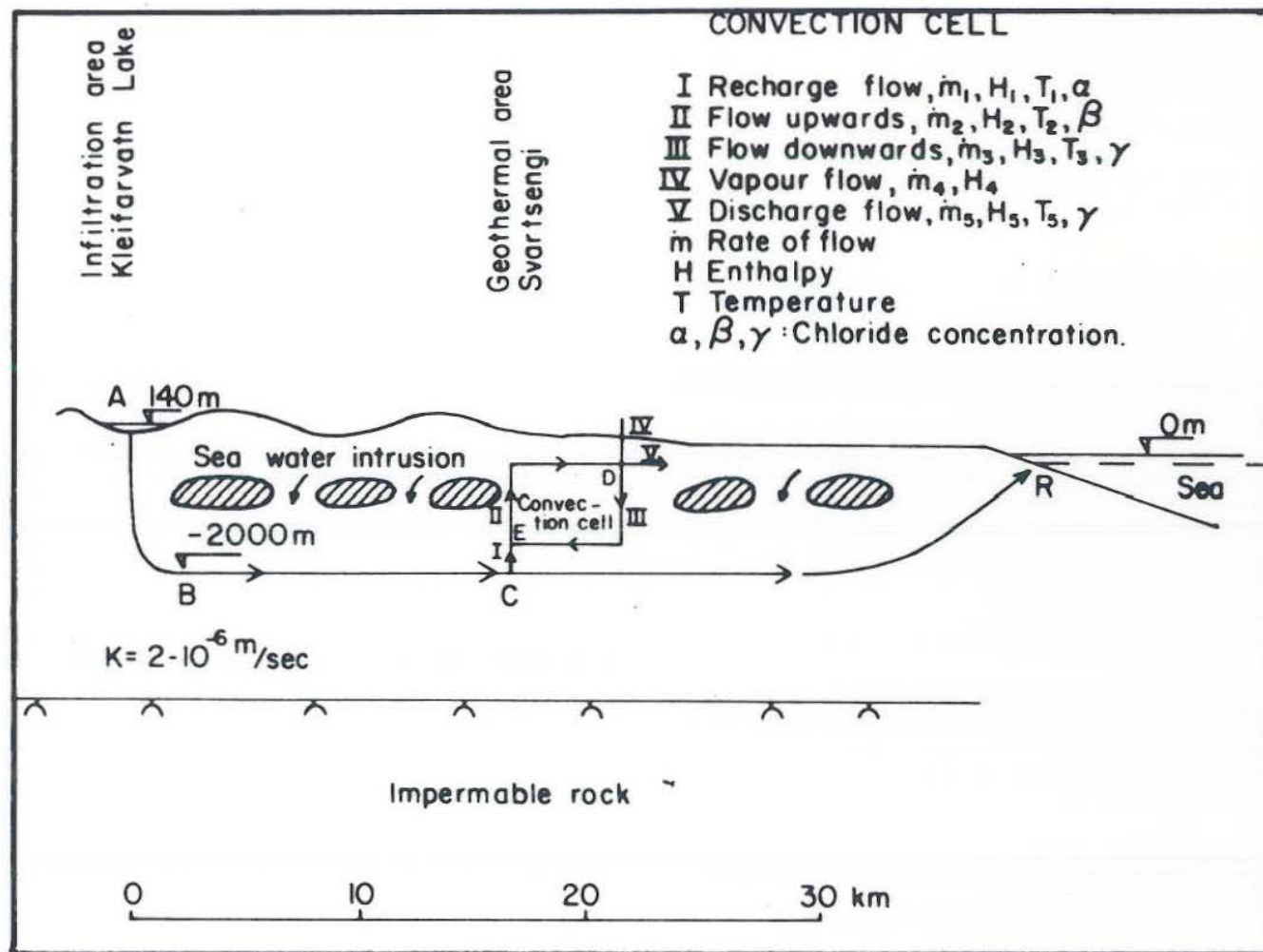


Fig. 2.6 Section along the Reykjanes peninsula showing possible infiltration streamline and the hybrid convection model. (From Kjaran, et.al., 1979).

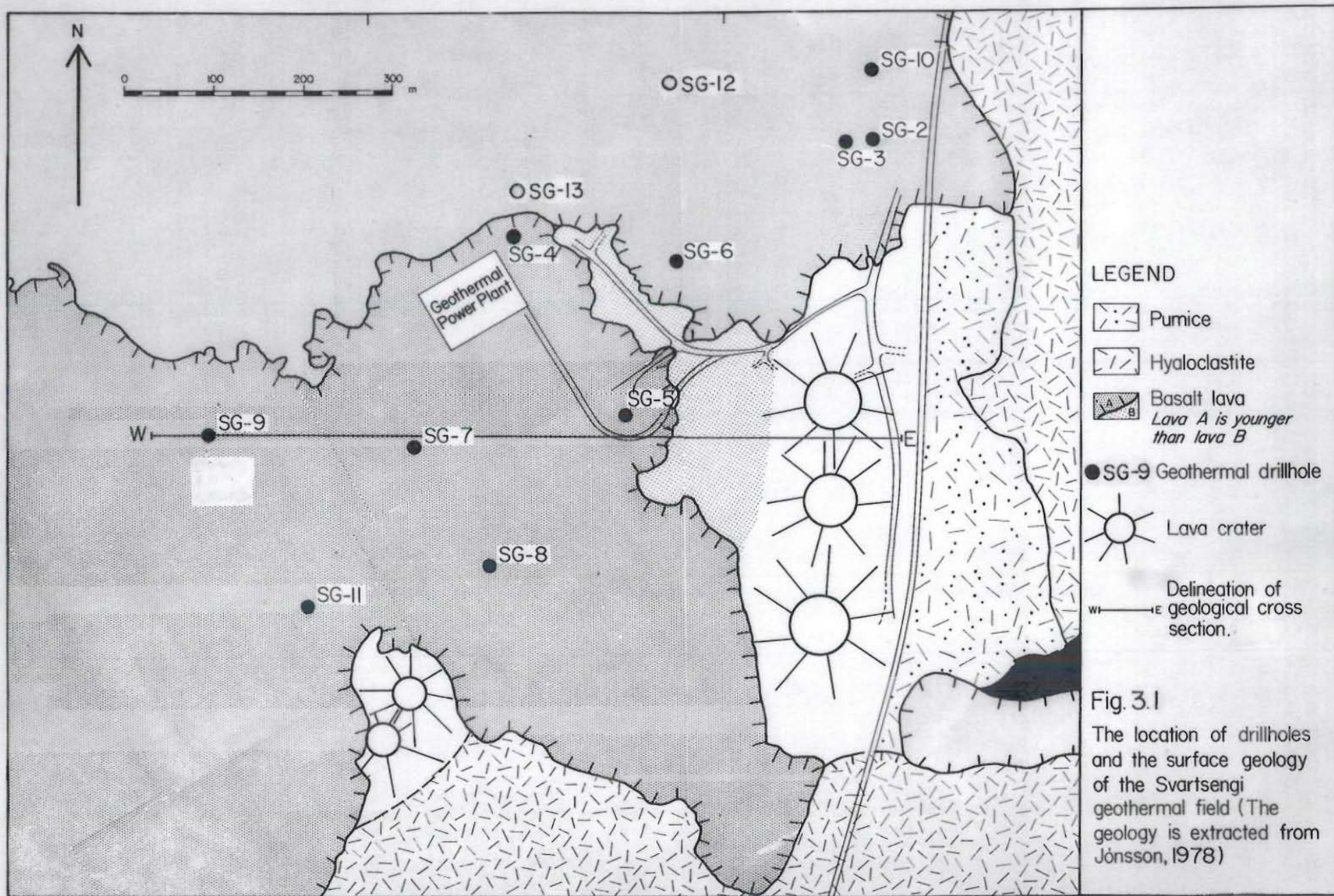
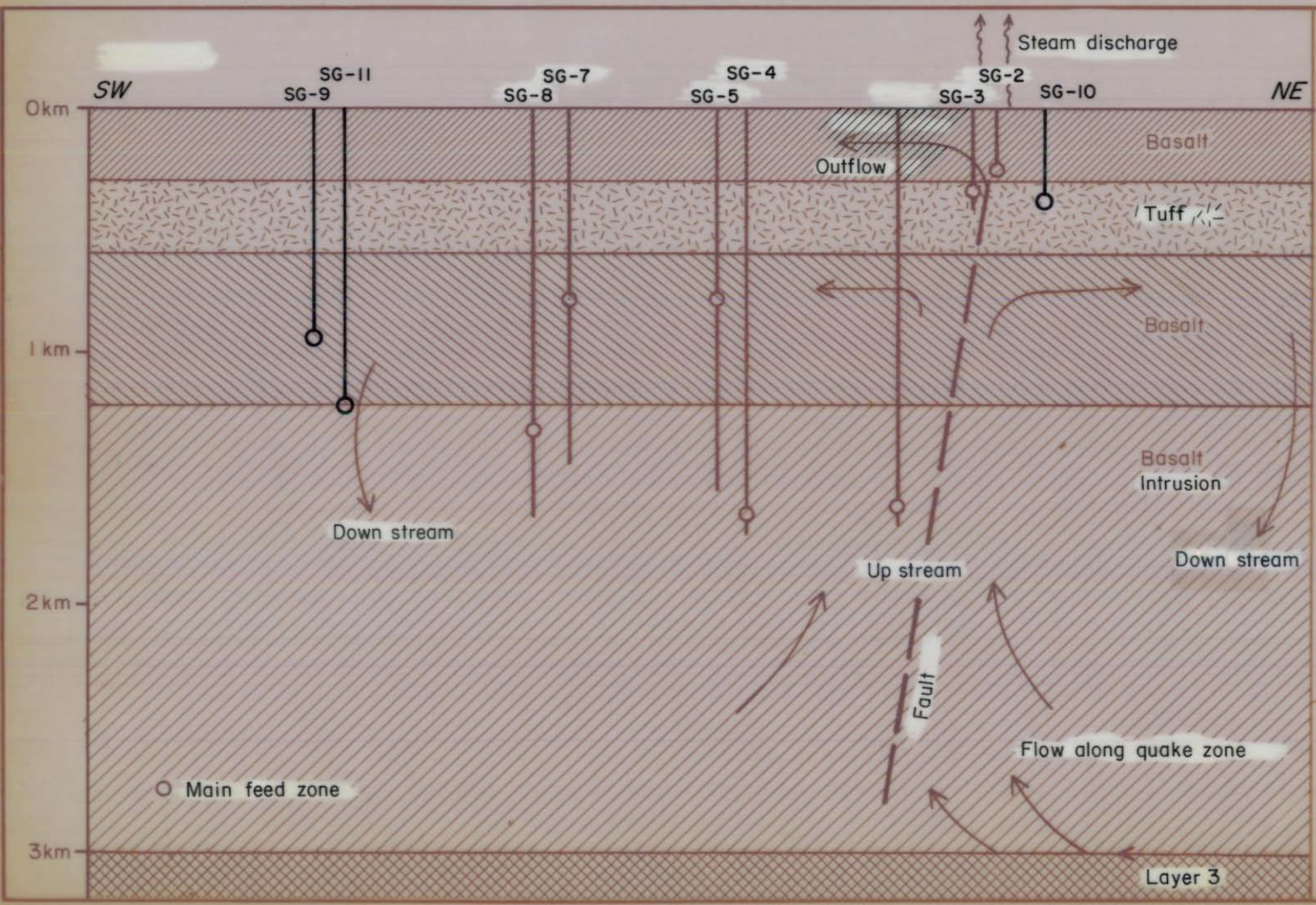


Fig. 3.2 SW - NE VERTICAL SECTION SHOWING SOME GEOLOGICAL FEATURES



27. maí 1980
SPK/Gyða
Svartsenji
F-19673

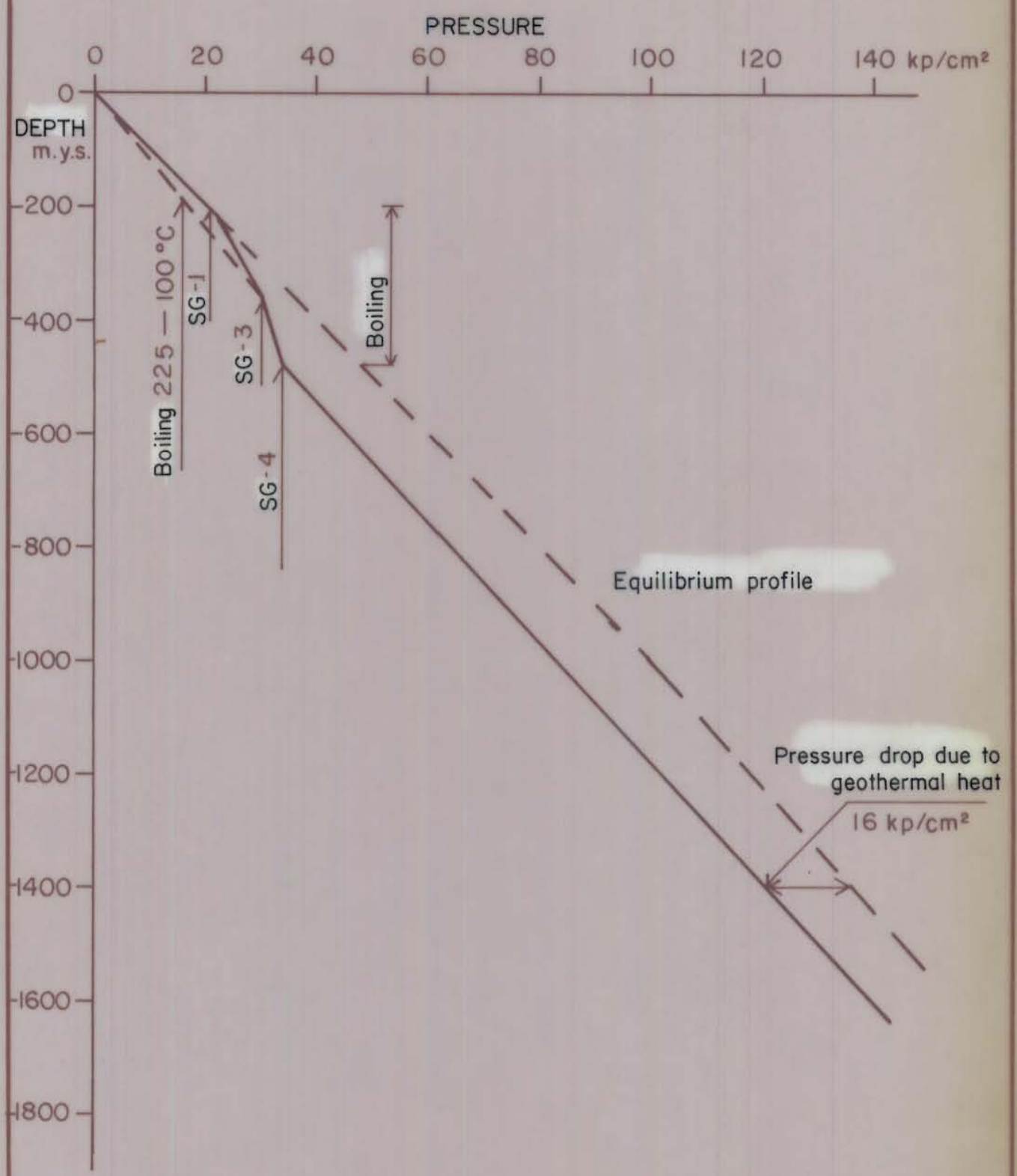
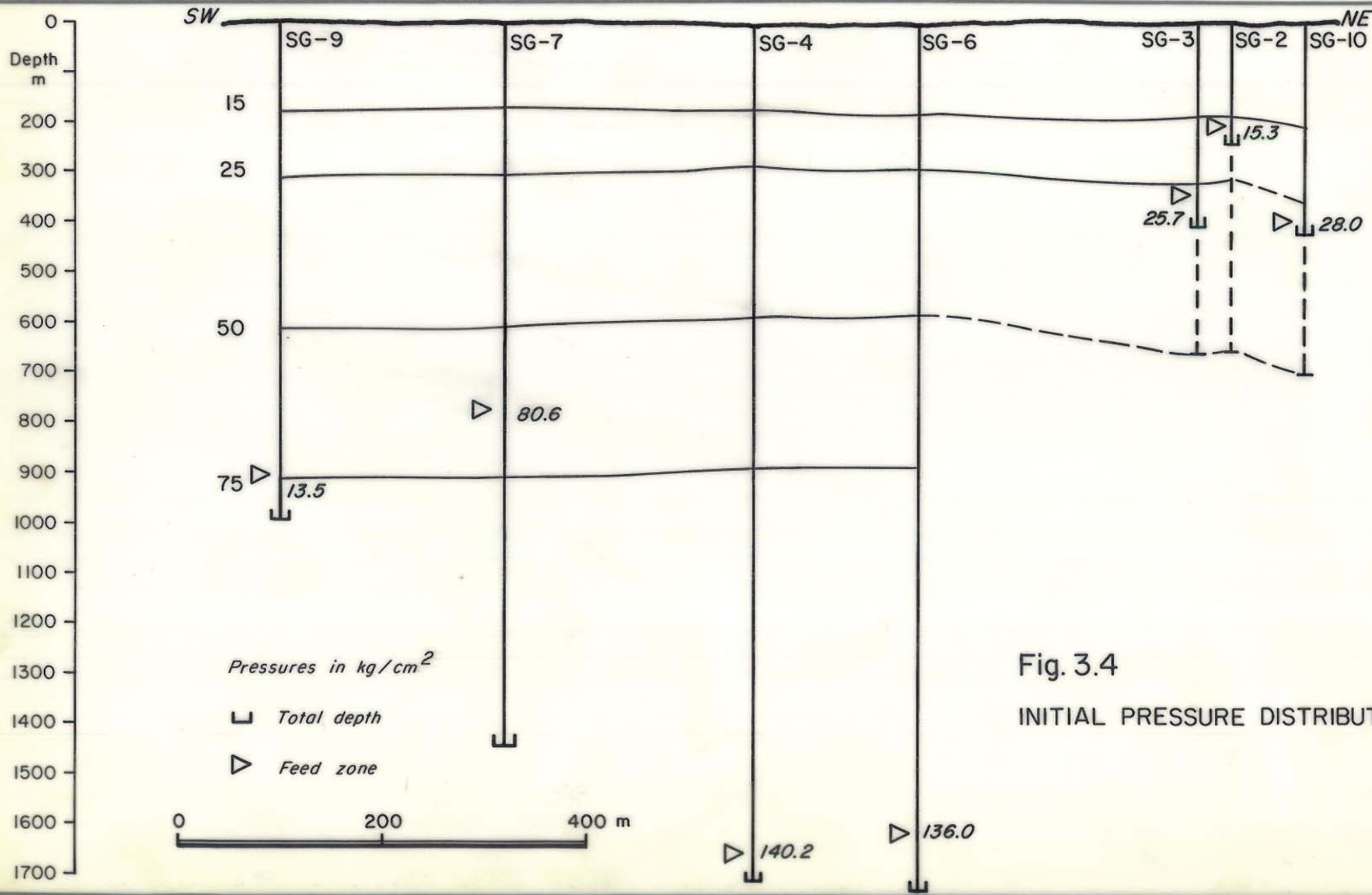


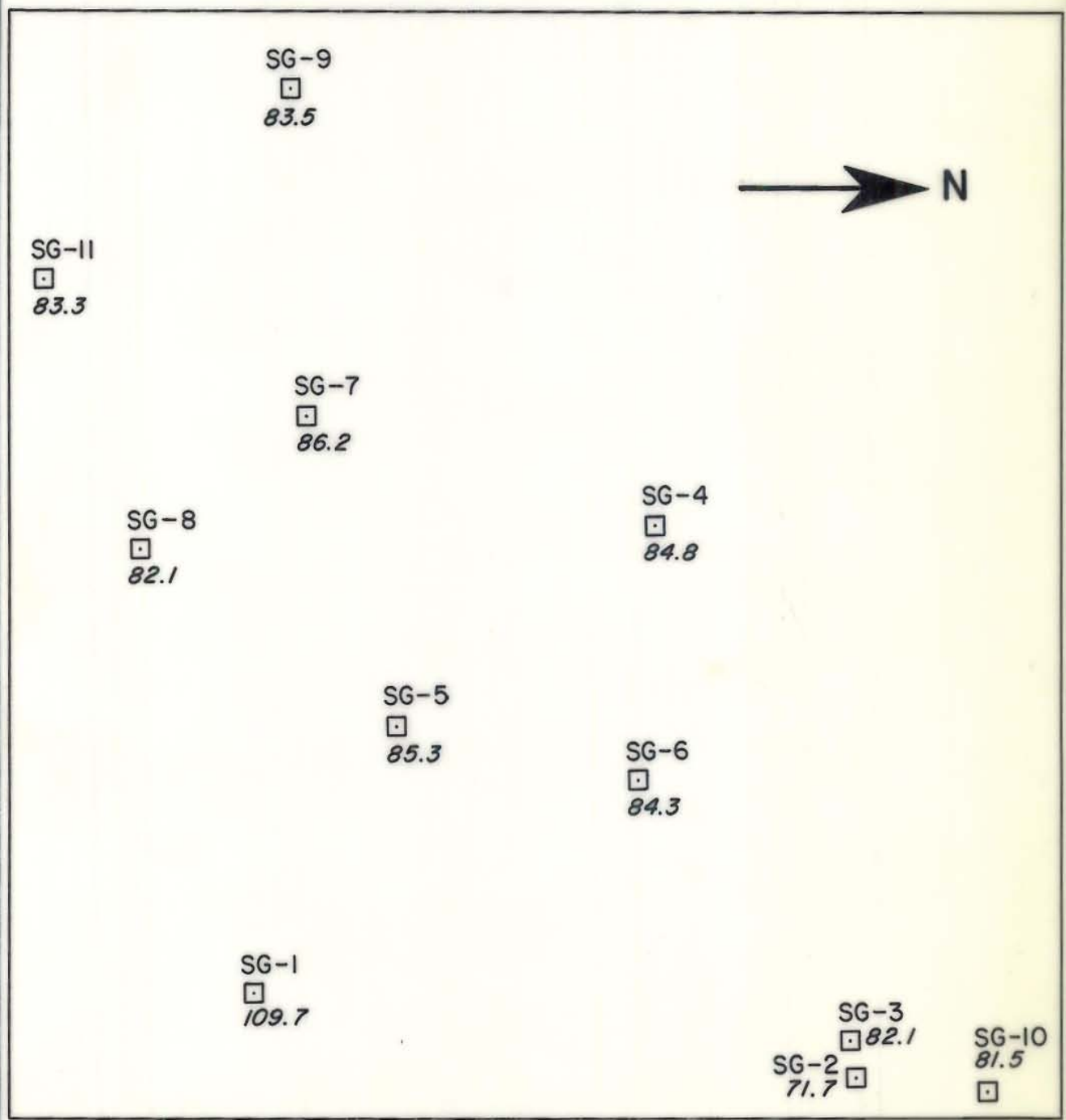
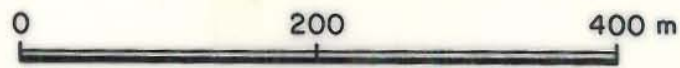
Fig. 3.3 EARLY PRESSURE LOGS SHOWING DIFFERENCES IN FLUID DENSITIES



JHD-HSP-2300-JRR
81.09.1172-GSJ

Fig. 3.4
INITIAL PRESSURE DISTRIBUTION

JHD-HSP-2300-JRR
81.09.1170-GSJ



Pressures in kg / cm²

Fig. 3.5 HORIZONTAL PRESSURE DISTRIBUTION AT 1000 M REFERENCE DEPTH

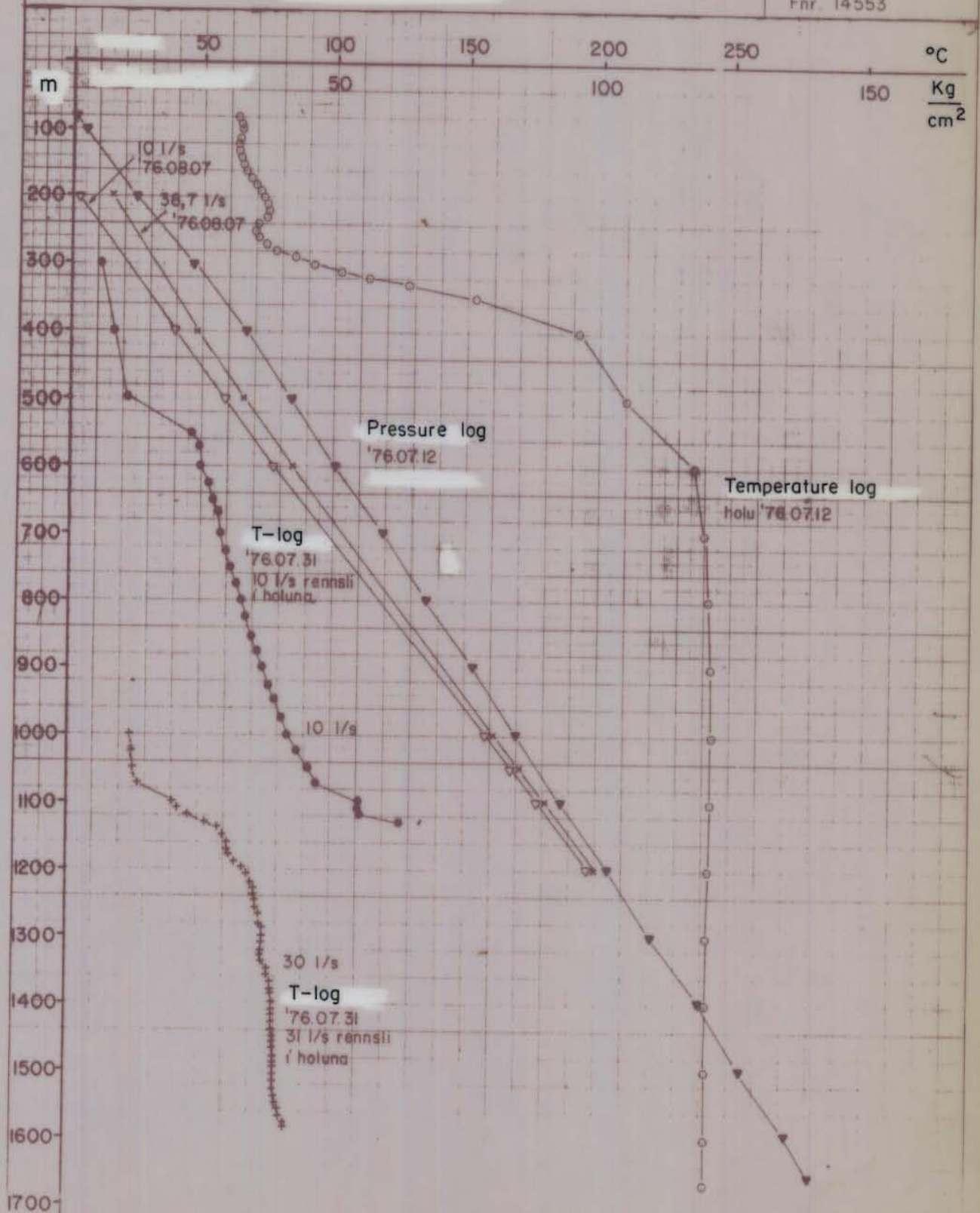


Fig. 3.6 SG-4 COMPLETION AND EARLY P-T LOGS

ORKUSTOFNUN
Jarðhitadeild

24.6.'75 SA/SL

Tnr.27 Tnr.1195

J-Svartse. J-Hitam

Fnr.11812

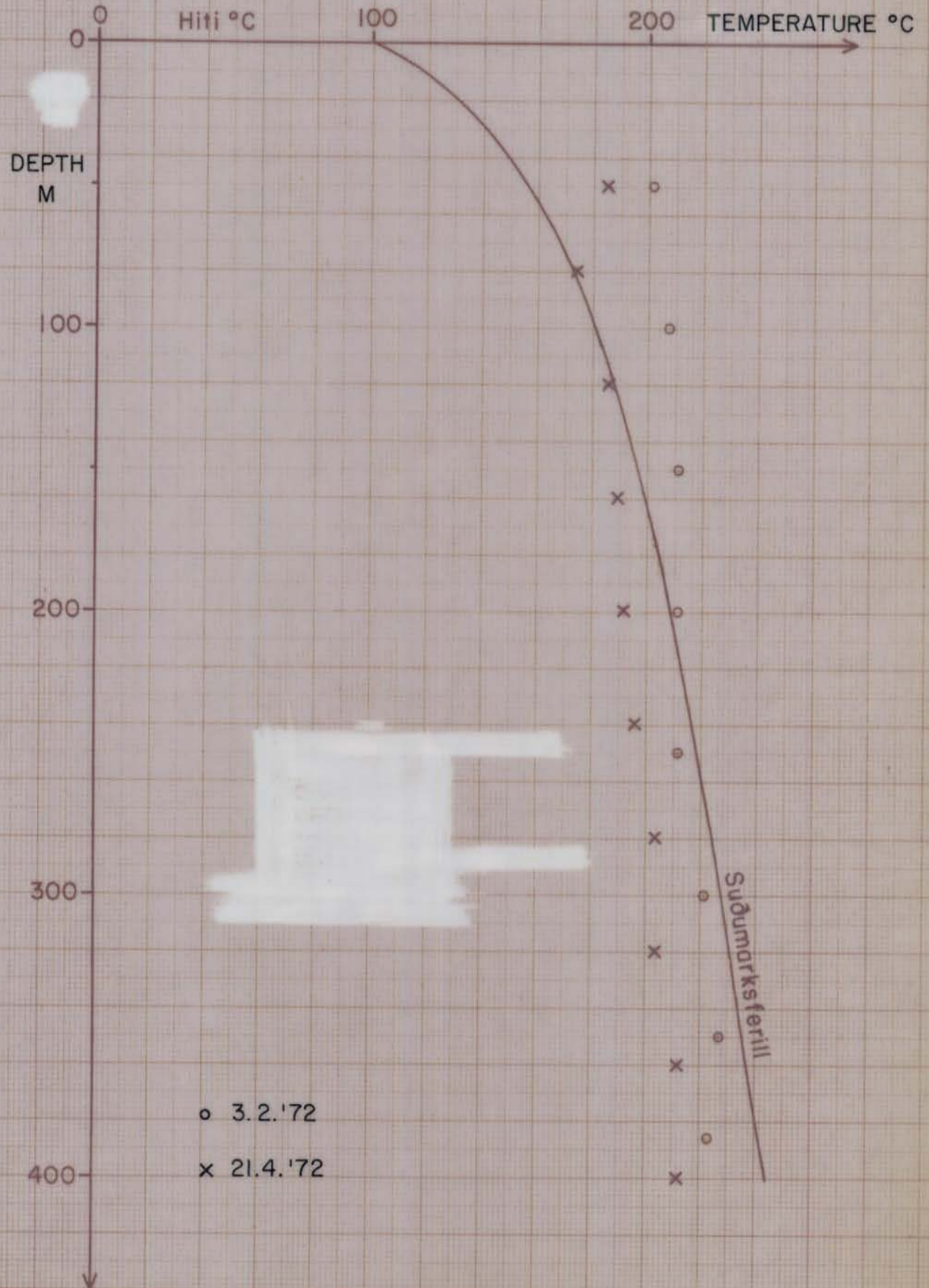
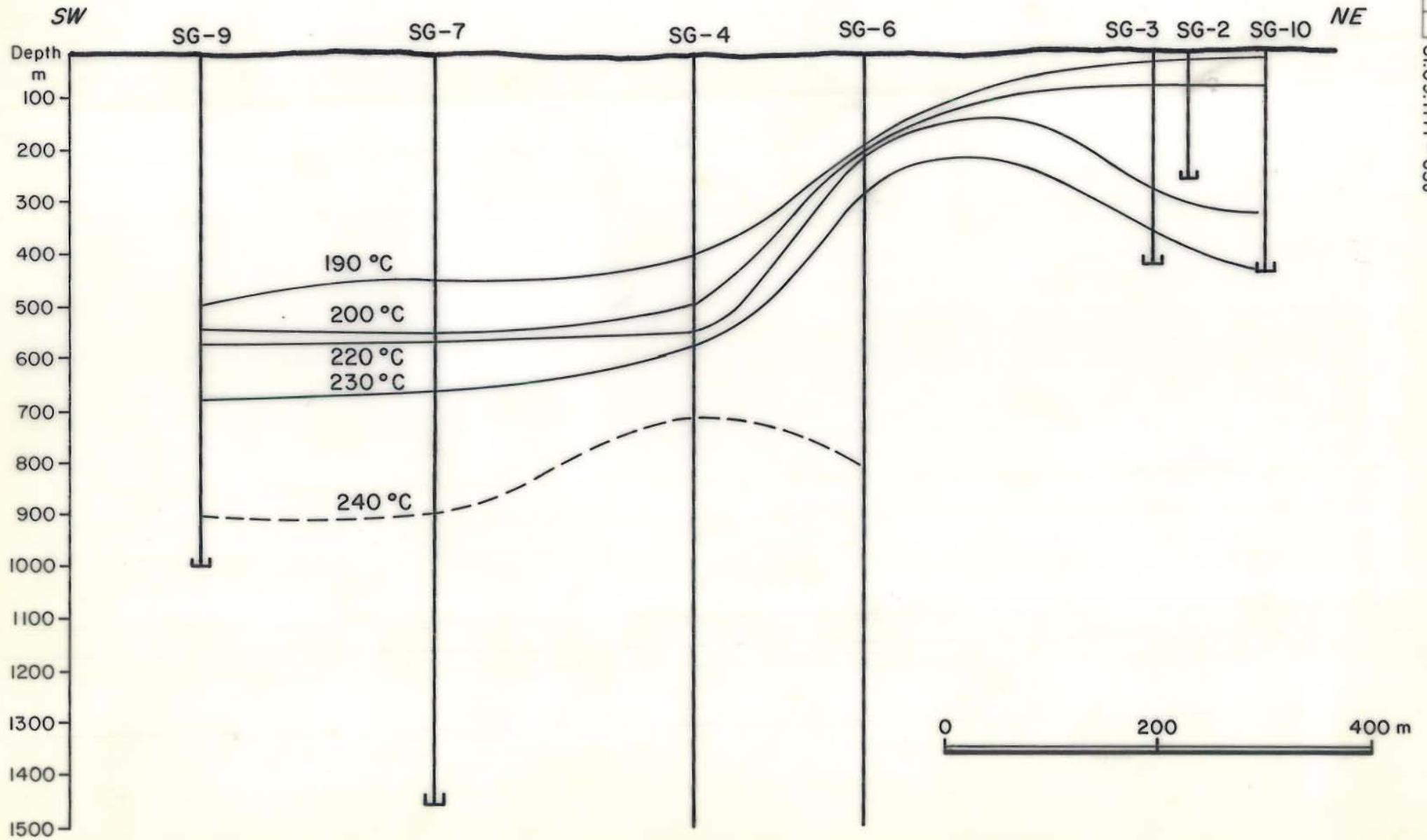


Fig.3.7 SG-3 TEMPERATURE LOG

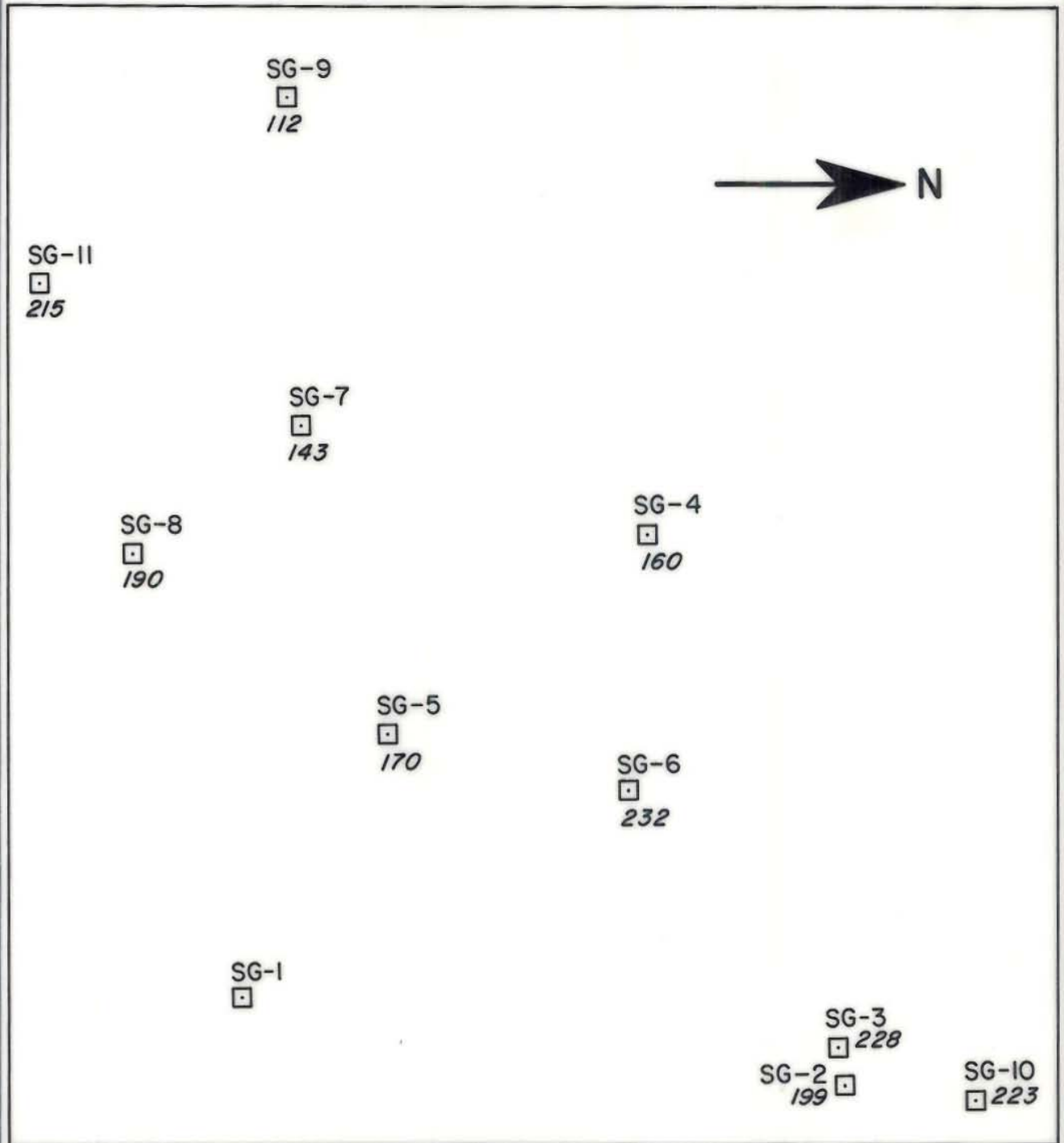
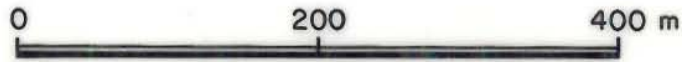


JHD-HSP-2300-JRR
81.09.1171-GSJ

Fig. 3.8 A VERTICAL SECTION SHOWING TEMPERATURE DISTRIBUTION



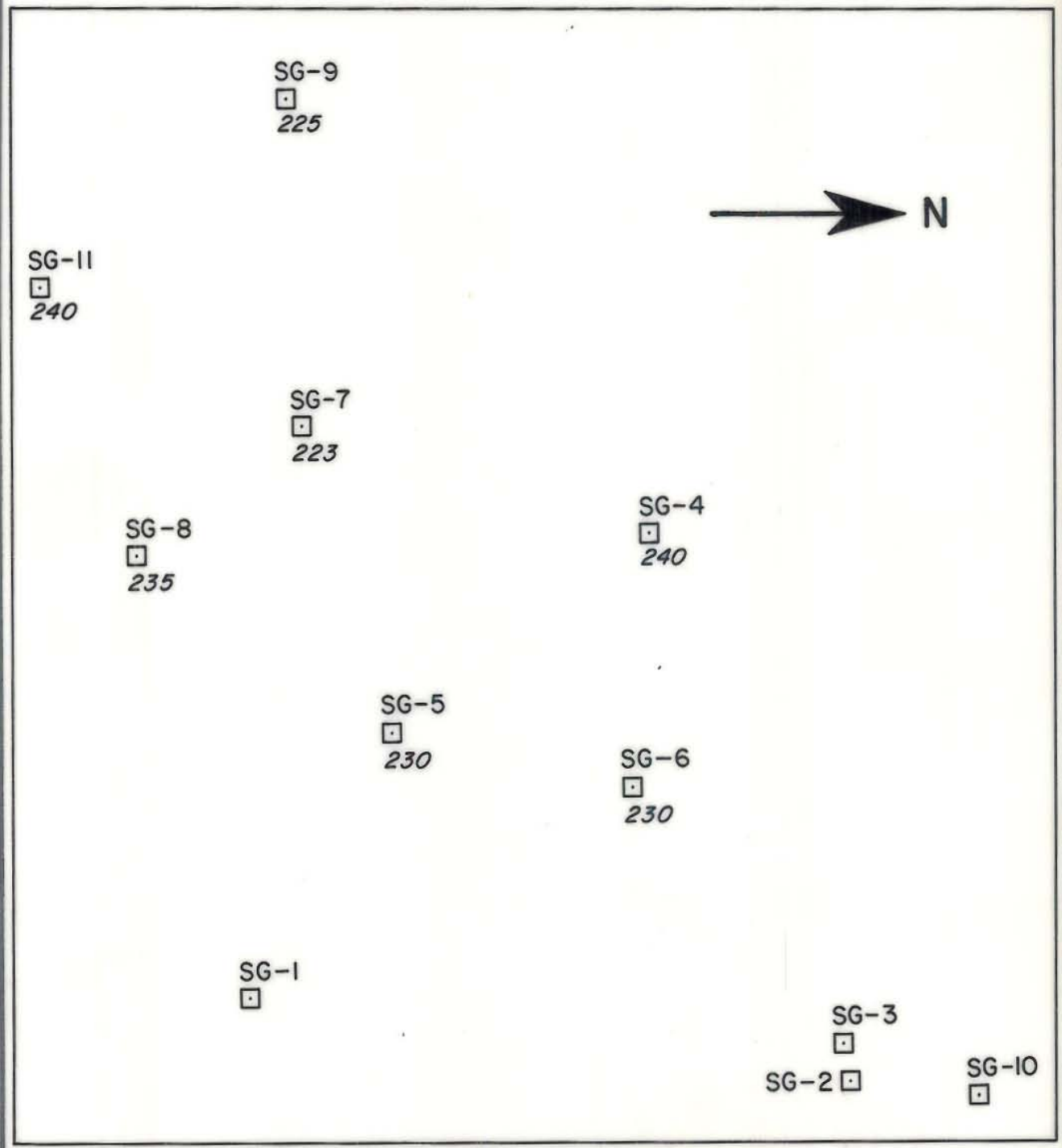
JHD-HSP-2300-JRR
81.09.1173-GSJ



Temperatures in °C

Fig. 3.9 TEMPERATURE PROFILE AT 350 M DEPTH

JHD-HSP-2300-JRR
81.09.1174-GSJ



* Temperatures in °C

Fig. 3.10 TEMPERATURE DISTRIBUTION AT 700 M DEPTH

JHD-HSP-2300-JRR
81.09.1175-GSJ

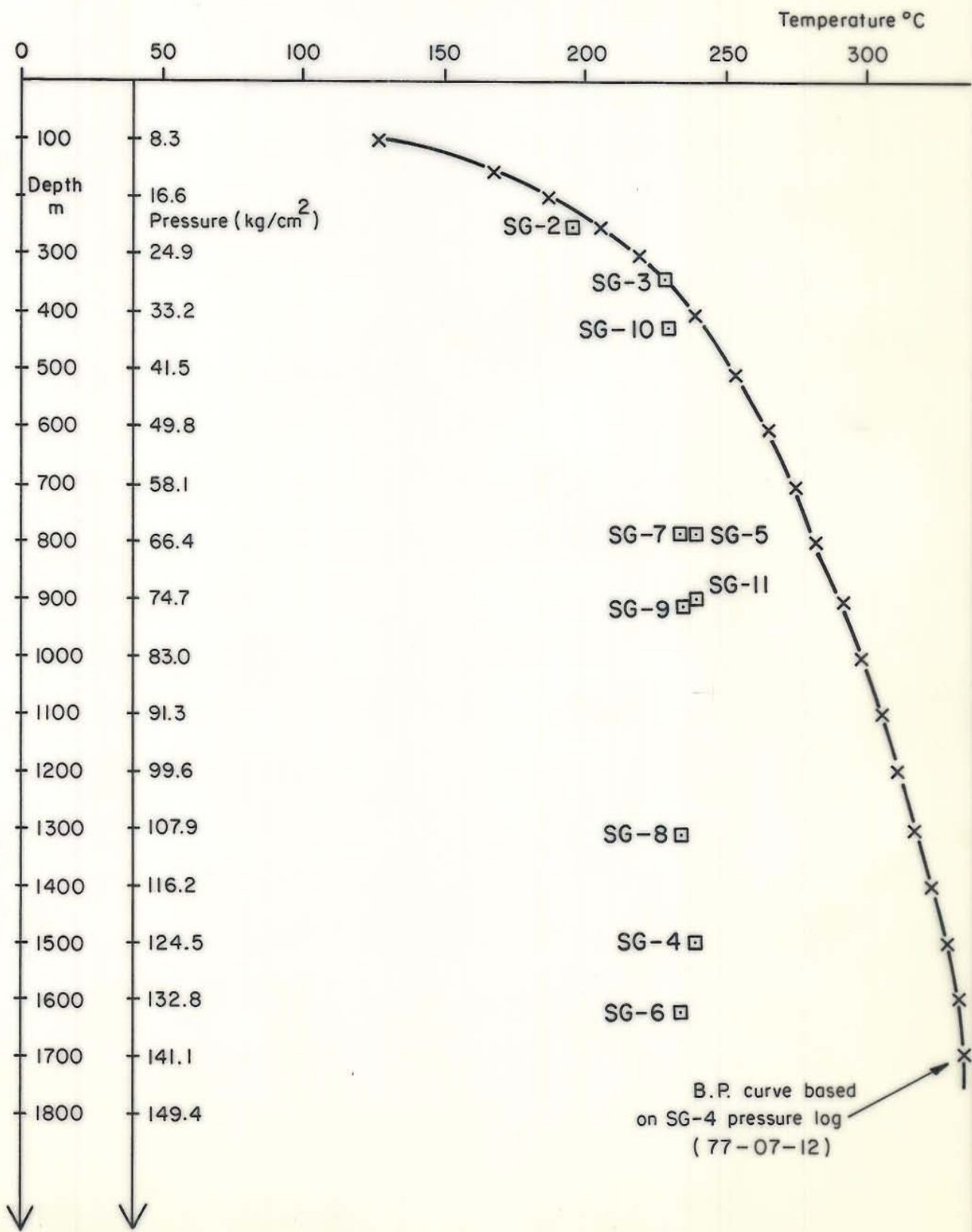


Fig. 3.11 PRESSURE-TEMPERATURE SATURATION RELATION

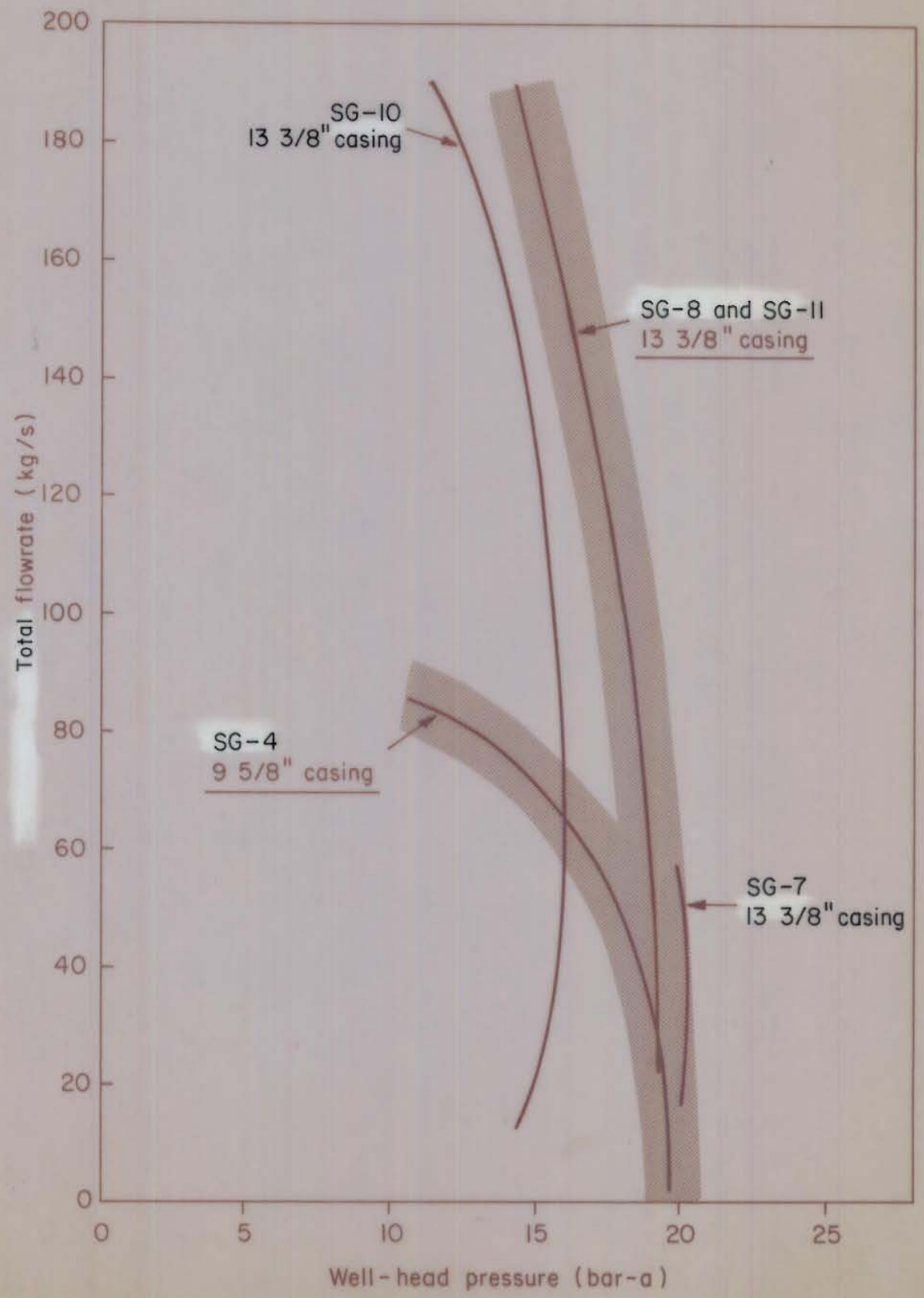


Fig. 3.12 TYPICAL BORE OUTPUT CHARACTERISTIC OF SVARTSENGI WELLS

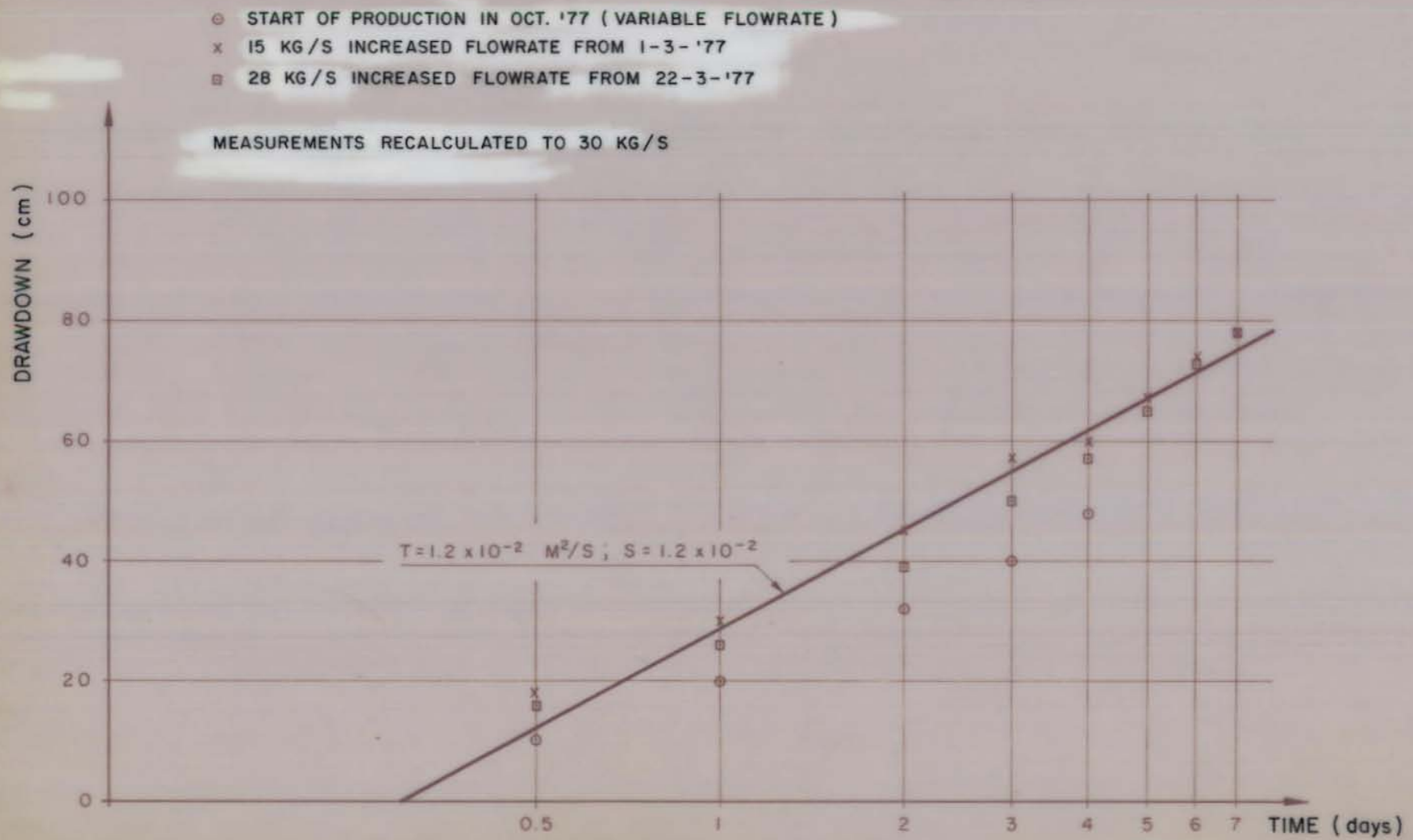


Fig. 4.1 RESULTS OF INITIAL MEASUREMENTS OF STORATIVITY (S) AND TRANSMISSIVITY (T)

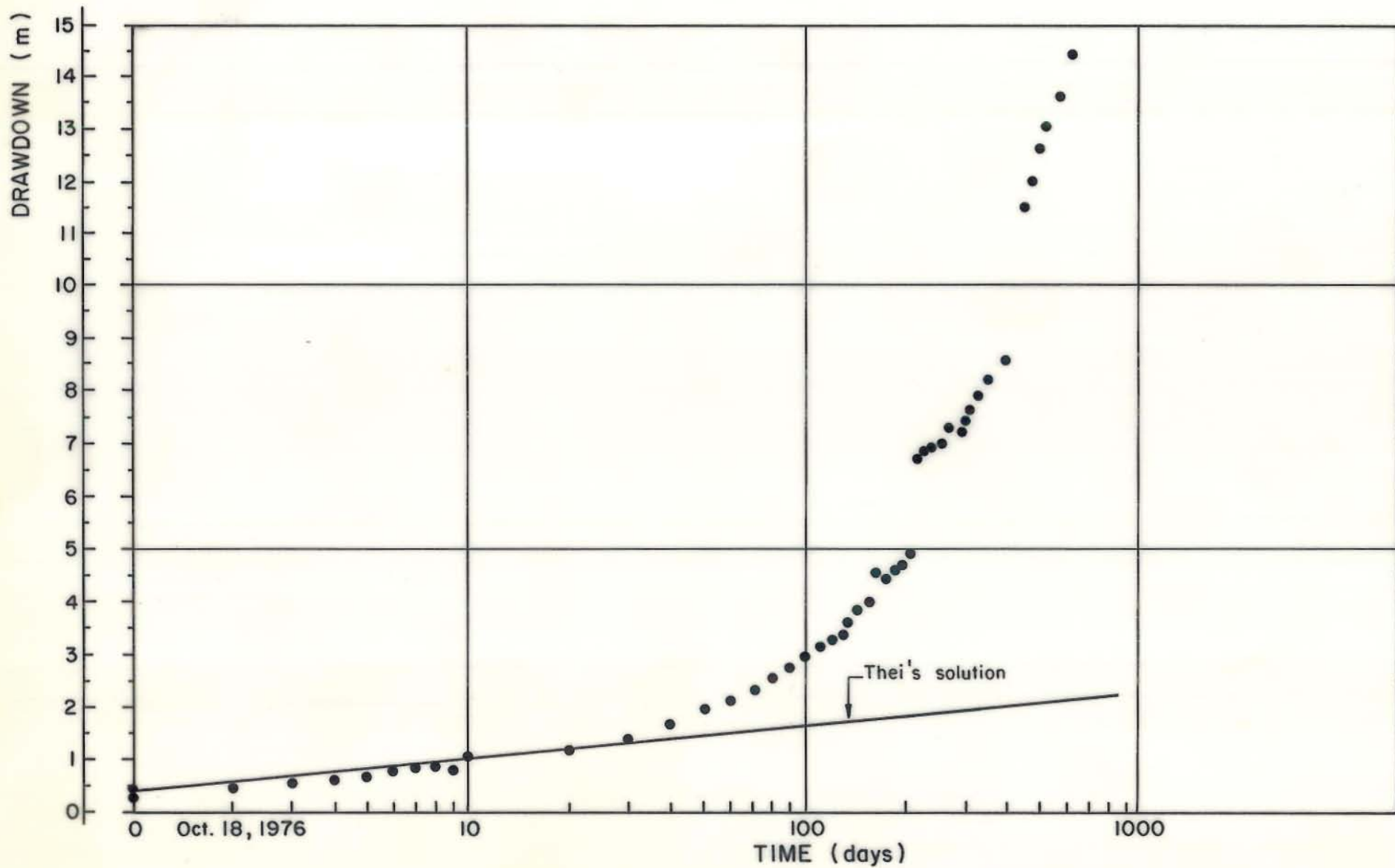


Fig. 4.2 MEASURED DRAWDOWN (0-970 DAYS) IN SG-5

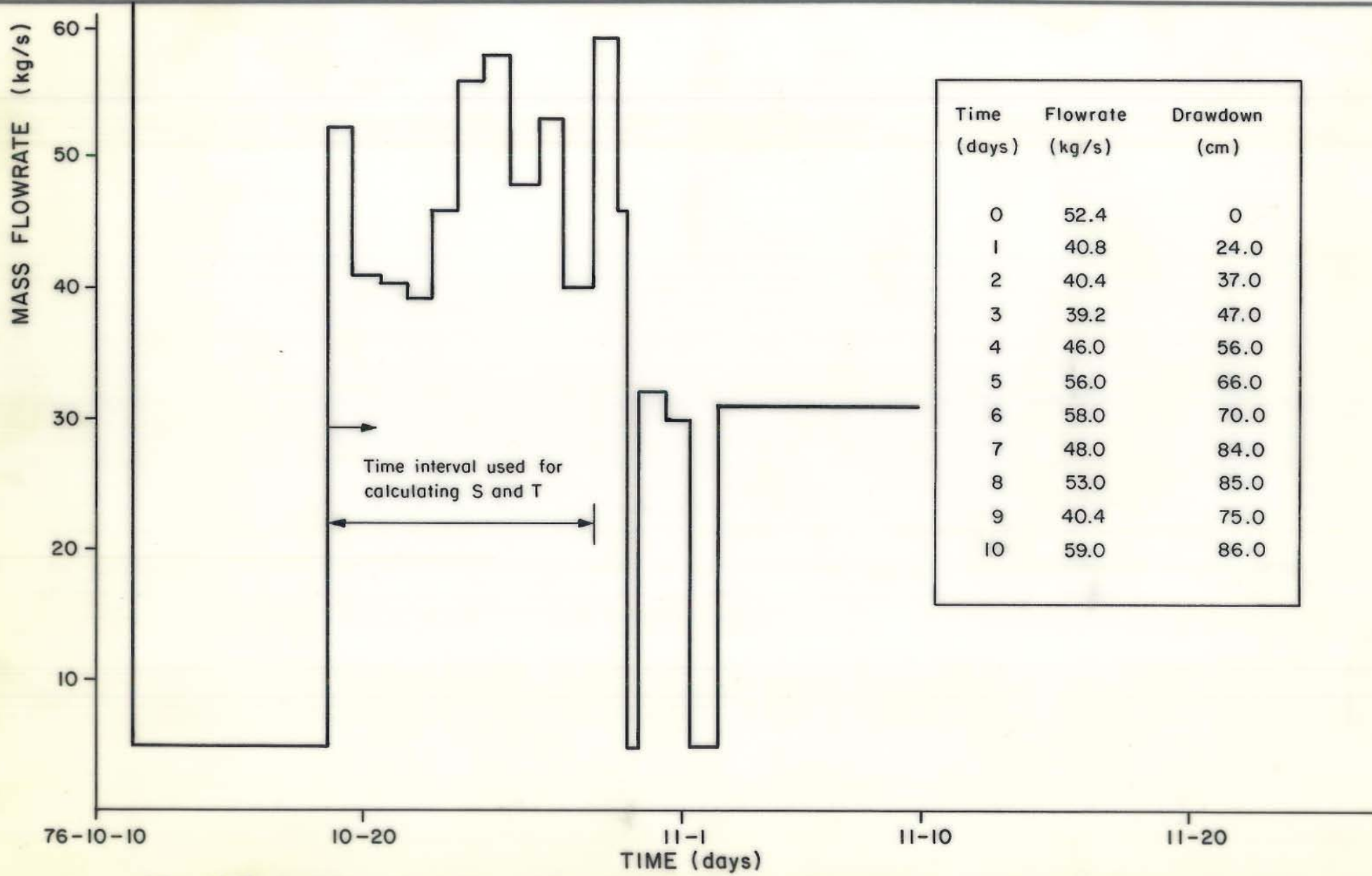


Fig. 4.3 FLOWRATE DATA USED FOR TEST A. (76-10-18 TO 76-10-28)

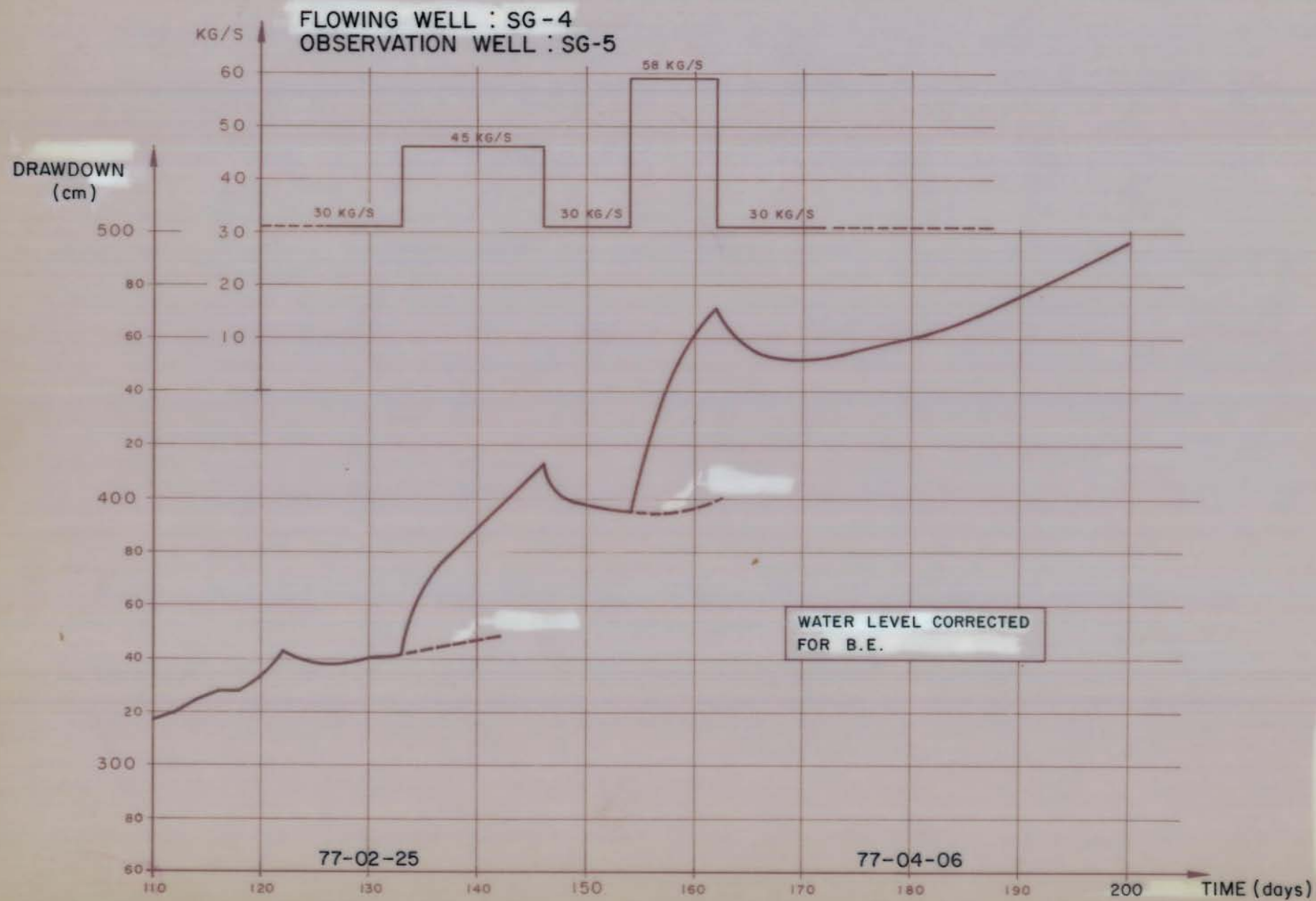


Fig. 4.4 FLOWRATE AND DRAWDOWN DATA FOR TEST B AND C (77-02-25 TO 77-04-06)

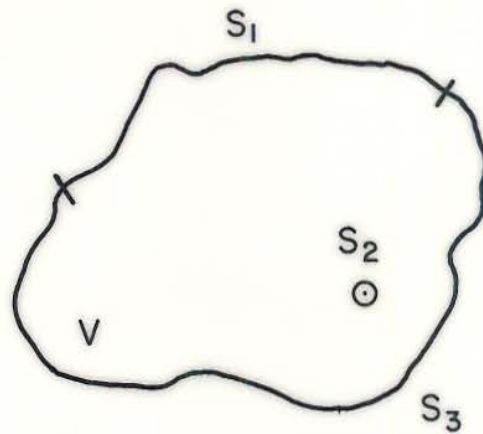


Fig. 4.5 a DEFINITION OF BOUNDARIES FOR EQUATION (1)
(BARELLI AND PALAMA, 1980)

S_1 : Part of boundary defining reservoir field pressure

S_2 : Part of boundary representing the well where flowrate variation occurs

S_3 : Part of boundary on which flowrate is defined

V : Volume boundary of the reservoir

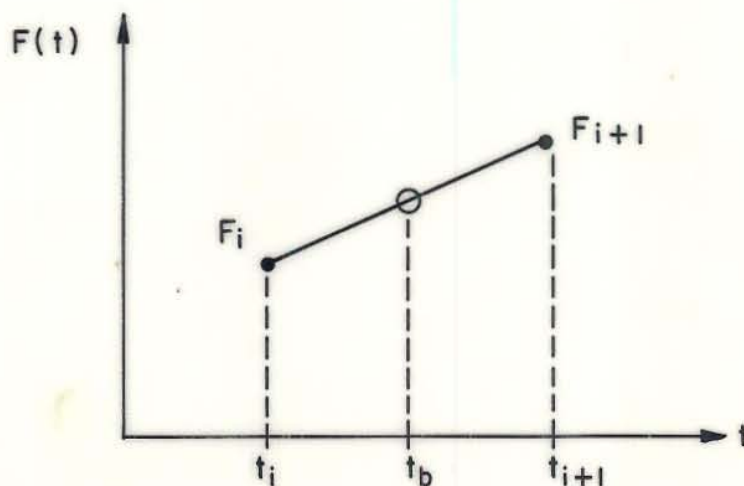


Fig. 4.5 b LINEAR INTERPOLATION SCHEME FOR EQUATION (5)

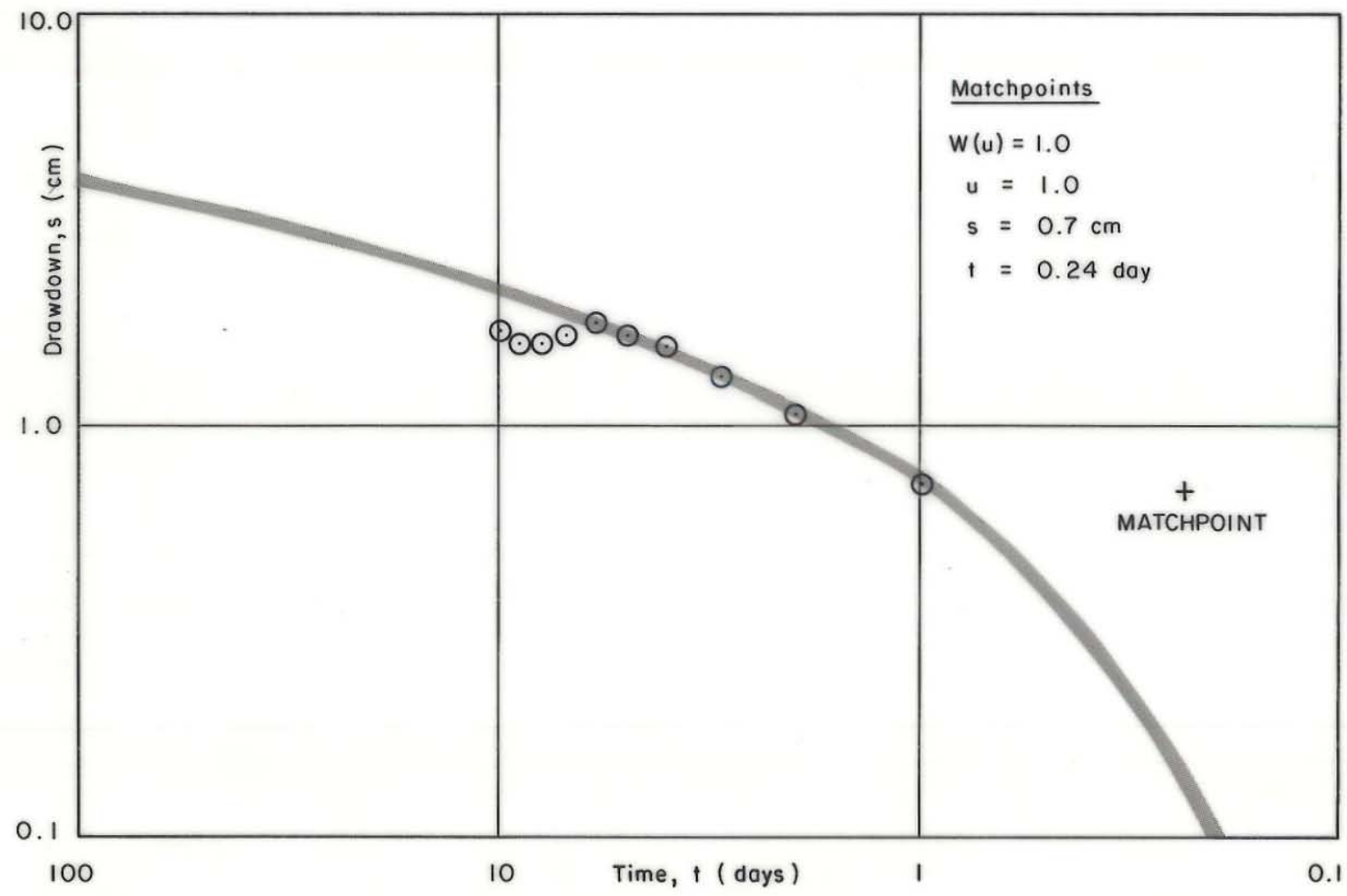


Fig. 4.6 TYPE CURVE MATCHING WITH COMPUTED U.R.F. FOR THE FIRST 10 DAYS

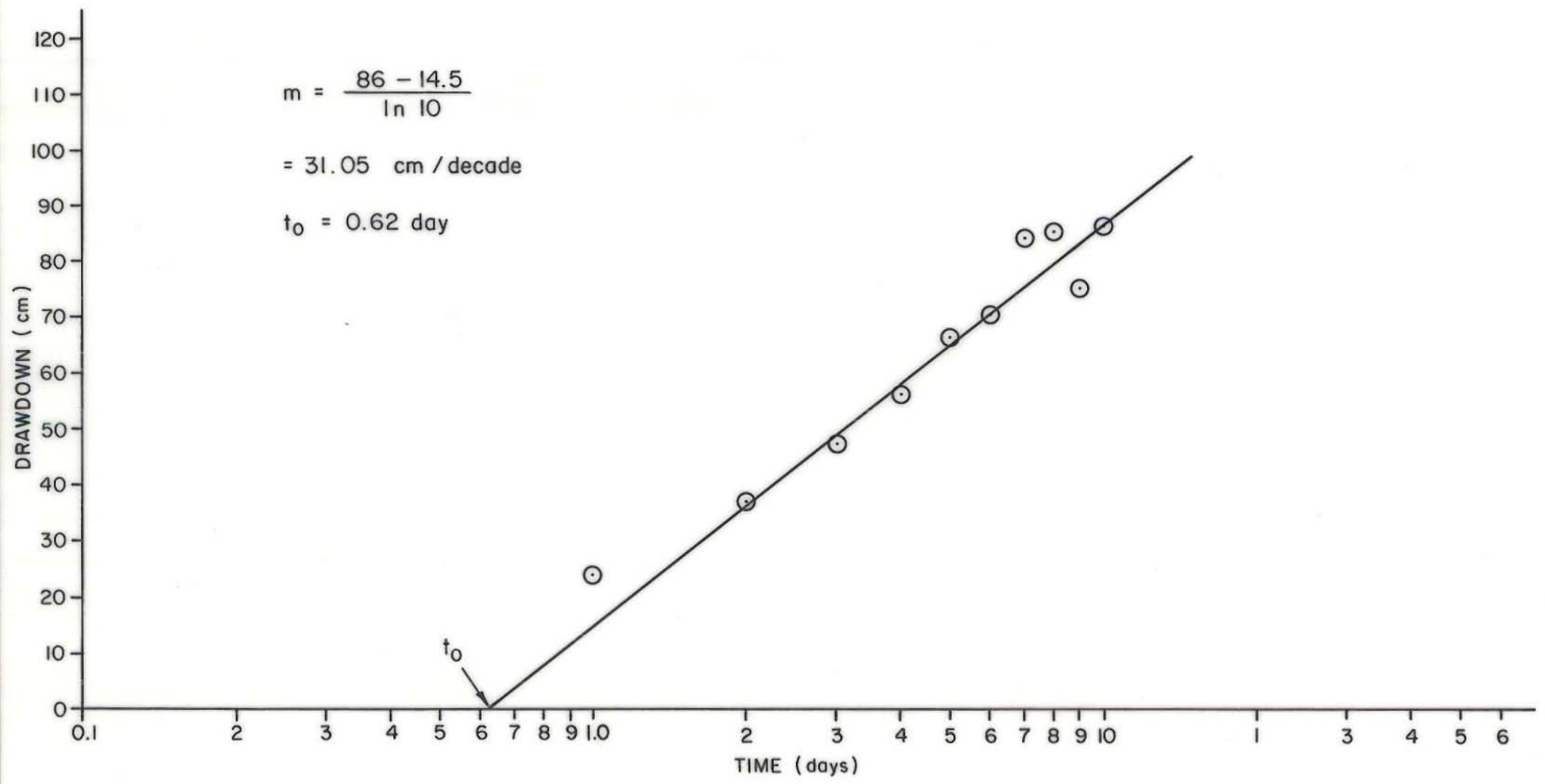


Fig. 4.7 SEMI - LOG PLOT OF DRAWDOWN DATA FOR THE FIRST 10 DAYS

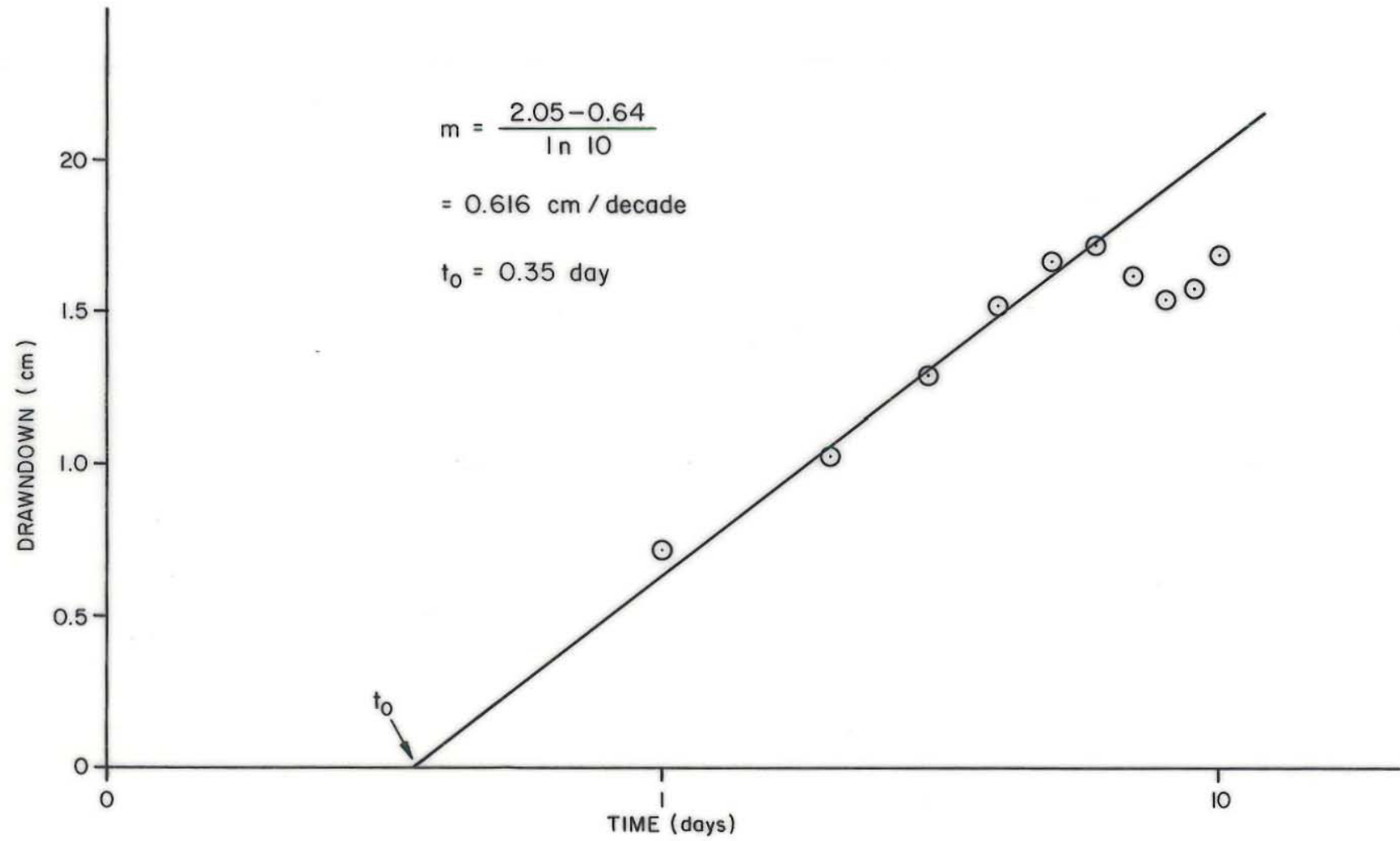


Fig. 4.8 SEMI-LOG PLOT OF THE UNIT RESPONSE FUNCTION FOR THE FIRST 10 DAYS

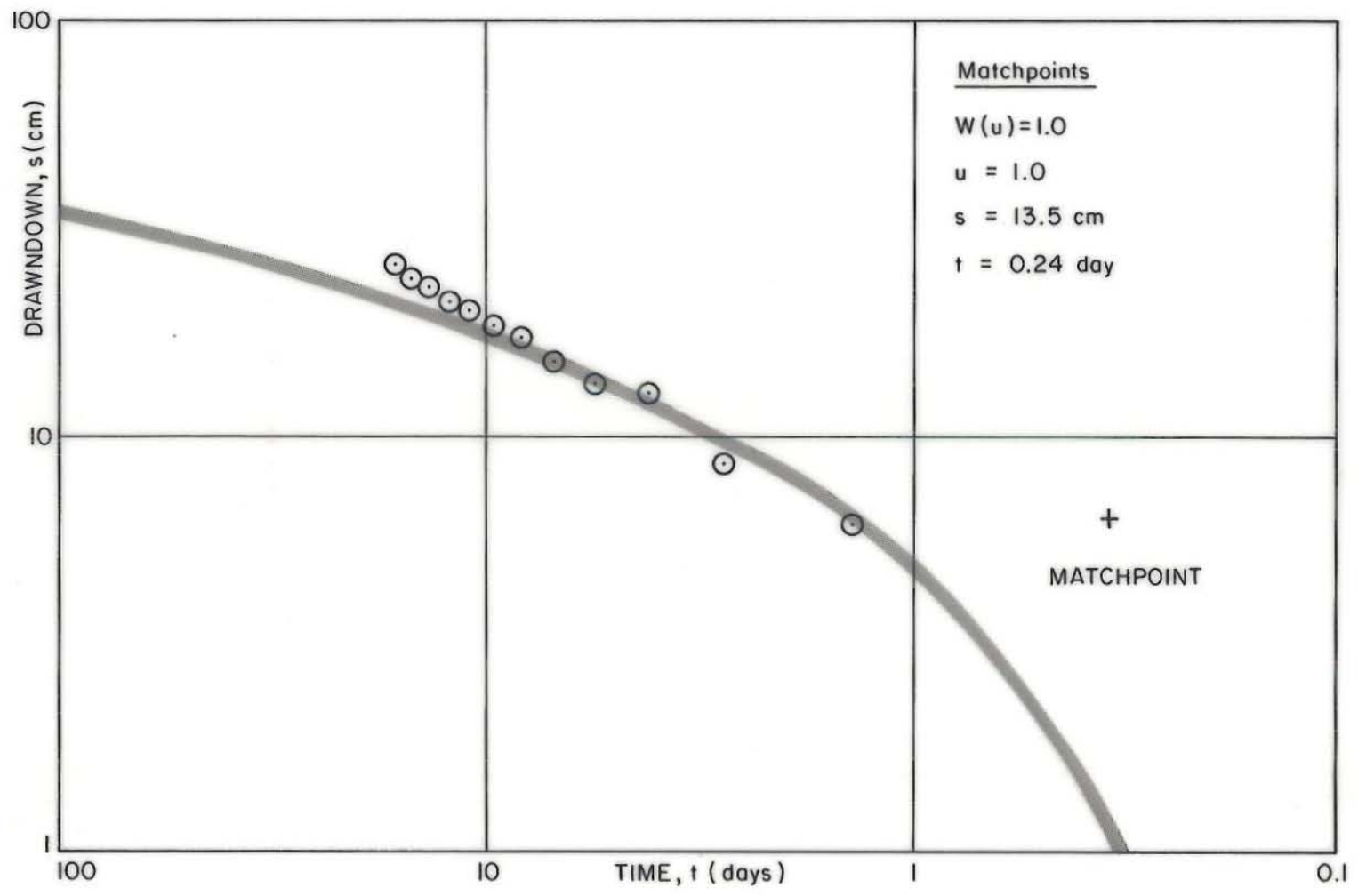


Fig. 4.9 TYPE CURVE MATCHING WITH MEASURED DRAWDOWN FROM 77-02-25 TO 77-03-17

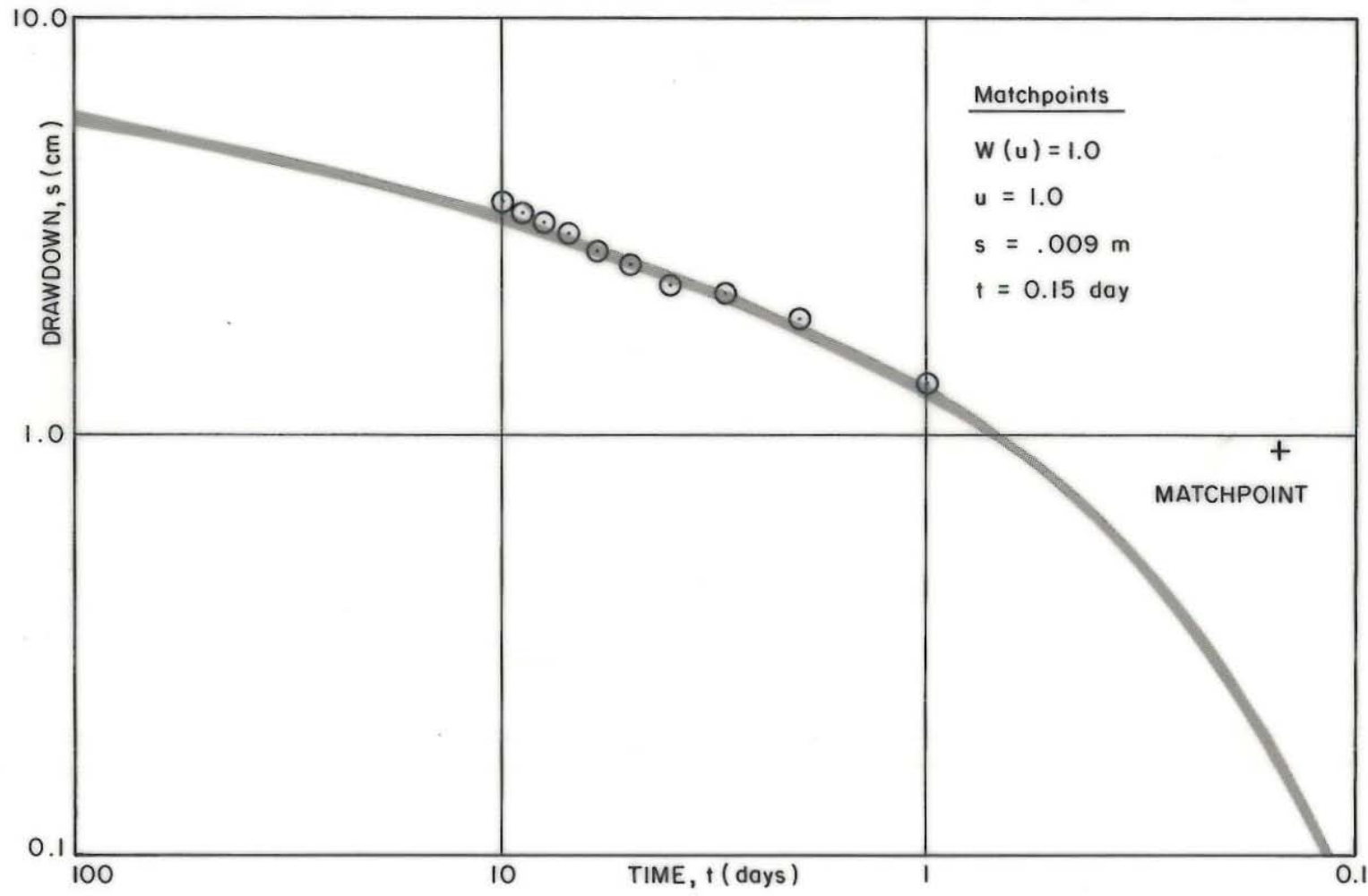


Fig. 4.10 TYPE CURVE MATCHING WITH UNIT RESPONSE FUNCTION DATA FROM 77-02-25 TO 77-03-17

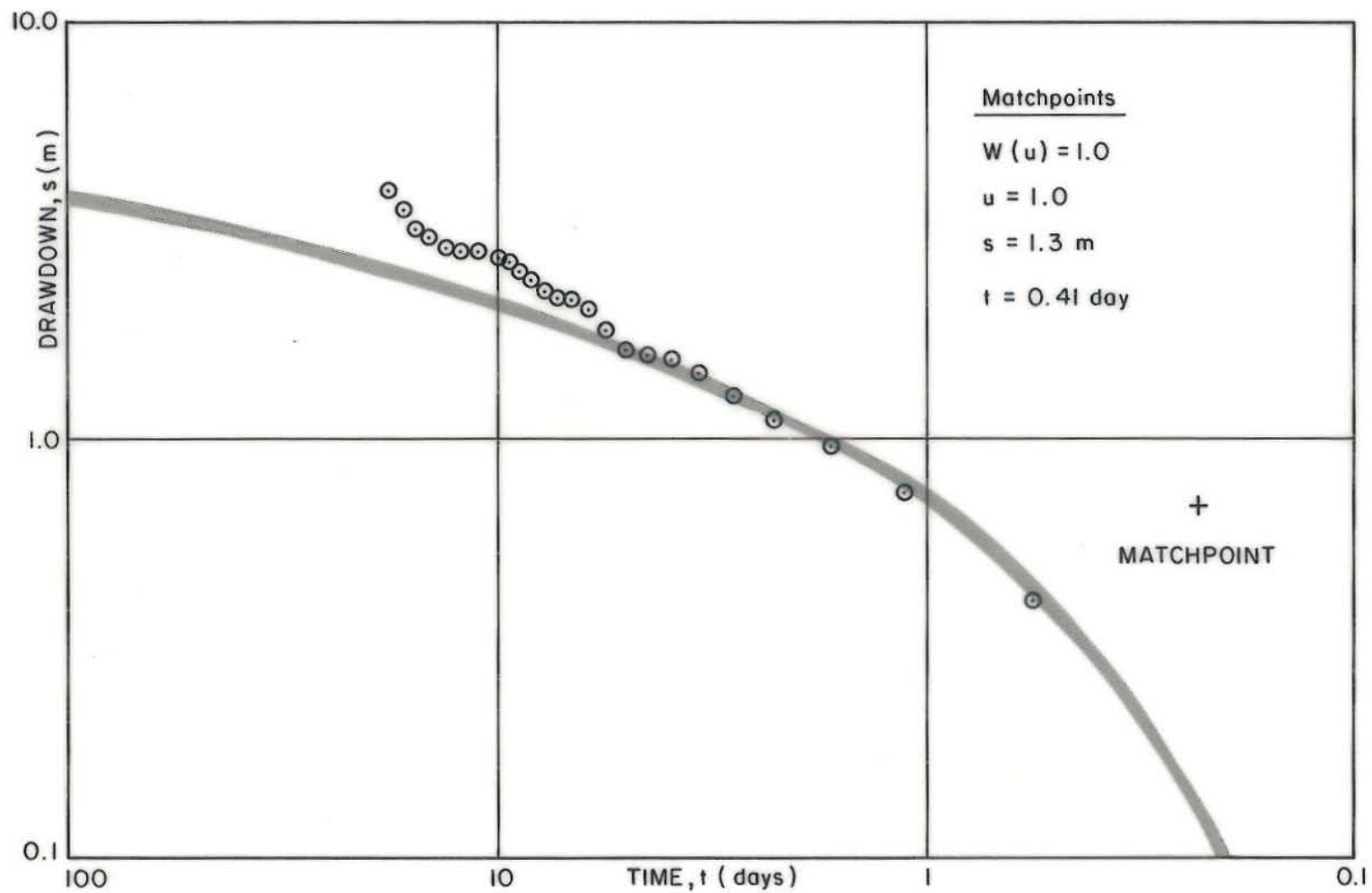


Fig. 4.11 TYPE CURVE MATCHING WITH VALUES OF UNIT-RESPONSE FUNCTION FROM 77-02-28 TO 77-04-06

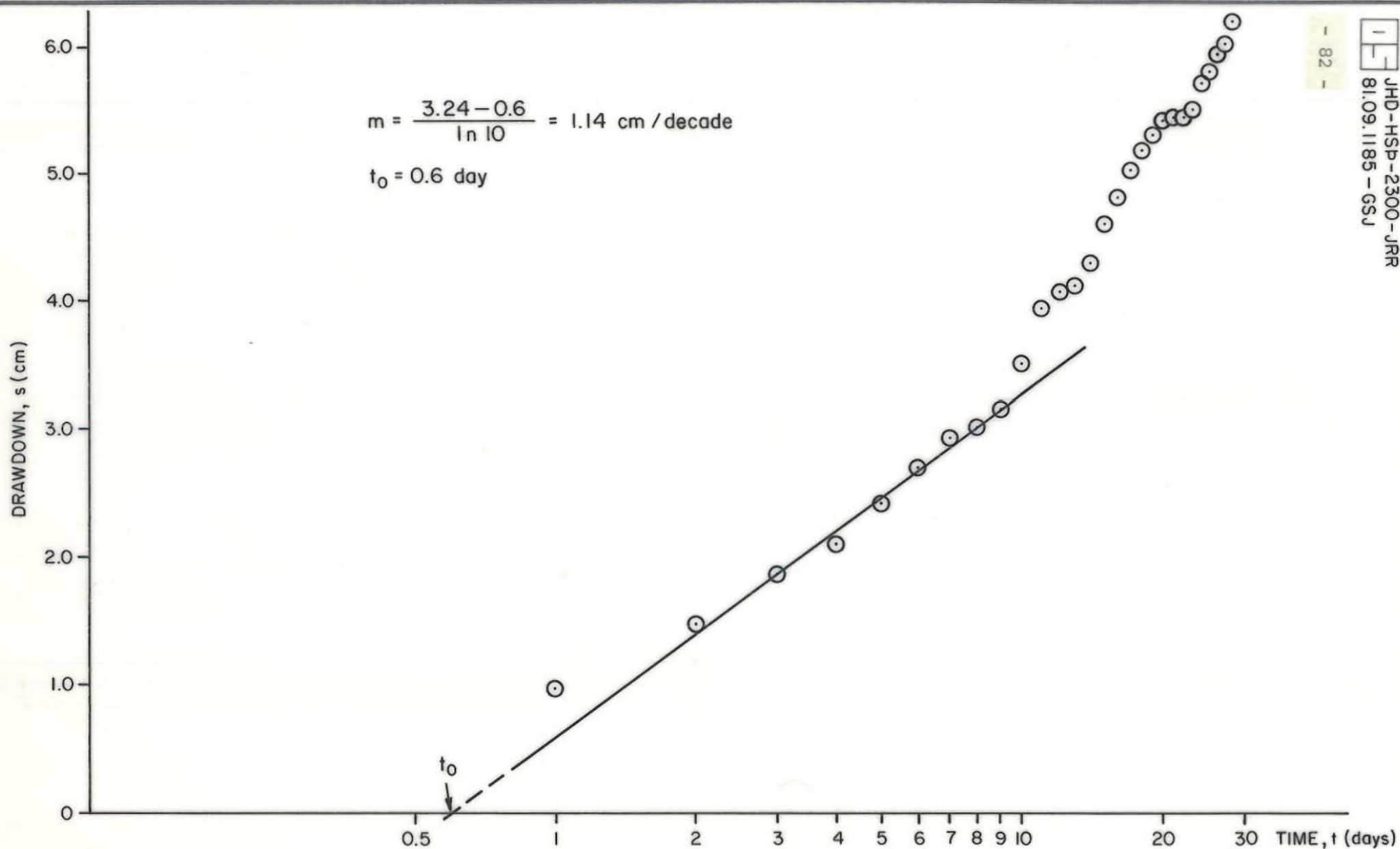


Fig. 4.12 SEMI-LOG PLOT OF UNIT RESPONSE FUNCTION FROM 77-02-28 TO 77-04-06

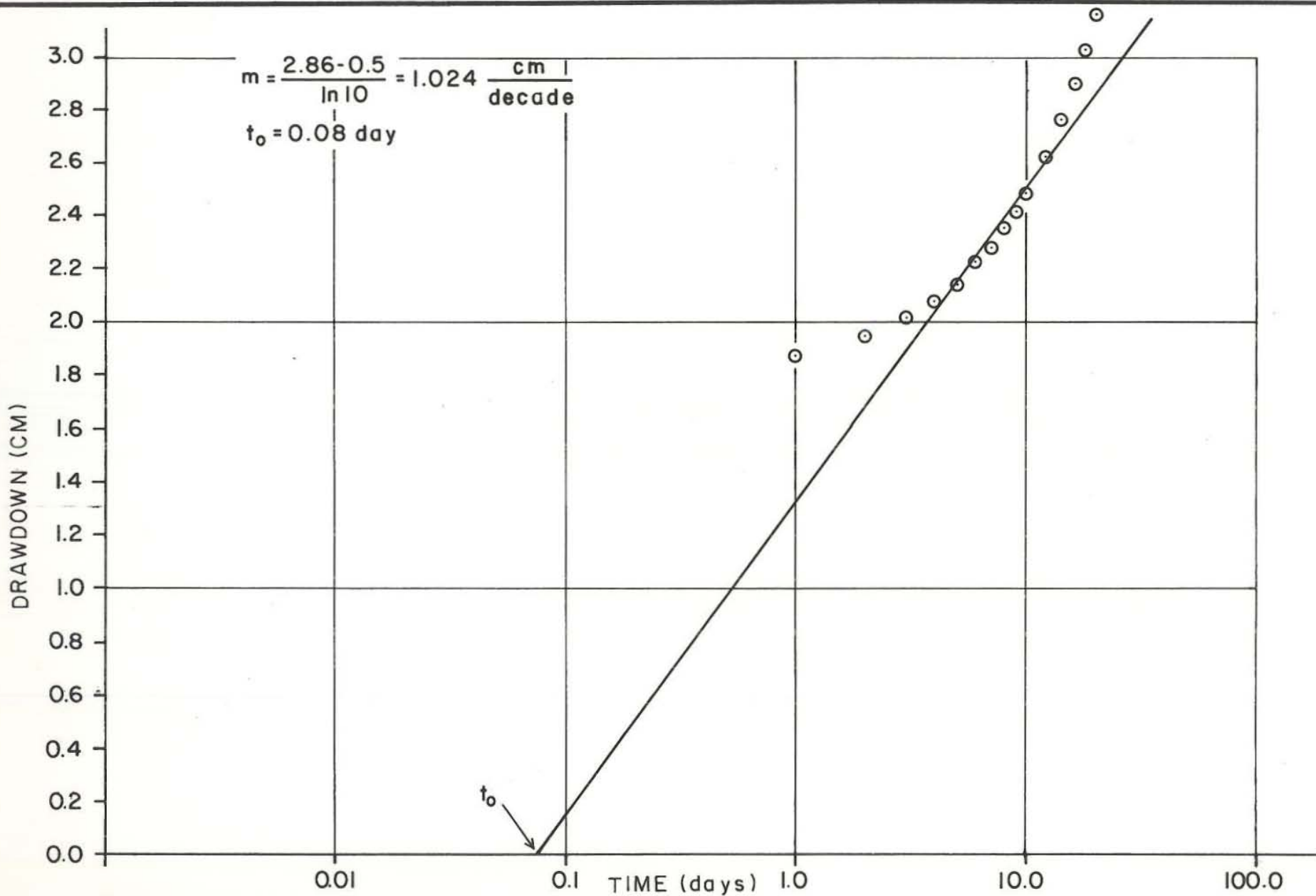


Fig. 4.13 Semi-log plot of 0-10 day drawdown. Computed from unit response function for 0-900 days

JHD-HSB-2300 J.R.R.
81.10.1205, T/Sy J.

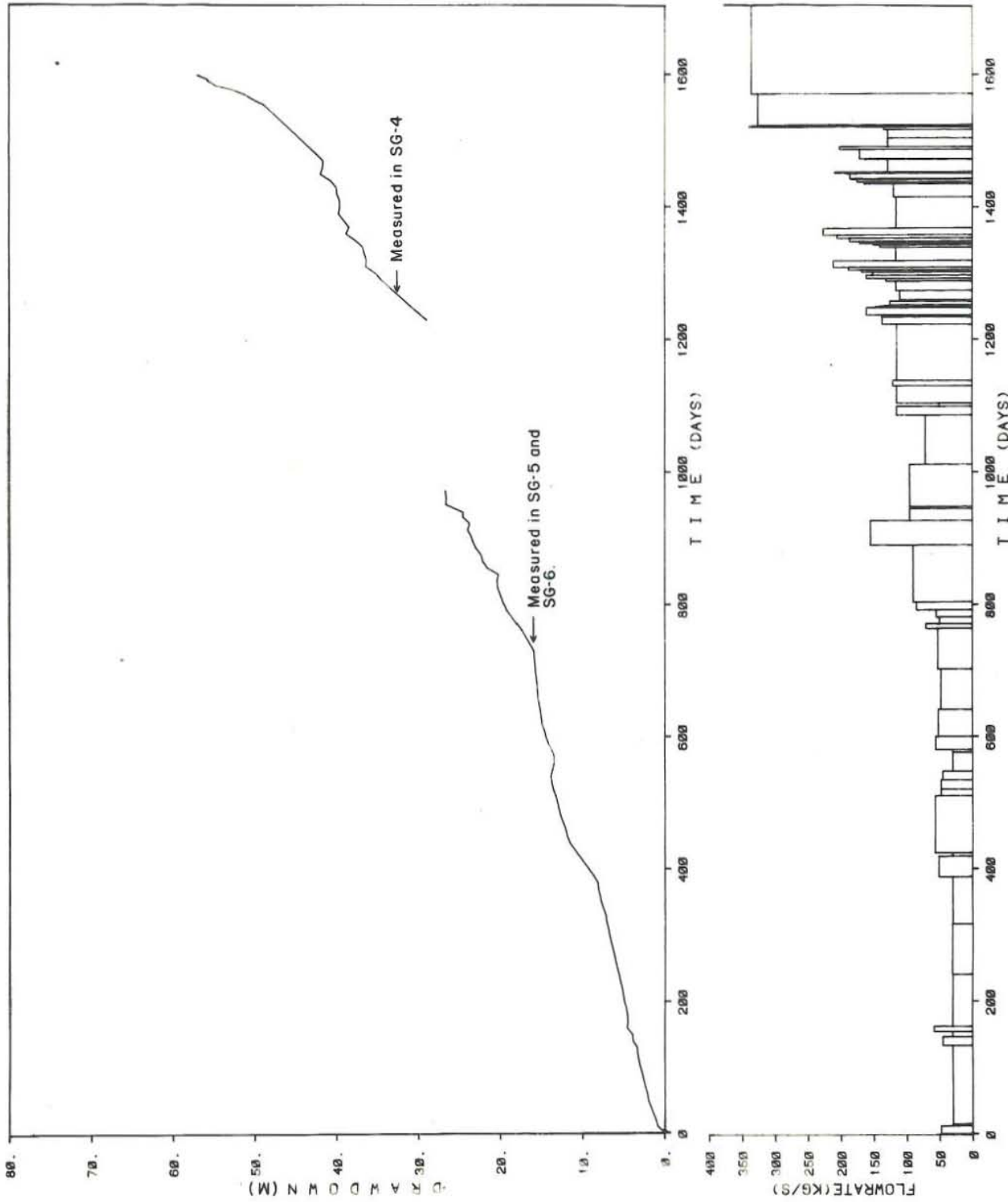


FIG. 4.14. DRAWDOWN HISTORY (0 - 1600 DAYS)
SVARTSENGI GEOTHERMAL FIELD

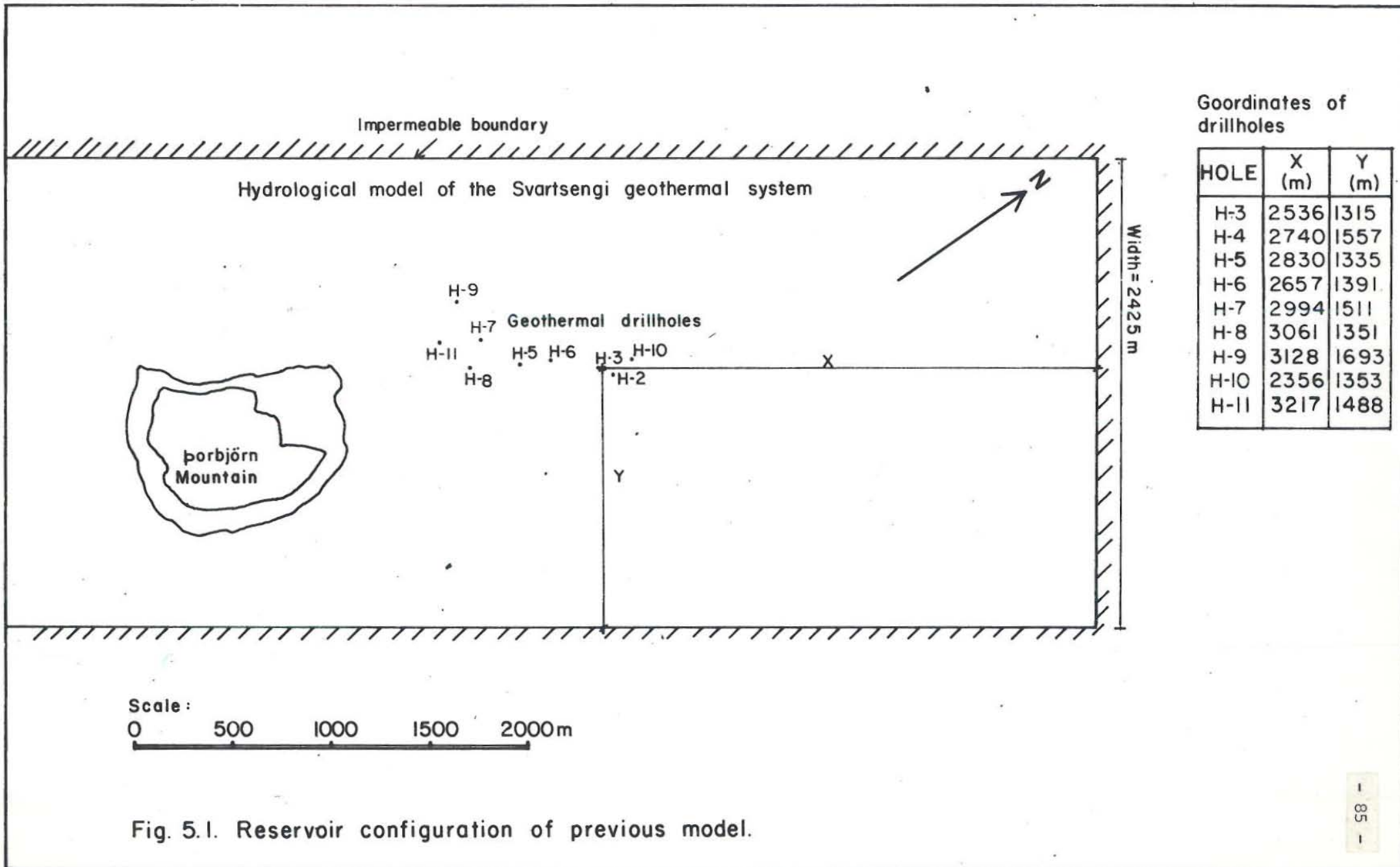


Fig. 5.1. Reservoir configuration of previous model.

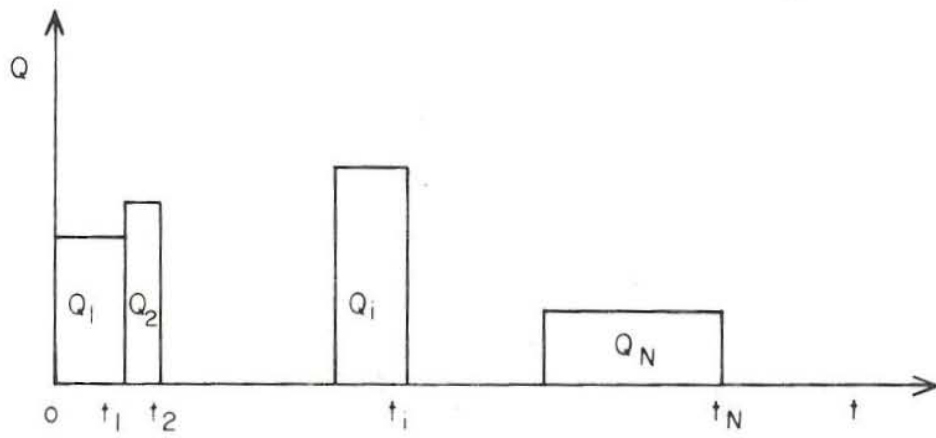


Fig 5.2. Discrete pumping rates.

F-18971



JHD-HSP-9000-GKH-JRR
81.10.1215.-EBF

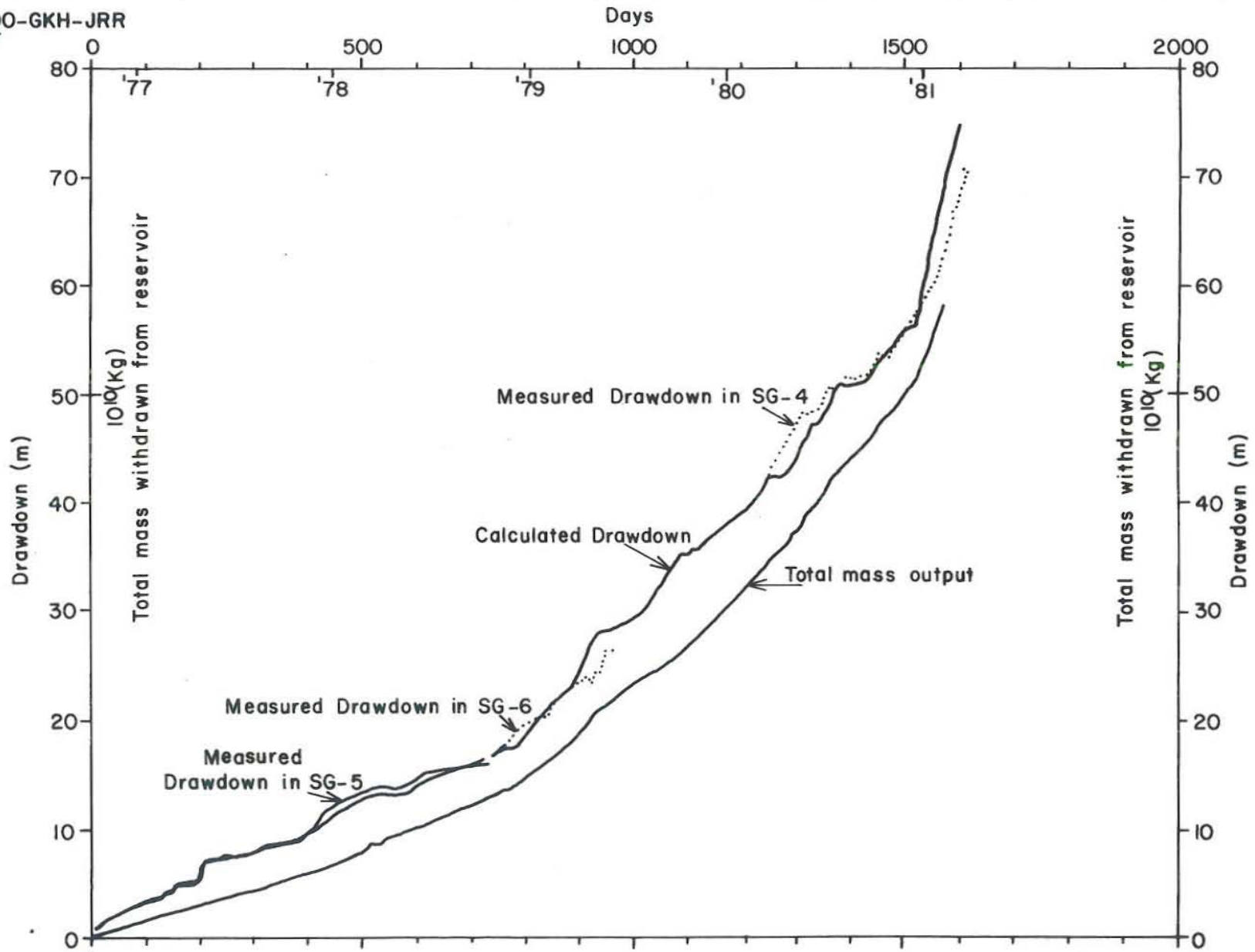


Fig. 5.3. Measured vs. calculated drawdown for previous model. (From Halldórsson, 1981)

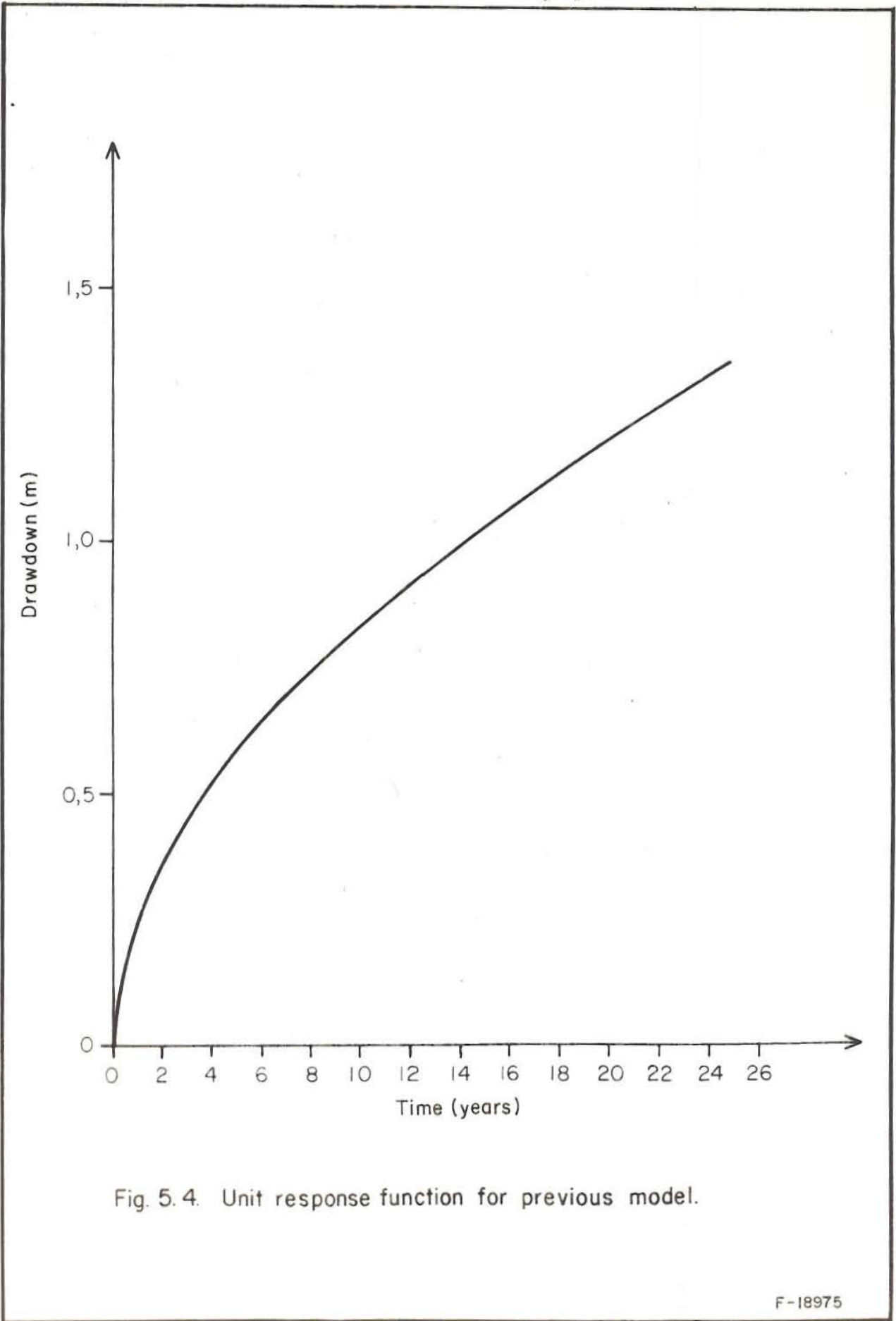


Fig. 5.4. Unit response function for previous model.

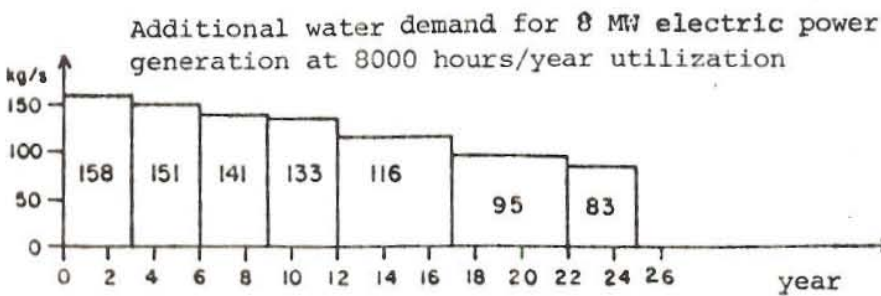
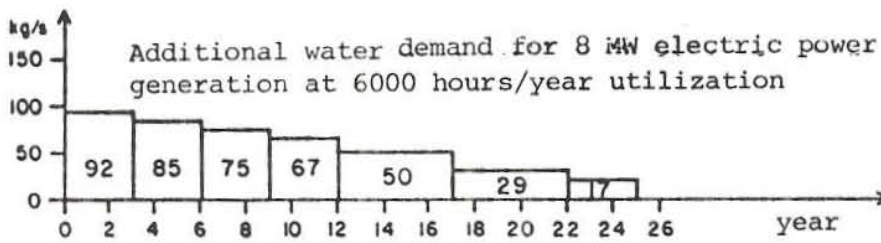
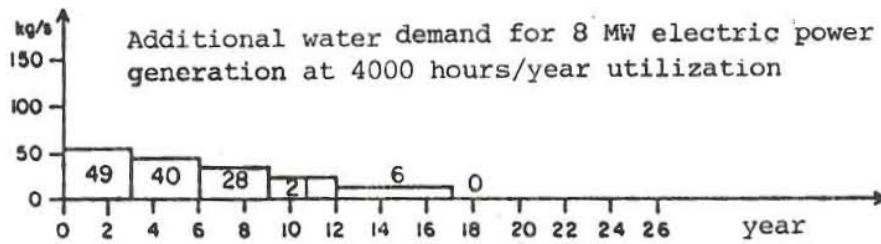
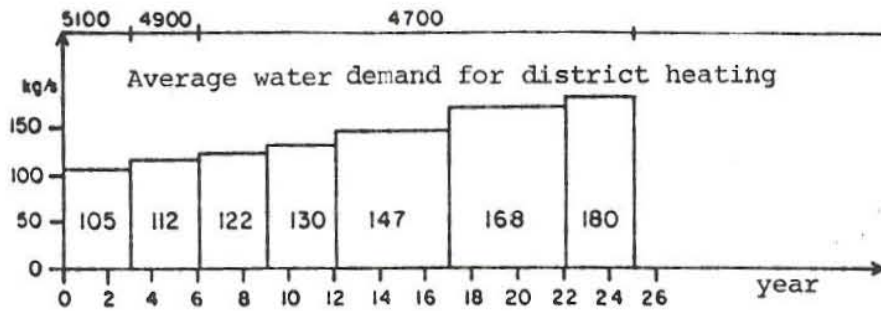
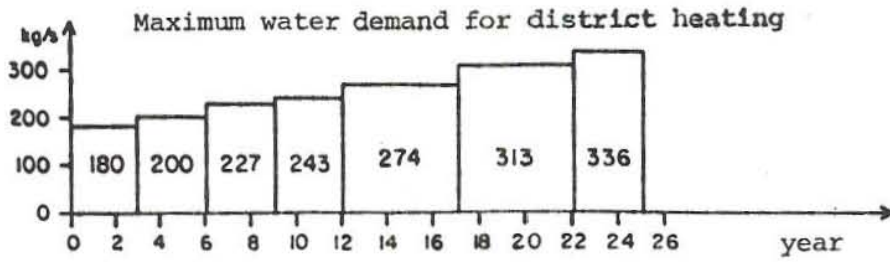


Fig. 5.5 Future production requirements



ORKUSTOFNUN
Straumfræðistöð

HITAVEITA SUDURNESJA, SVARTSENGI

79-10-31

S.P.K/Sy.J.

Vinnslut Svartse.

F 18793

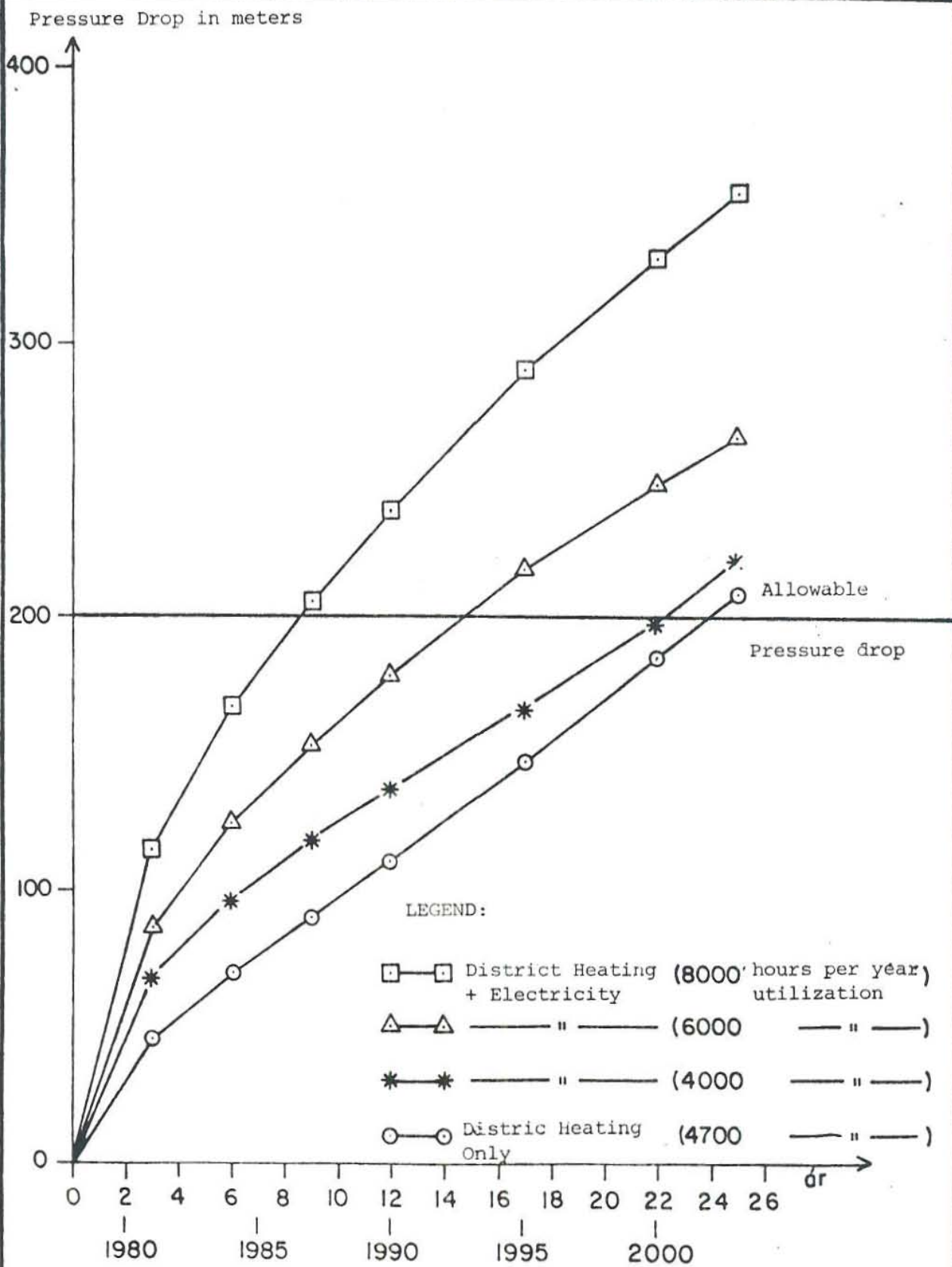


Fig. 5.6. Forecasted drawdowns, for previous model.

Equation of family of curves
for different reservoir pressure PA

$$\left(\frac{W}{177 PA - 53.5}\right)^2 + \left(\frac{P_o}{0.355 PA - 10.6}\right)^2 = 1$$

W Mass flow, kg / s

P_o Wellhead pressure, bar abs

Δ Measurements in SG-4

PA = 88 bar, reservoir
pressure at 1000 m
below sea level

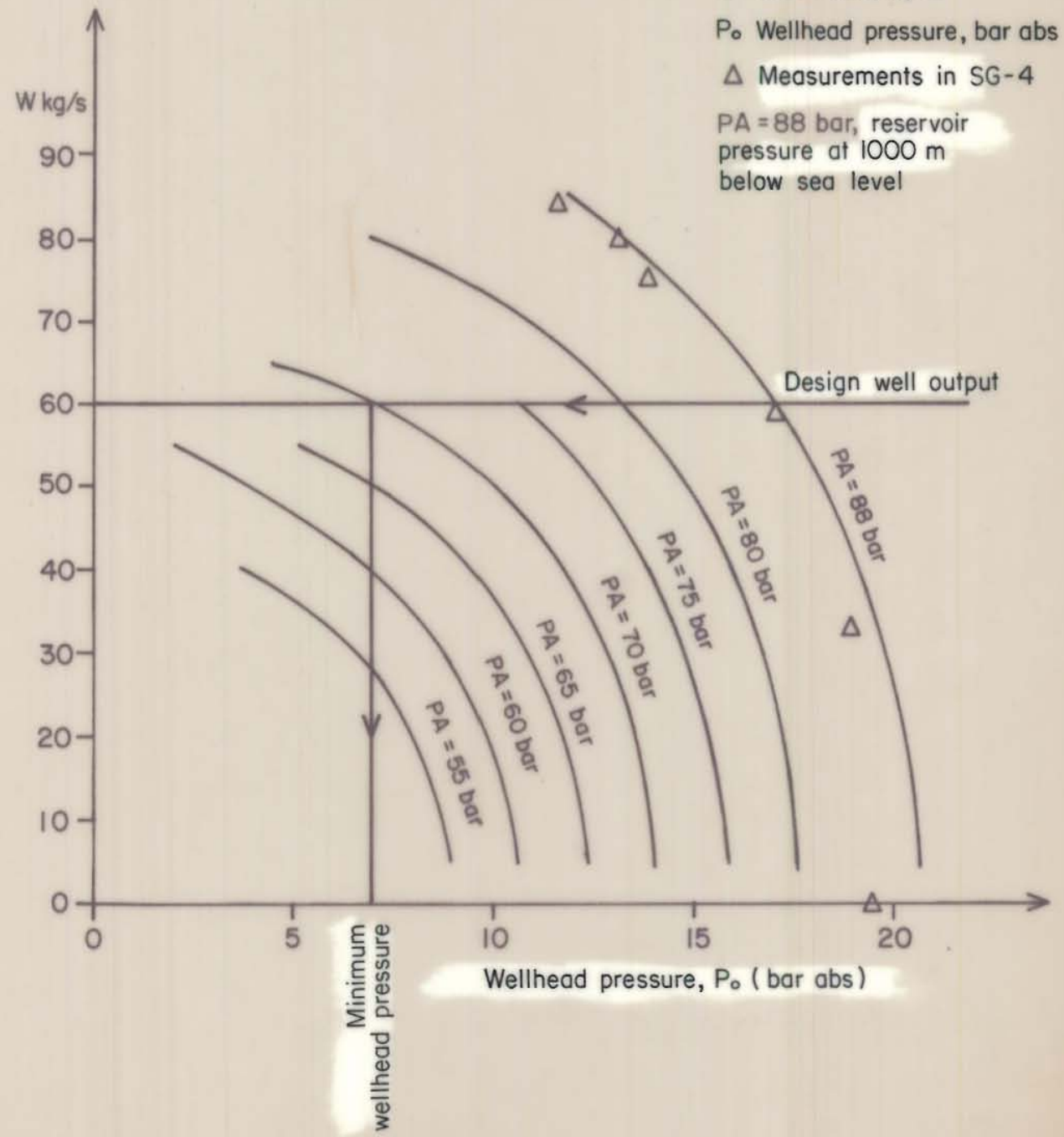


Fig. 5.7 RESULTS OF NUMERICAL TWO PHASE FLOW CALCULATIONS FOR WELLS FOR DIFFERENT RESERVOIR PRESSURES AT 1000 M DEPTH

UF JHD-HSP-2300 J.R.R.
81.10. 1216. T/Sy J.

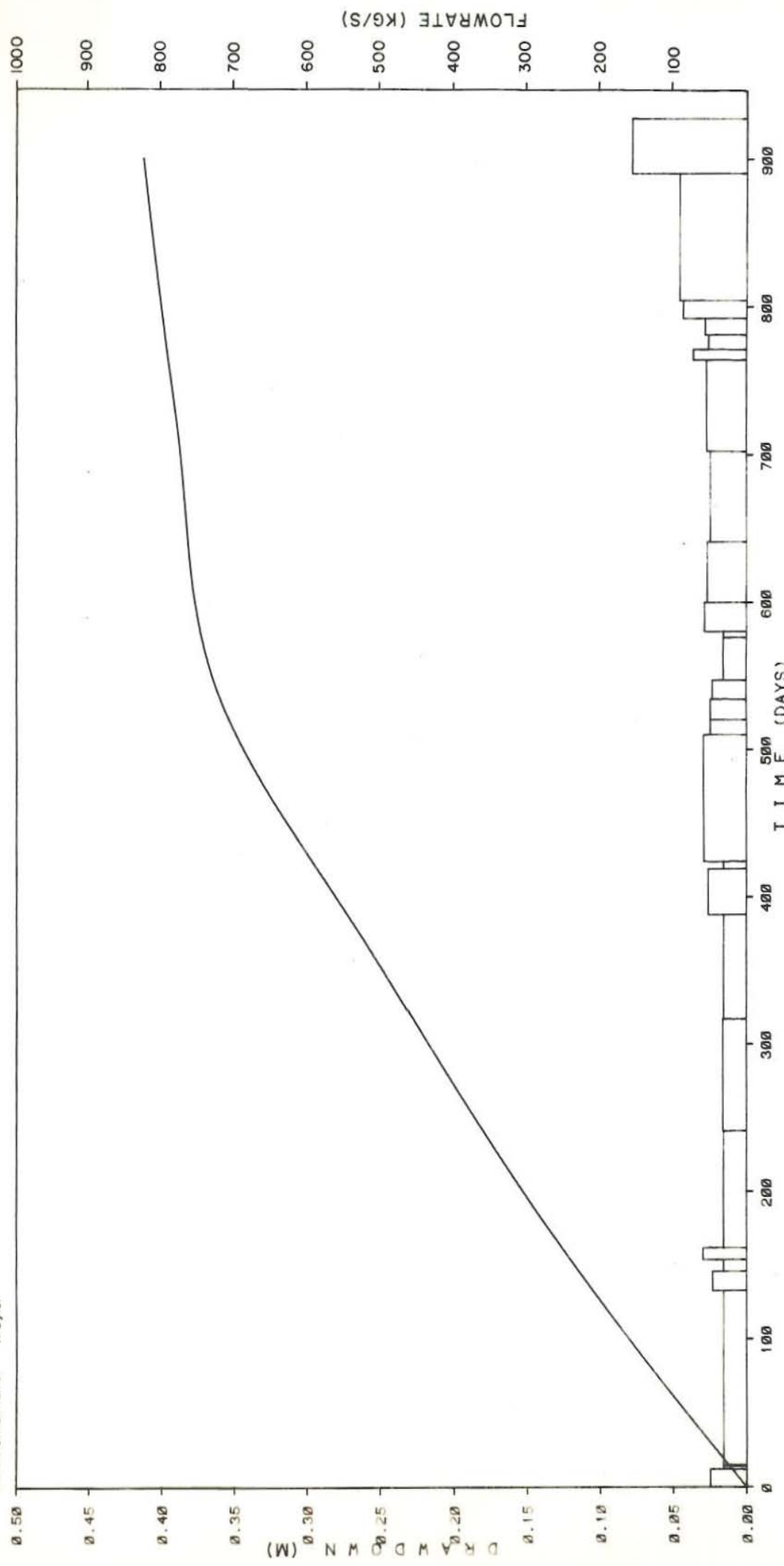


FIG.5.8 UNIT RESPONSE FUNCTION (Ø - 970 DAYS)
SVARTSENGI GEOTHERMAL FIELD

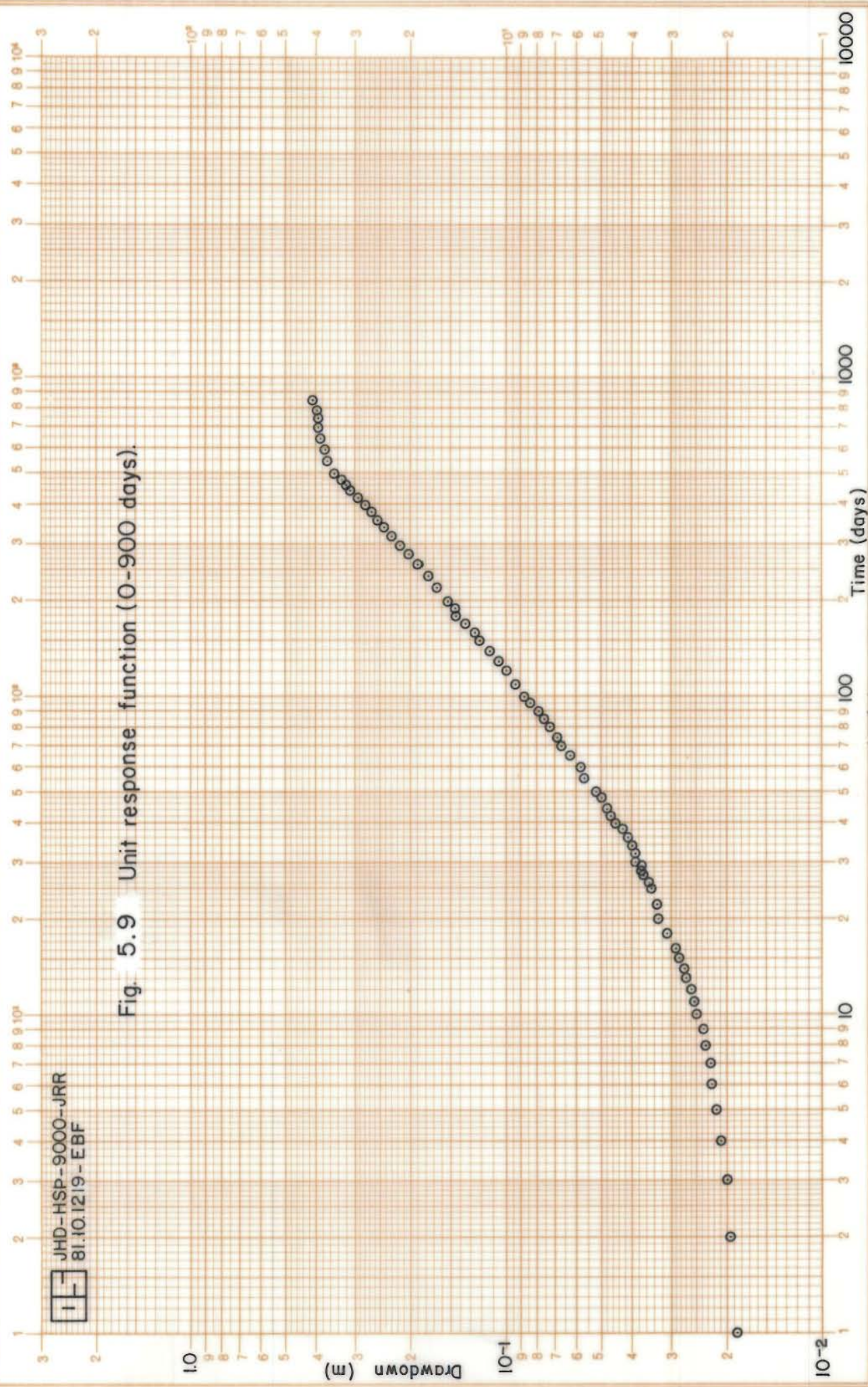
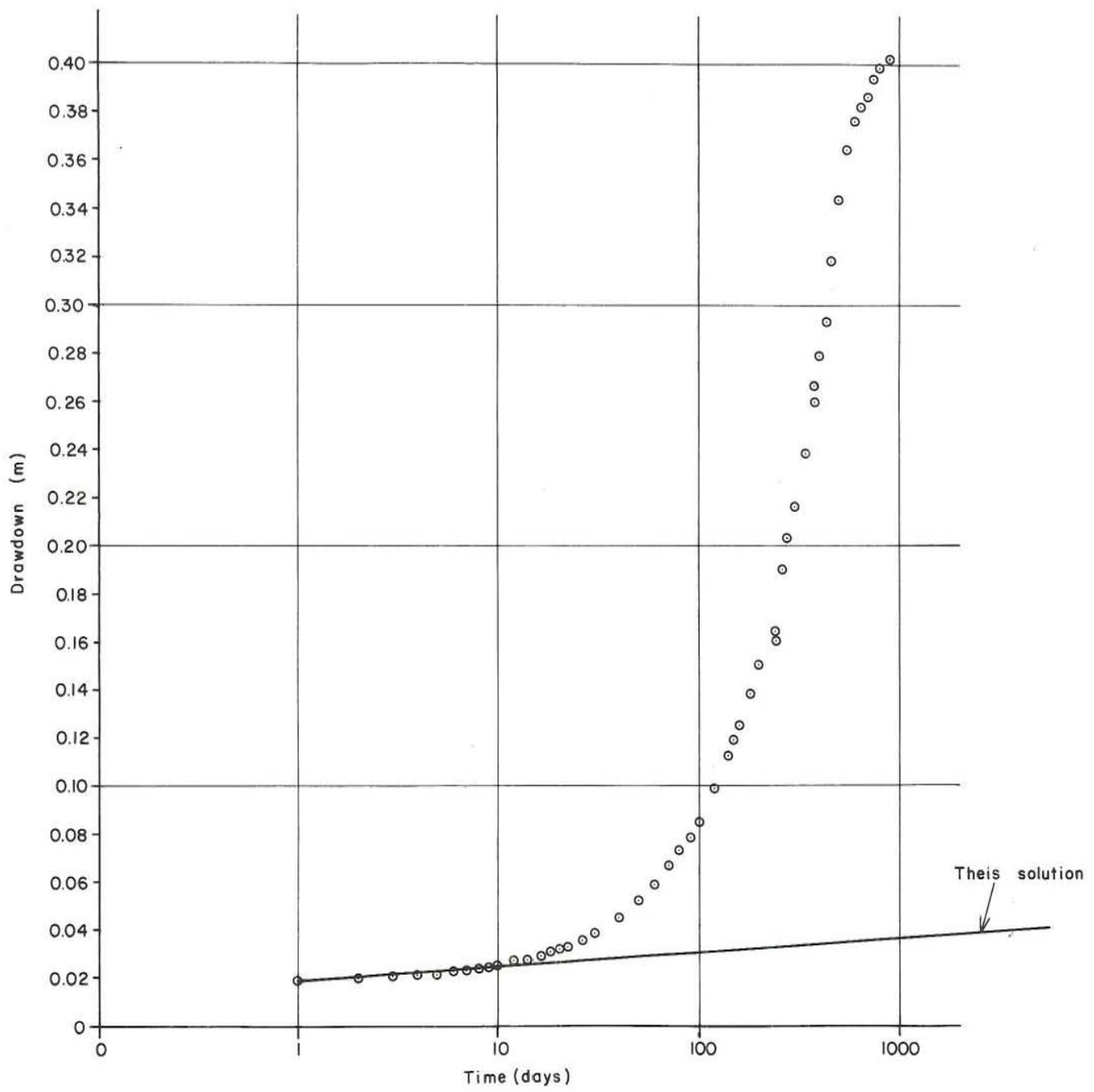


Fig. 5.9 Unit response function (0-900 days).

JHD-HSP-9000-JRR
81.10.1220-EBF

Fig. 5.10 Unit response function (0-900 days).



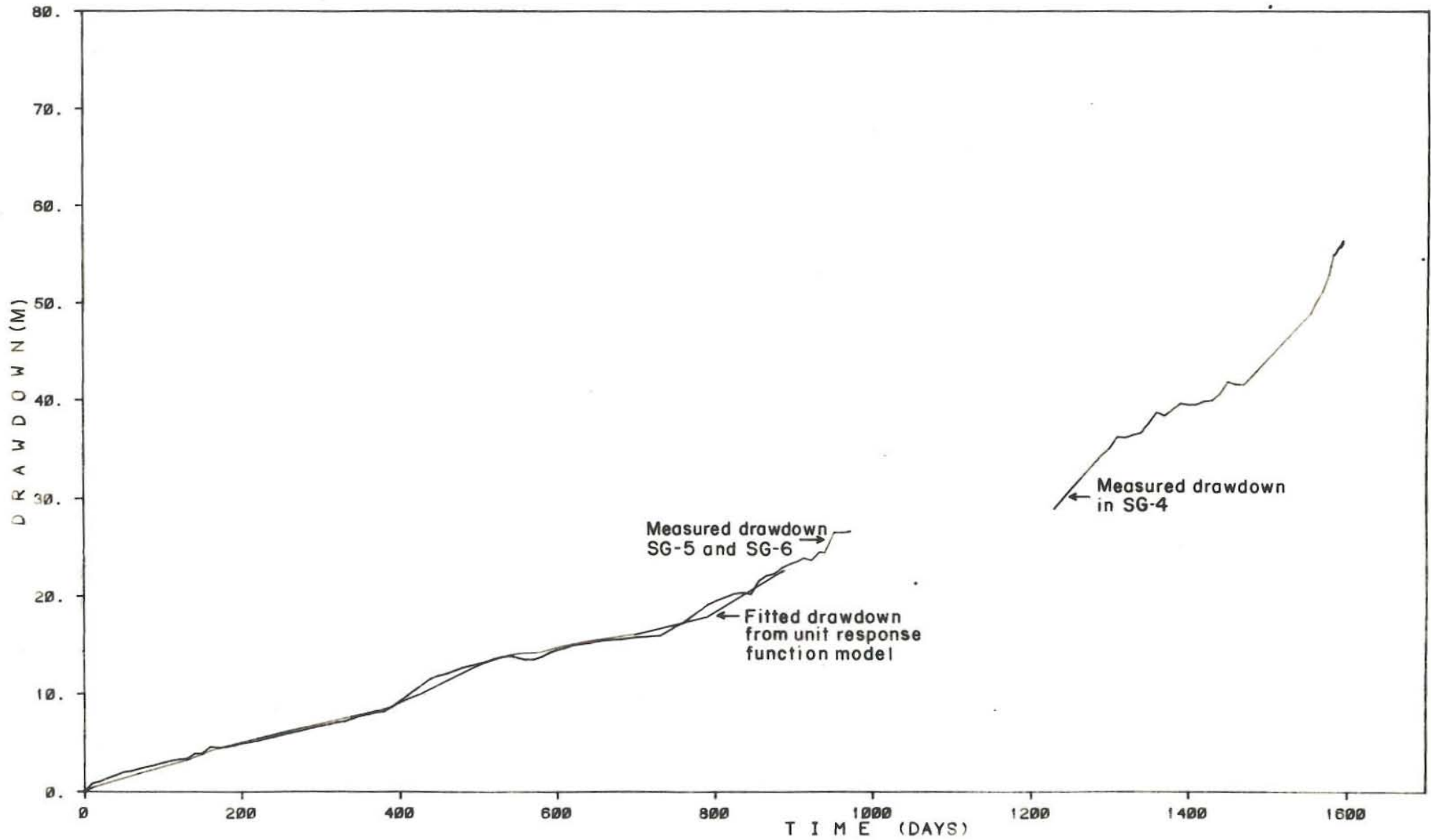


FIG. 5.II MEASURED AND FITTED DRAWDOWN FROM U.R.F. (0-900 DAYS)
SVARTSENGI GEOTHERMAL FIELD

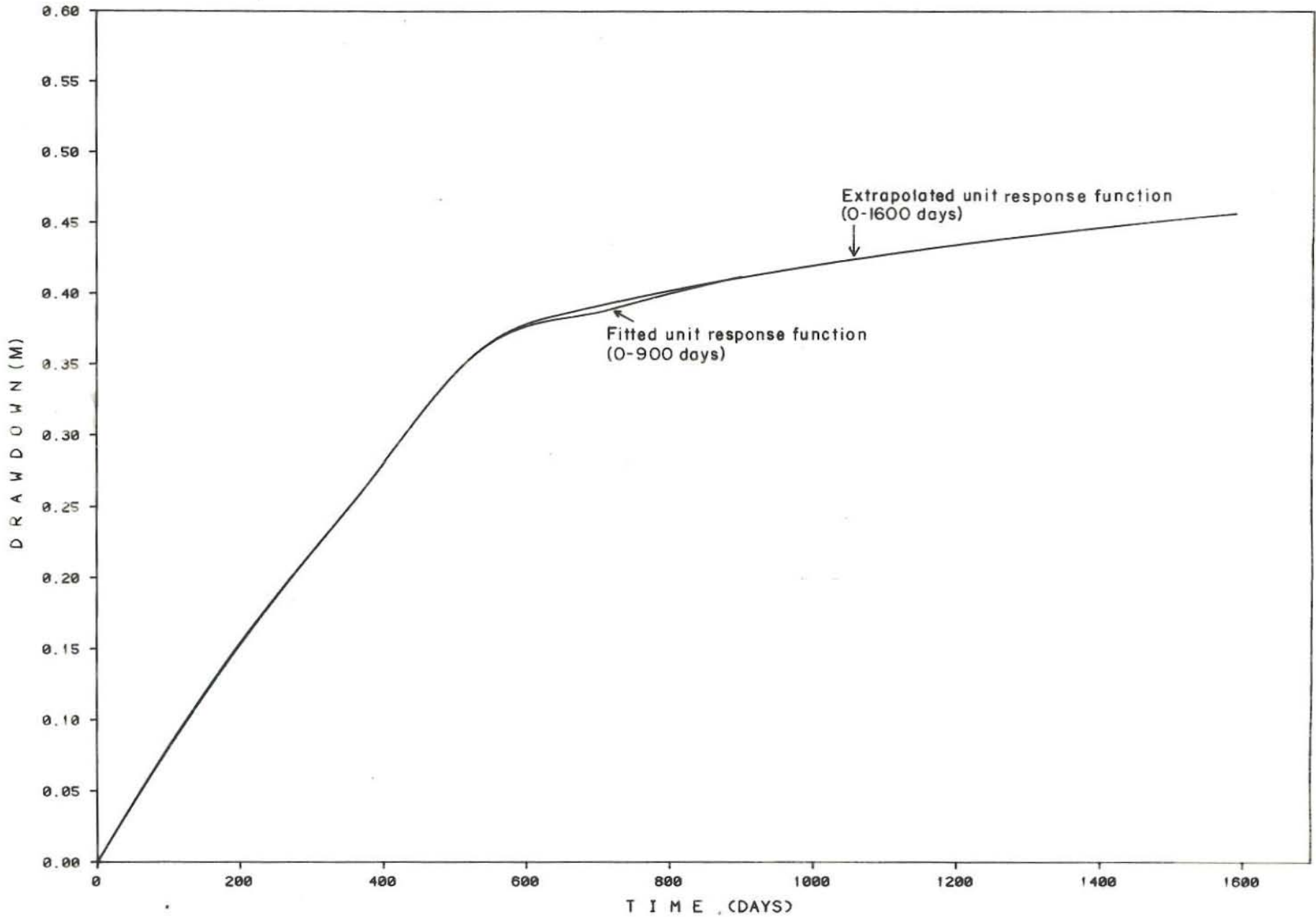


FIG. 5.12 UNIT RESPONSE FUNCTION (0 - 1600 DAYS)
SVARTSENGI GEOTHERMAL FIELD

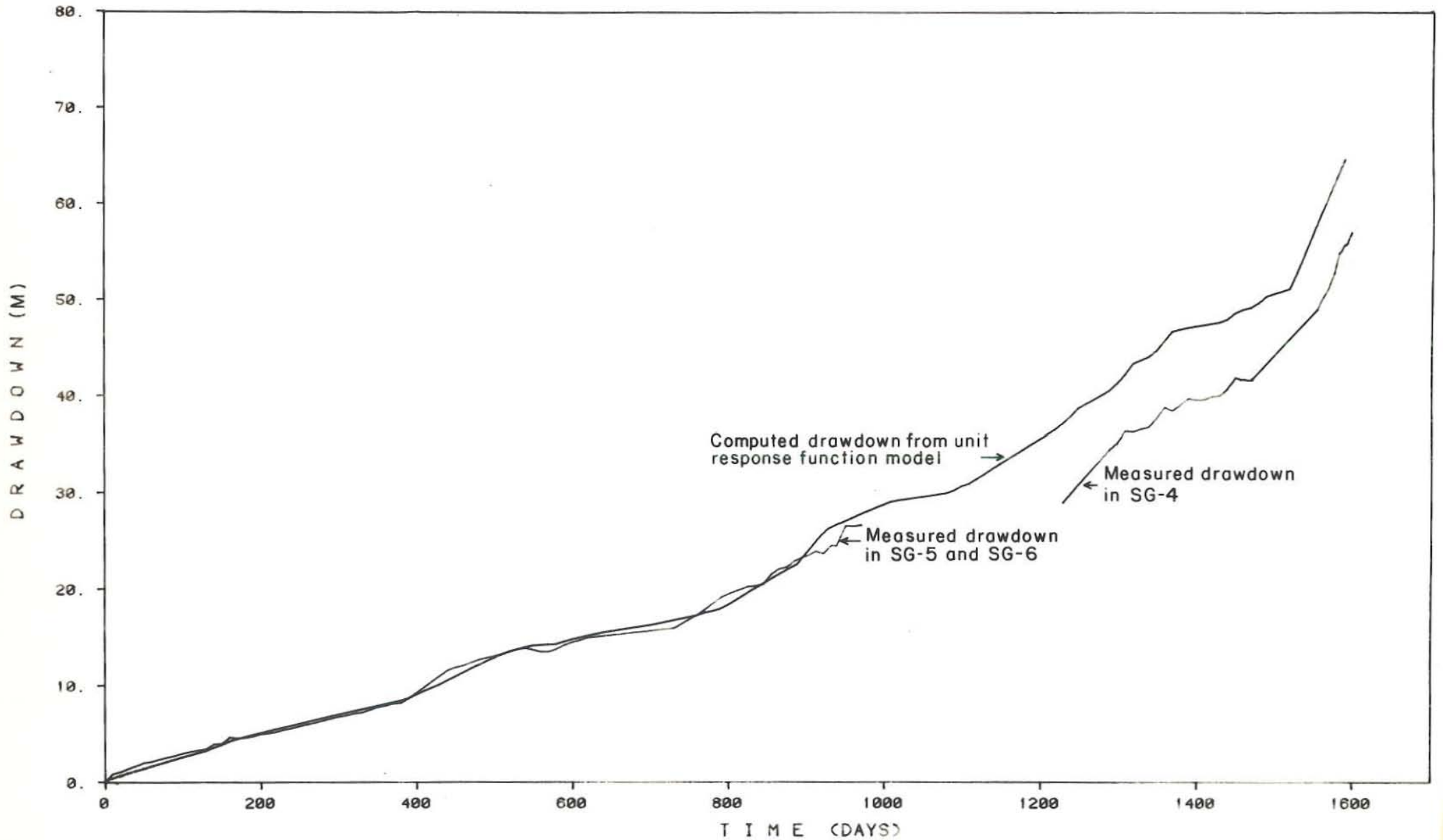


FIG. 5.13 MEASURED VS. COMPUTED DRAWDOWN (0-1600 DAYS)
SVARTSENGI GEOTHERMAL FIELD

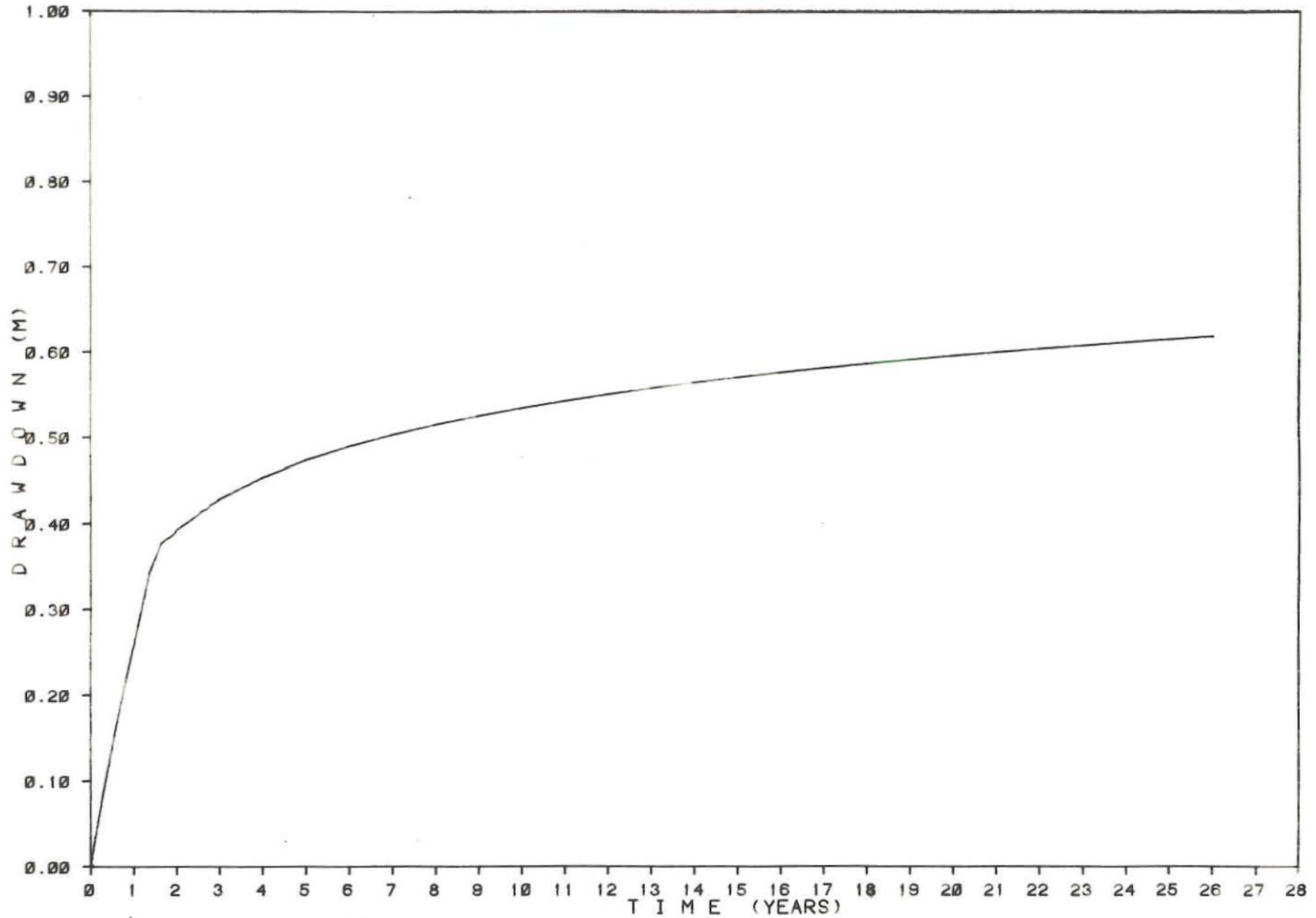


FIG. 5.14 PROJECTED UNIT RESPONSE FUNCTION (0-25 YEARS)
SVARTSENGI GEOTHERMAL FIELD

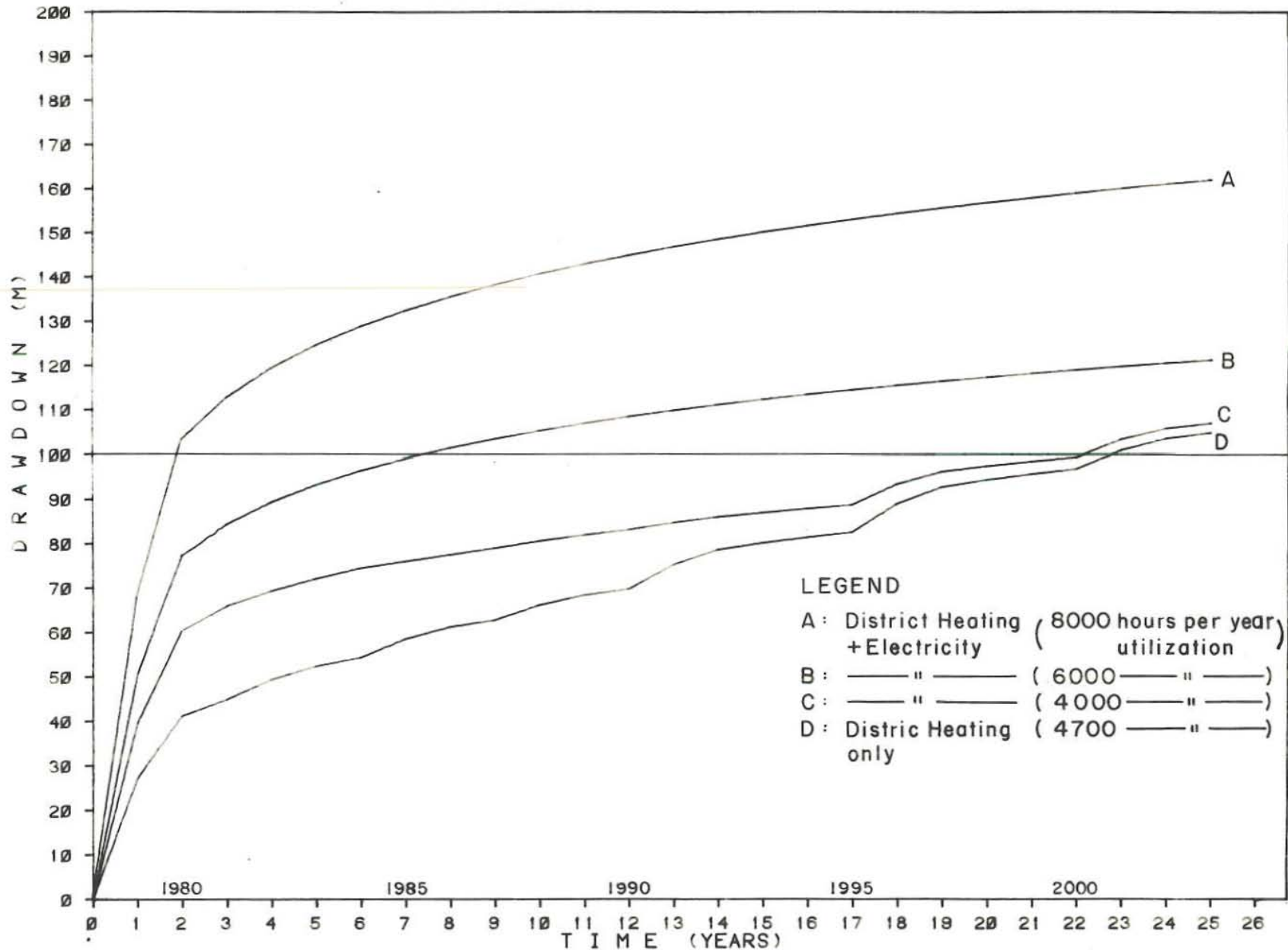


FIG.5.15 CALCULATED DRAWDOWNS FROM UNIT RESPONSE FUNCTION
 SVARTSENGI GEOTHERMAL FIELD

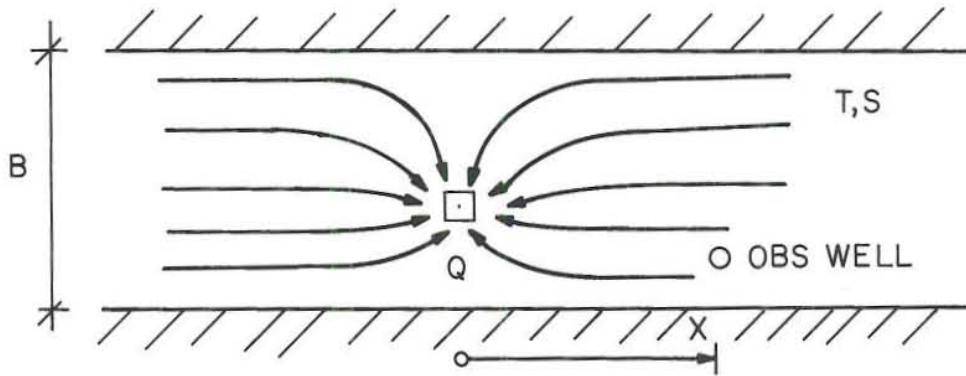


Fig. 5.16.A. Flow in an esker by pumpage from a well.
(From Gustafson, et.al., 1976)

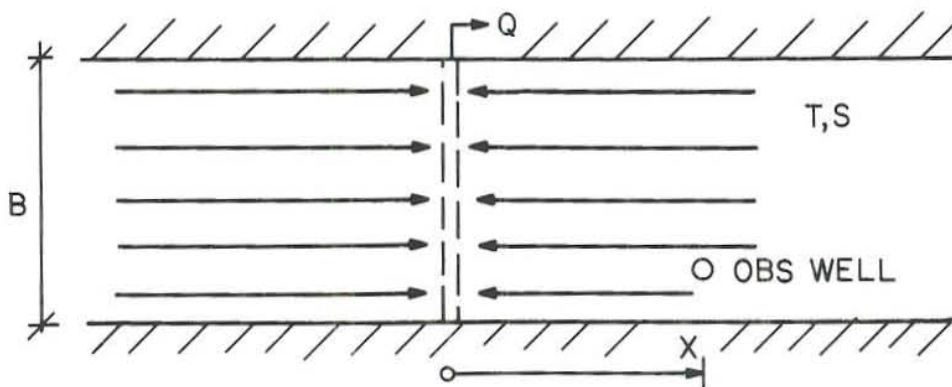


Fig. 5.16.B. Auxiliary hydraulic system for calculating the hydraulic properties of an esker.
(From Gustafson, et.al., 1976).

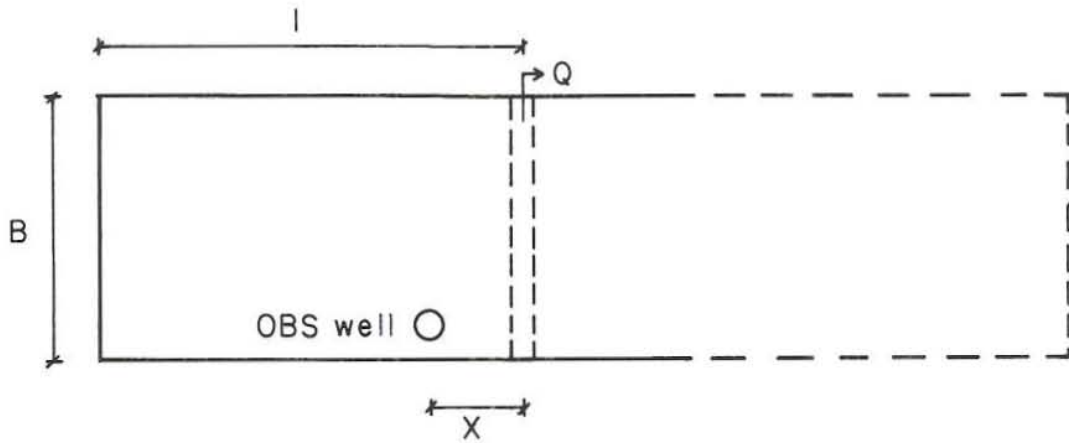


Fig. 5.16 C. Svartsengi reservoir configuration

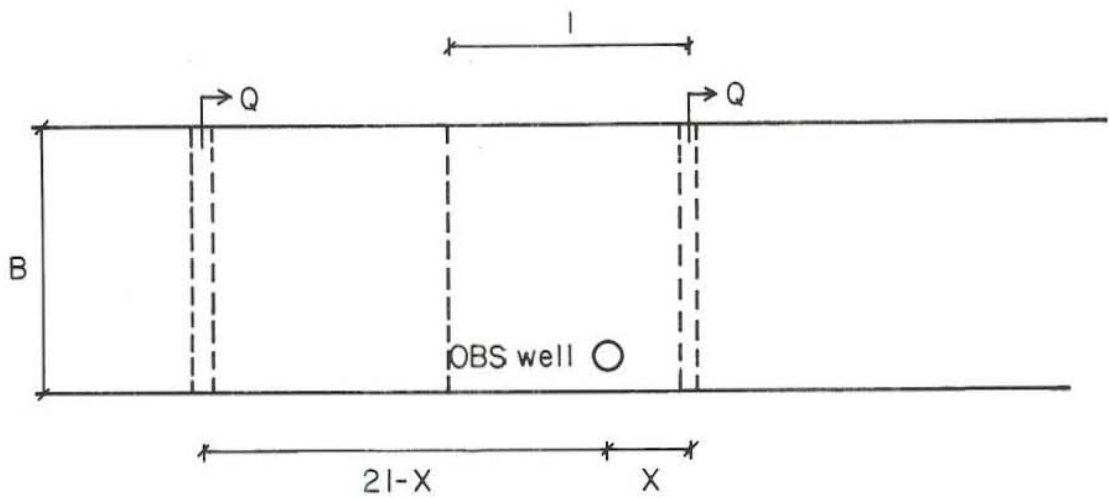


Fig. 5.16 D. Equivalent two-well system

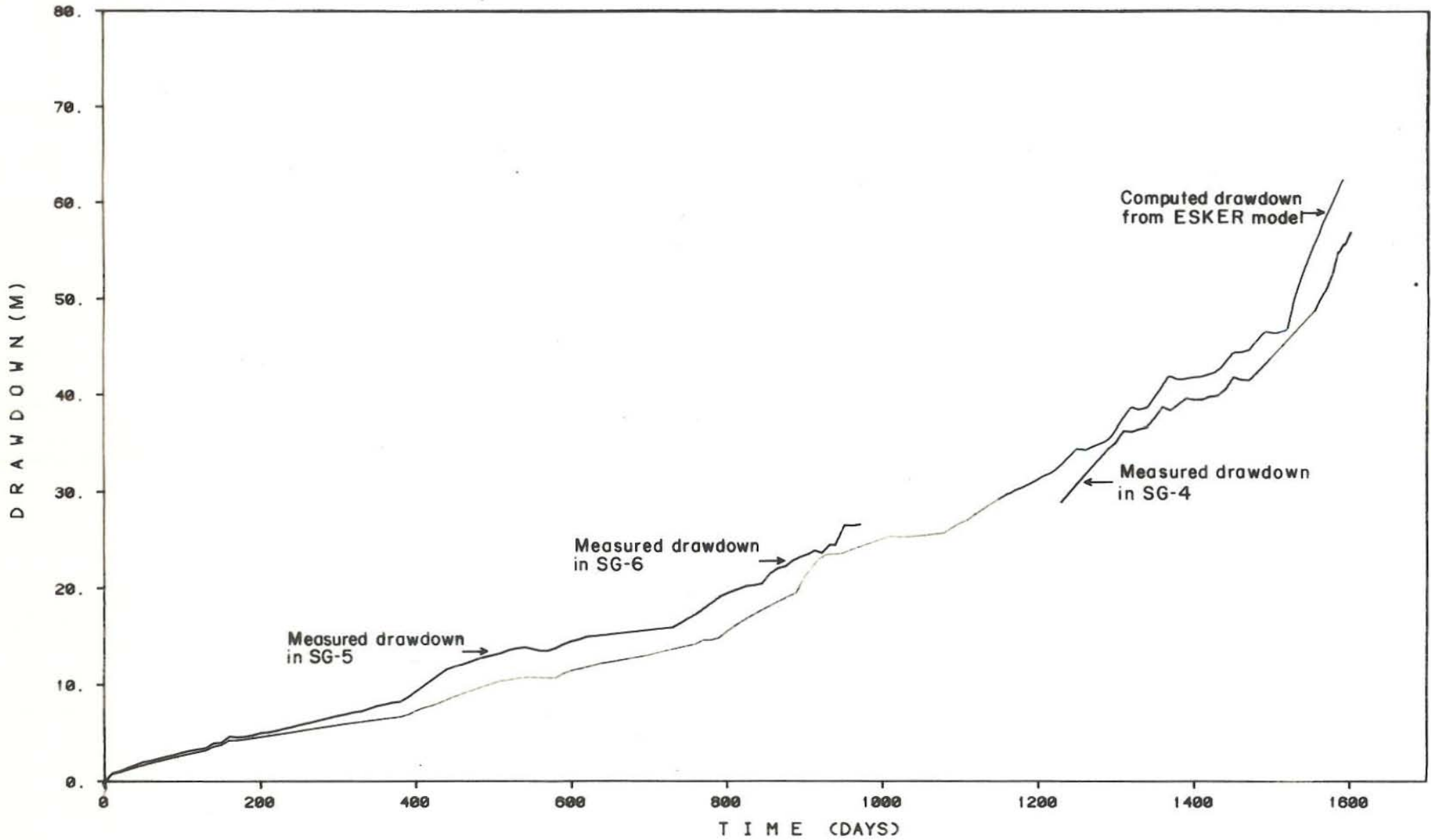


FIG. 5.17 MEASURED VS. COMPUTED DRAWDOWN (0-1600 DAYS)
SVARTSENGI GEOTHERMAL FIELD

JHD-HSD-2300, J.R.R.
81.10. 1211. T/Sy.J.

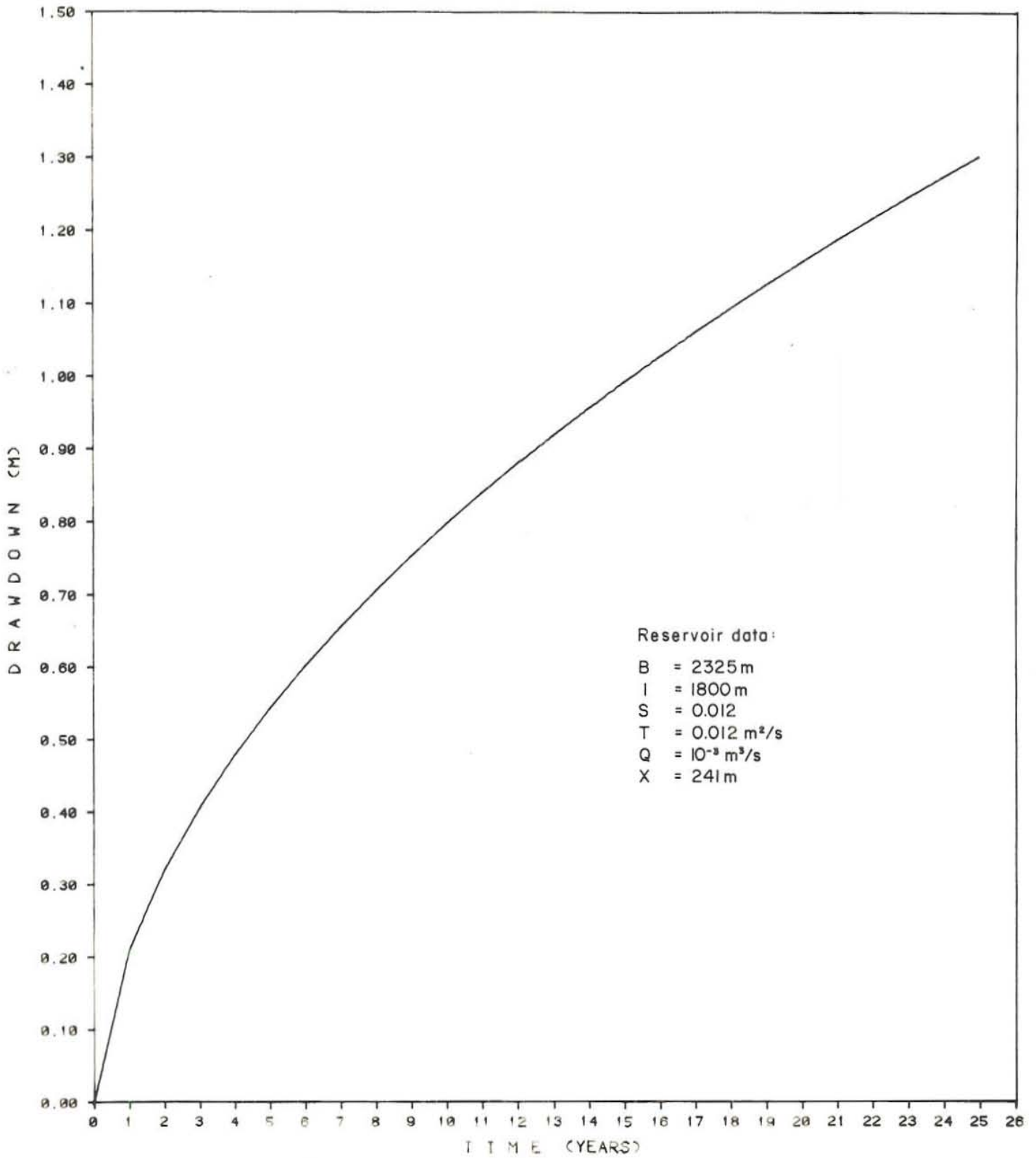


FIG. 5.18 PROJECTED ESKER MODEL (0-25YRS)
SVARTSENGI GEOTHERMAL FIELD

APPENDIX A. DRAWDOWN HISTORY

SKRA DOWN,HIS

1981-10-15

=====

	1	2
1	0.000000	0.000000
2	10.00000	0.860000
3	20.00000	1.080000
4	30.00000	1.400000
5	40.00000	1.700000
6	50.00000	2.020000
7	60.00000	2.140000
8	70.00000	2.380000
9	80.00000	2.580000
10	90.00000	2.760000
11	100.0000	3.000000
12	110.0000	3.180000
13	120.0000	3.320000
14	130.0000	3.440000
15	140.0000	3.940000
16	150.0000	4.000000
17	160.0000	4.640000
18	170.0000	4.540000
19	180.0000	4.620000
20	190.0000	4.760000
21	200.0000	5.000000
22	210.0000	5.080000
23	220.0000	5.220000
24	230.0000	5.440000
25	240.0000	5.600000
26	250.0000	5.820000
27	260.0000	6.000000
28	270.0000	6.180000
29	280.0000	6.380000
30	290.0000	6.580000
31	300.0000	6.780000
32	310.0000	6.920000
33	320.0000	7.120000
34	330.0000	7.220000
35	340.0000	7.500000
36	350.0000	7.780000
37	360.0000	7.940000
38	370.0000	8.140000
39	380.0000	8.220000
40	390.0000	8.700000
41	400.0000	9.280000
42	410.0000	9.840000
43	420.0000	10.44000
44	430.0000	11.02000
45	440.0000	11.60000
46	450.0000	11.90000
47	460.0000	12.10000
48	470.0000	12.40000
49	480.0000	12.70000
50	490.0000	12.90000
51	500.0000	13.10000
52	510.0000	13.30000
53	520.0000	13.60000
54	530.0000	13.80000
55	540.0000	13.90000
56	550.0000	13.70000
57	560.0000	13.50000
58	570.0000	13.50000
59	580.0000	13.80000
60	590.0000	14.20000

1981-10-15

=====

	1	2
61	600.0000	14.50000
62	610.0000	14.70000
63	620.0000	15.00000
64	731.0000	15.98000
65	763.0000	17.48000
66	792.0000	19.18000
67	803.0000	19.58000
68	813.0000	19.88000
69	826.0000	20.26000
70	836.0000	20.34000
71	846.0000	20.51000
72	856.0000	21.54000
73	866.0000	22.09000
74	876.0000	22.29000
75	886.0000	22.92000
76	896.0000	23.29000
77	906.0000	23.58000
78	913.0000	23.91000
79	923.0000	23.65000
80	933.0000	24.51000
81	940.0000	24.46000
82	952.0000	26.54000
83	962.0000	26.49000
84	972.0000	26.62000

ORKUSTOFNUM
1981-10-15

SKRA NDH4.DAT

=====

	1	2
1	1230,000	28,95000
2	1240,000	29,87000
3	1250,000	30,83000
4	1290,000	34,42000
5	1300,000	35,12000
6	1310,000	36,31000
7	1320,000	36,22000
8	1330,000	36,52000
9	1340,000	36,70000
10	1350,000	37,62000
11	1360,000	38,74000
12	1370,000	38,36000
13	1390,000	39,63000
14	1400,000	39,48000
15	1410,000	39,51000
16	1420,000	39,84000
17	1430,000	39,93000
18	1440,000	40,61000
19	1450,000	41,84000
20	1460,000	41,55000
21	1470,000	41,50000
22	1480,000	42,34000
23	1555,000	48,84000
24	1560,000	49,73000
25	1570,000	51,12000
26	1578,000	52,79000
27	1584,000	54,84000
28	1585,000	54,78000
29	1586,000	54,93000
30	1587,000	55,04000
31	1588,000	55,22000
32	1589,000	55,40000
33	1590,000	55,51000
34	1591,000	55,65000
35	1592,000	55,56000
36	1593,000	55,65000
37	1594,000	55,79000
38	1595,000	55,98000
39	1596,000	56,21000
40	1597,000	56,38000
41	1598,000	56,54000
42	1599,000	56,71000
43	1600,000	56,90000
44	1601,000	57,03000
45	1602,000	57,18000
46	1603,000	57,34000
47	1604,000	57,49000
48	1605,000	57,71000
49	1606,000	57,75000
50	1607,000	57,92000
51	1608,000	58,10000
52	1609,000	58,24000
53	1610,000	58,39000
54	1611,000	58,58000
55	1612,000	58,70000
56	1613,000	58,83000
57	1613,000	59,68000

APPENDIX B. FLOWRATE HISTORY

GRKUSTOFNUN
1981-10-15

SKRA PUMP.HIS

=====

	1	2
1	0.0000000	48.00000
2	12.00000	30.00000
3	14.00000	5.000000
4	15.00000	30.00000
5	133.0000	45.00000
6	146.0000	30.00000
7	154.0000	58.00000
8	162.0000	30.00000
9	241.0000	31.00000
10	317.0000	30.00000
11	388.0000	51.00000
12	419.0000	30.00000
13	424.0000	57.00000
14	510.0000	48.00000
15	520.0000	48.00000
16	534.0000	45.00000
17	547.0000	30.00000
18	576.0000	30.00000
19	580.0000	56.00000
20	600.0000	52.00000
21	641.0000	48.00000
22	702.0000	53.00000
23	764.0000	71.00000
24	771.0000	50.00000
25	781.0000	55.00000
26	792.0000	85.00000
27	804.0000	90.00000
28	890.0000	155.0000
29	927.0000	95.00000
30	945.0000	65.00000
31	948.0000	95.00000
32	1012.000	71.00000
33	1086.000	115.0000
34	1099.000	50.00000
35	1104.000	115.0000
36	1130.000	121.0000
37	1138.000	115.0000
38	1223.000	137.0000
39	1234.000	131.0000
40	1235.000	138.0000
41	1237.000	161.0000
42	1248.000	147.0000
43	1250.000	134.0000
44	1251.000	115.0000
45	1252.000	125.0000
46	1258.000	60.00000
47	1260.000	110.0000
48	1274.000	116.0000
49	1288.000	131.0000
50	1292.000	161.0000
51	1297.000	151.0000
52	1302.000	168.0000
53	1305.000	188.0000
54	1309.000	211.0000
55	1319.000	116.0000
56	1339.000	140.0000
57	1343.000	150.0000
58	1345.000	171.0000
59	1348.000	186.0000
60	1353.000	205.0000

ORKUSTOFNUN

SKRA PUMP,HIS

1981-10-15

=====

	1	2
61	1358.000	226.0000
62	1368.000	116.0000
63	1415.000	120.0000
64	1435.000	164.0000
65	1437.000	163.0000
66	1438.000	175.0000
67	1442.000	183.0000
68	1443.000	186.0000
69	1451.000	192.0000
70	1452.000	209.0000
71	1453.000	129.0000
72	1472.000	164.0000
73	1473.000	172.0000
74	1487.000	202.0000
75	1491.000	129.0000
76	1504.000	129.0000
77	1517.000	135.0000
78	1521.000	339.0000
79	1523.000	279.0000
80	1524.000	326.0000
81	1571.000	336.0000

APPENDIX C. TOTAL MASS OUTPUT HISTORY

ORKUSTOFNUN
1981-10-15

SKRA FLOW.HIS

=====

	1	2
1	0,0000000	0,0000000
2	12,00000	0,5000000E-01
3	14,00000	0,5500000E-01
4	15,00000	0,5500000E-01
5	133,0000	0,3600000
6	146,0000	0,4100000
7	154,0000	0,4300000
8	162,0000	0,4700000
9	241,0000	0,6800000
10	317,0000	0,8800000
11	388,0000	1,100000
12	419,0000	1,200000
13	424,0000	1,200000
14	510,0000	1,600000
15	520,0000	1,700000
16	520,0000	1,700000
17	534,0000	1,700000
18	547,0000	1,800000
19	576,0000	1,900000
20	580,0000	1,900000
21	600,0000	2,000000
22	641,0000	2,150000
23	702,0000	2,400000
24	764,0000	2,700000
25	771,0000	2,700000
26	781,0000	2,770000
27	792,0000	2,830000
28	804,0000	2,910000
29	890,0000	3,580000
30	927,0000	4,080000
31	945,0000	4,230000
32	948,0000	4,240000
33	1012,000	4,770000
34	1086,000	5,220000
35	1099,000	5,350000
36	1104,000	5,370000
37	1130,000	5,630000
38	1138,000	5,720000
39	1223,000	6,560000
40	1234,000	6,690000
41	1235,000	6,700000
42	1237,000	6,720000
43	1248,000	6,880000
44	1250,000	6,900000
45	1251,000	6,920000
46	1252,000	6,930000
47	1258,000	6,990000
48	1260,000	7,000000
49	1274,000	7,130000
50	1288,000	7,270000
51	1292,000	7,320000
52	1297,000	7,390000
53	1302,000	7,450000
54	1305,000	7,500000
55	1309,000	7,560000
56	1319,000	7,740000
57	1339,000	7,940000
58	1343,000	7,990000
59	1345,000	8,030000
60	1348,000	8,080000

ORKUSTOFNUN

SKRA FLOW.HIS

1981-10-15

=====

	1	2
61	1353,000	8,160000
62	1358,000	8,250000
63	1368,000	8,440000
64	1415,000	8,910000
65	1435,000	9,120000
66	1437,000	9,140000
67	1438,000	9,160000
68	1442,000	9,220000
69	1443,000	9,240000
70	1451,000	9,360000
71	1452,000	9,380000
72	1453,000	9,400000
73	1472,000	9,610000
74	1473,000	9,620000
75	1487,000	9,770000
76	1491,000	9,840000
77	1504,000	10,030000
78	1517,000	10,170000
79	1521,000	10,220000
80	1523,000	10,280000
81	1524,000	10,300000
82	1571,000	11,630000
83	1604,000	12,590000